

DTIC FILE COPY

1

FJSRL-TR-89-0009

FRANK J. SEILER RESEARCH LABORATORY

**THEORETICAL STUDY OF THE TOWNES-MERRITT
EFFECT IN LEVEL CROSSING EXPERIMENTS**

SEPTEMBER 1989

DTIC
ELECTE
OCT 03 1989
S B D

MAJOR W.R. WHITE

APPROVED FOR PUBLIC RELEASE;
DISTRIBUTION UNLIMITED.

2301-F1

AIR FORCE SYSTEMS COMMAND

UNITED STATES AIR FORCE

89 10 2 144

AD-A213 165



FJSRL-TR-89-0009

This document was prepared by the Laser Physics Division, Directorate of Lasers and Aerospace Mechanics, Frank J. Seiler Research Laboratory, United States Air Force Academy, CO. The research was conducted under Project Work Unit Number 2301-F1-72, Major William R. White was the Project Scientist in charge of the work.


When U.S. Government drawings, specifications or other data are used for any purpose other than a definitely related government procurement operation, the government thereby incurs no responsibility nor any obligation whatsoever, and the fact that the government may have formulated, furnished or in any way supplied the said drawings, specifications or other data is not to be regarded by implication or otherwise, as in any manner licensing the holder or any other person or corporation or conveying any rights or permission to manufacture, use or sell any patented invention that may in any way be related thereto.

Inquiries concerning the technical content of this document should be addressed to the Frank J. Seiler Research Laboratory (AFSC), FJSRL/NH, USAF Academy, CO 80840-6528. Phone (719) 472-3122.

[This report has been reviewed by the Commander and is releasable to the National Technical Information Service (NTIS). At NTIS it will be available to the general public, including foreign nations.]

This technical report has been reviewed and is approved for publication.


WILLIAM R. WHITE, Major, USAF
Chief, Laser Physics Division


ROBERT F. REILMAN, JR., Major, USAF
Director, Lasers & Aerospace Mechanics


WILLIAM G. THORPE, Lt Col USAF
Commander

Copies of this report should not be returned unless return is required by security considerations, contractual obligations, or notice on a specific document.

Printed in the United States of America. Qualified requestors may obtain additional copies from the Defense Documentation Center. [All others should apply to: National Technical Information Service, 6285 Port Royal Road, Springfield, Virginia 22161.]

REPORT DOCUMENTATION PAGE				Form Approved OMB No. 0704-0188										
1a. REPORT SECURITY CLASSIFICATION UNCLASSIFIED			1b. RESTRICTIVE MARKINGS											
2a. SECURITY CLASSIFICATION AUTHORITY			3. DISTRIBUTION / AVAILABILITY OF REPORT Approved for public release; distribution unlimited											
2b. DECLASSIFICATION / DOWNGRADING SCHEDULE			5. MONITORING ORGANIZATION REPORT NUMBER(S)											
4. PERFORMING ORGANIZATION REPORT NUMBER(S) AFIT/DS/ENP/89-2 FJSRL-TR-89-0009			7a. NAME OF MONITORING ORGANIZATION											
6a. NAME OF PERFORMING ORGANIZATION School of Engineering		6b. OFFICE SYMBOL (if applicable) AFIT/ENP	7b. ADDRESS (City, State, and ZIP Code)											
6c. ADDRESS (City, State, and ZIP Code) Air Force Institute of Technology Wright-Patterson AFB OH 45433			9. PROCUREMENT INSTRUMENT IDENTIFICATION NUMBER											
8a. NAME OF FUNDING / SPONSORING ORGANIZATION Frank J. Seiler Research Lab		8b. OFFICE SYMBOL (if applicable) FJSRL/NH	10. SOURCE OF FUNDING NUMBERS											
8c. ADDRESS (City, State, and ZIP Code) USAF Academy CO 80840-6528			PROGRAM ELEMENT NO.	PROJECT NO.	TASK NO.									
11. TITLE (Include Security Classification) Theoretical Study of the Townes-Merritt Effect in Level Crossing Experiments (U)														
12. PERSONAL AUTHOR(S) William Roc White, B.S., M.S., Major, USAF														
13a. TYPE OF REPORT PhD Dissertation		13b. TIME COVERED FROM _____ TO _____		14. DATE OF REPORT (Year, Month, Day) 1989 September										
15. PAGE COUNT 112														
16. SUPPLEMENTARY NOTATION <i>Continued from Pg. 1</i>														
17. COSATI CODES			18. SUBJECT TERMS (Continue on reverse if necessary and identify by block number.)											
<table border="1" style="width: 100%; border-collapse: collapse;"> <thead> <tr> <th style="width: 33%;">FIELD</th> <th style="width: 33%;">GROUP</th> <th style="width: 33%;">SUB-GROUP</th> </tr> </thead> <tbody> <tr> <td>20</td> <td>05</td> <td></td> </tr> <tr> <td>20</td> <td>10</td> <td></td> </tr> </tbody> </table>			FIELD	GROUP	SUB-GROUP	20	05		20	10		Spectroscopy, Level Crossings, Quantum Beats, Absorption Sidebands, Nonlinear Optics, Quantum Optics <i>SC(11)</i>		
FIELD	GROUP	SUB-GROUP												
20	05													
20	10													
19. ABSTRACT (Continue on reverse if necessary and identify by block number) A high resolution spectroscopic technique using a nonresonant RF field in a level crossing experiment is proposed. Absorption sidebands, originally observed by Townes and Merritt (1947), are analyzed using a quantum electrodynamics (QED) approach. A model is developed using the Heisenberg operator formalism and the adiabatic approximation to describe the atomic dynamics. Results agree with a dressed states approach and the original experiment. The model is extended to a three level atom to describe level crossings and quantum beats for linear and quadratic Stark shifted atoms. Expressions are developed to define level crossing conditions and estimate critical experimental parameters. <i>Keywords:</i> Dissertation Chairman: Richard J. Cook, Lt Col, USAF Adjunct Professor of Physics														
20. DISTRIBUTION / AVAILABILITY OF ABSTRACT <input checked="" type="checkbox"/> UNCLASSIFIED/UNLIMITED <input type="checkbox"/> SAME AS RPT <input type="checkbox"/> DTIC USERS			21. ABSTRACT SECURITY CLASSIFICATION UNCLASSIFIED											
22a. NAME OF RESPONSIBLE INDIVIDUAL Richard J. Cook, Lt Col, USAF			22b. TELEPHONE (Include Area Code) 613 472 3122		22c. OFFICE SYMBOL FJSRL/NH									

THEORETICAL STUDY OF THE TOWNES-MERRITT EFFECT
IN LEVEL CROSSING EXPERIMENTS

DISSERTATION

William Roc White, B.S., M.S.

Major, USAF

September 1989

Approved for public release; distribution unlimited

Preface

This paper culminates a nearly five year effort in pursuit of a PhD degree on a part time basis. The last two years were spent on this particular research. The primary aim of this study was to propose a new high resolution spectroscopic technique using a nonresonant field to effect a level crossing. The theoretical description of the Townes-Merritt effect, quantum beats, and level crossings are covered, as well as a brief look at some of the important experimental parameters. An actual experiment is suggested as a logical follow-on effort. A secondary objective was to gain a more detailed education in quantum electrodynamics (QED) and nonlinear effects such as level crossings and quantum beats. Several useful techniques in atomic physics are covered in this paper, which hopefully, the reader may find useful.

There are several people to whom I owe many thanks in the completion of this program. First, I wish to thank Dr. Richard J. Cook who has both inspired me in this field of study and has ultimately made it possible for me to pursue and complete this program. It has been an absolute pleasure to work with and learn from him. I also owe deep appreciation to Dr. Ronald L. Bagley for his willingness to support my desire to take on such a program and constant urging to complete it. Finally, and most of all, I wish to thank my family, Kristen, Lara, and particularly my wife Barbara, for their continued support and patience in this often trying task. It is to them that I truly owe this opportunity to attain a lifelong goal.

Table of Contents

	Page
Preface	ii
List of Figures	iv
Abstract	v
I. Introduction	1
II. Background	6
Townes-Merritt Effect	6
Level Crossings and Quantum Beats	8
III. QED Description of the Townes-Merritt Effect	18
Heisenberg Operator Formalism	18
Adiabatic Approximation	24
Townes-Merritt Effect	30
Quantum Electrodynamic Approach	39
Dressed States Model	46
Quantum Beats in a Two Level Atom	53
IV. Quantum Beats and Level Crossings	56
Three Level Atom	56
Linear Stark Shift	58
Quadratic Stark Shift	60
Quantum Beats Calculation	63
Linear Stark Shift	66
Dressed States Calculation	68
Quadratic Stark Shift	70
Level Crossing Calculation	73
Linear Stark Shift	75
Quadratic Stark Shift	86
V. Experimental Feasibility	89
VI. Conclusion	101
Bibliography	103
Vita	105



For	
<input checked="checked" type="checkbox"/> For <input type="checkbox"/> For <input type="checkbox"/> For	
By	
Distribution/	
Availability Codes	
Dist	Avail and/or Special
A-1	

List of Figures

Figure	Page
1. Absorption Sidebands	1
2. Energy Level Diagram	3
3. Experimental Setup	4
4. Three Level Atomic System	9
5. Level Crossing Experiment	10
6. Quantum Beats	11
7. Fluorescent Intensity at Level Crossing	17
8. Two Level Atom	20
9. Absorption Cross-Section	24
10. Absorption Cross-Section in a Nonresonant Field	36
11. Dressed States for a Two Level Atom	46
12. Quantum Beats in a Two Level Atom	54
13. Dressed States for a Three Level Atom	57
14. Level Crossing Geometry	79
15. Level Crossing Signal for a Linear Stark Shift	80
16. Level Crossing Signal for a Linear Quadratic Shift	88
17. RF Field Strength Required for a Quadratic Shift	92
18. Level Crossing Signal for $\phi = \pi/4$	99

Abstract

A high resolution spectroscopic technique using a nonresonant RF field in a level crossing experiment is proposed. Absorption sidebands, originally observed by Townes and Merritt (1947), are analyzed using a quantum electrodynamic (QED) approach. A model is developed using the Heisenberg operator formalism and the adiabatic approximation to describe the atomic dynamics. Results agree with a dressed states approach and the original experiment. The model is extended to a three level atom to describe level crossings and quantum beats for linear and quadratic Stark shifted atoms. Expressions are developed to define level crossing conditions and estimate critical experimental parameters.

THEORETICAL STUDY OF THE TOWNES-MERRITT EFFECT IN LEVEL CROSSING EXPERIMENTS

I. Introduction

→ The aim of this study is to develop the theory to describe the effect of an external nonresonant electromagnetic field on level crossing experiments. The primary motivation rests in the possibility of using these effects to obtain greater accuracy in high resolution spectroscopy. The basis for such a study began with the observation, by Townes and Merritt in 1947, of sidebands in the absorption spectra of the OCS $J = 1 \rightarrow 2$ transition when the sample was placed in a nonresonant oscillating electric field [1]. These sidebands, shown in Figure 1, occur at intervals equal to twice the modulating field frequency. The original semiclassical analysis uses time-dependent perturbation theory to describe the frequency dependence and relative amplitudes of the sidebands [2] with good agreement to the experiment. The proposed application of this "Townes-Merritt Effect" involves the determination of energy differences between nearby atomic/molecular levels by causing respective sidebands to overlap or cross.

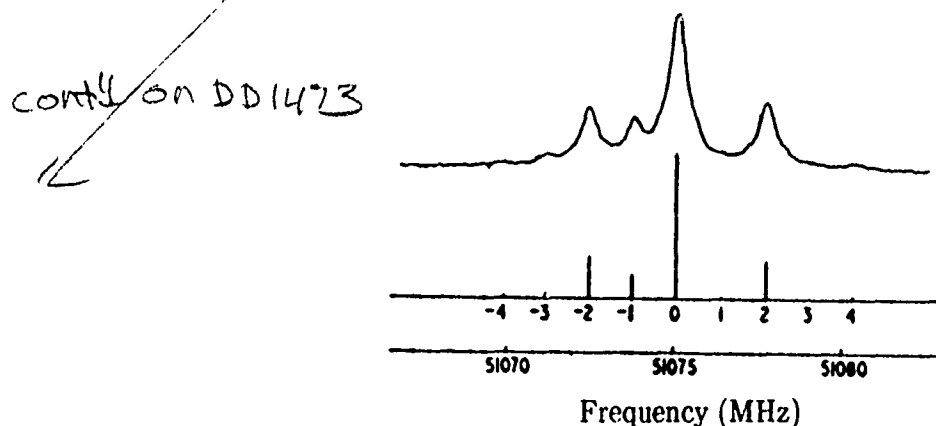


Figure 1. Absorption sidebands in a combined static and RF Field [26]. Theoretical pattern is below experimental result.

Level crossings and a closely related phenomenon, quantum beats, can occur when there exist two nearby energy levels which can each transition to a lower state. Both result from interference between the fluorescence patterns of the two independent transitions when they are coherently excited with a short pulse. Quantum beats manifest themselves in an oscillation of the total fluorescence at a frequency proportional to the energy difference of the excited states. Level crossings result in a rotation of the overall fluorescence pattern which may be detected by a change in intensity or polarization in a given direction. These will be discussed in more detail later; but it is worth mentioning that an adequate description of the phenomenon requires a quantum electrodynamic (QED) model of the interaction [3,4], which will become the basis of this study.

Level crossing experiments are an established method used to measure the fine or hyperfine structure of atomic and molecular systems [5]. However in these cases, static fields (electric or magnetic) are used to cause the level crossing. Hereafter, atomic and molecular systems will be referred to as simply atomic. Individual levels split as a result of the Stark or Zeeman effect and orientation quantization of the atomic angular momentum. Then, depending on the field strength, a level crossing may occur. The indication of a level crossing is a change in the fluorescence pattern for the transition from the crossing levels to a lower level. The original energy level spacing can be determined from the field strength at which the crossing occurs. In the use of static fields, key problems present are: strong field strengths are generally required; it is difficult to generate static fields with uniform strength over the sample; and further measurement of the field strength can be a significant source of error [6].

Use of an external nonresonant oscillating field, for example in the radio frequency (RF) or microwave region, would appear to alleviate the problems

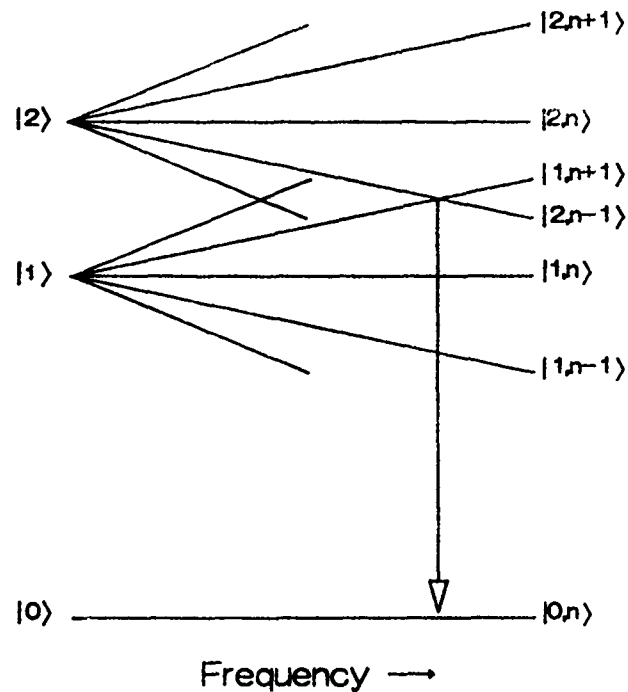


Figure 2. Energy Level Diagram for a combined atom-RF field system.

associated with static fields. The primary difference in the case of an RF field is that the level splitting is dependent on the external field frequency instead of field intensity. Figure 2 shows a typical energy level diagram of an atom in an RF field where the levels represent the combined atom-field system. Note the vertical scale is relative to the energy of the n photon state. The atom with no field applied has two closely spaced upper states, $|1\rangle$ and $|2\rangle$, each of which has an allowed transition to the ground state $|0\rangle$. As the field is applied with increasing frequency, the energy levels split and eventually cross. The notation used to describe specific combined states indicates the original atomic state and the photon number state n , for example $|1,n\rangle$. It is worth noting that for each atomic state there are an infinite number of combined states due to the infinite number of possible photon number states; however, population of these states depends on the field intensity. Hence, the strength of given transitions and observed level crossings would depend on the field strength.

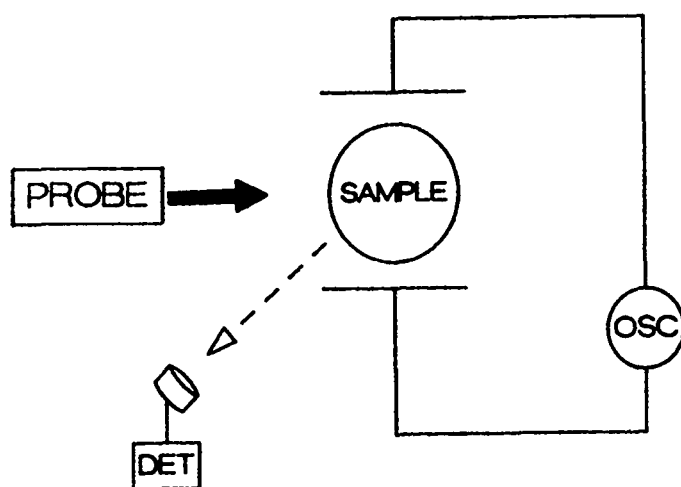


Figure 3. Experimental Setup

The potential advantages of the RF field approach result from the energy level dependence on field frequency. The level crossing points would depend primarily on field frequency which can be more accurately measured than field strength. This, in turn, would result in a more accurate determination of the original energy level separation. The major impact of field strength would be in the intensity of the transitions. Secondly, unlike the static case, the field uniformity is not a critical concern thus eliminating the principal source of error.

The proposed technique would involve an experimental setup similar to the schematic shown in Figure 3. An appropriate sample placed in a variable RF field is illuminated by a pulsed resonant probe beam to coherently excite the transitions. A detector placed off axis measures the fluorescence of the sample in order to observe quantum beats or to indicate a level crossing. The frequencies at which level crossings occur determine the original energy level spacing.

The main objective of this research is to develop the theory describing the resonant fluorescence of an atomic or molecular sample as a function of the frequency of an external nonresonant field. Of particular interest is a situation with closely spaced excited states which, due to the Townes-Merritt effect, split and

eventually result in level crossing. The original spacing can then be determined by the frequency at which the crossing occurs.

To lay the foundation, chapter II presents a review of the Townes–Merritt effect, quantum beats and the level crossing phenomenon. The original Townes–Merritt analysis used a semiclassical approach, which is not compatible with the description of level crossings; however, the results are useful as a comparison to a quantum electrodynamic (QED) model. The descriptions of quantum beats and level crossings provide the initial mathematical framework which will be used later in applying the Townes–Merritt effect.

Chapter III revisits the Townes–Merritt effect in the context of QED. The Heisenberg operator formalism is used to describe the atomic dynamics. Additionally, the calculations use the adiabatic approximation to describe the atom in the nonresonant RF field. The results are compared to a dressed states model to confirm the approach. The overall purpose is to understand the mechanisms involved in the Townes–Merritt sidebands in order to apply them to the cases of quantum beats and level crossings.

The three level atom is addressed in chapter IV. Calculations for the instantaneous energy states for an atom in an RF field are performed, following the adiabatic approach, for both linear and quadratic Stark shifts. These then are used in descriptions of the signals resulting from quantum beats and level crossings. Expressions describing the effect of the RF field are developed, which form the basis of using the level crossing method as a spectroscopic technique.

A final step, in chapter V, is to investigate the prospects for an experimental test of this method. Suitable atomic transitions, RF field strength and frequency, and required detection capability will be investigated. The intent here is to take an initial look at the feasibility of conducting this type of experiment.

II. Background

Townes-Merritt Effect

As a preliminary, a review of the original Townes-Merritt model is required since it will provide a comparison with any QED approach. Consider an absorption experiment in which the sample is placed in a rapidly varying nonresonant field and probed with a second resonant beam. The original calculations used semiclassical time-dependent perturbation theory to describe transitions from this dynamic Stark effect [2,7]. The wave equation for an atom in the nonresonant field is

$$i\hbar \frac{\partial |\psi\rangle}{\partial t} = [\hat{H}_0 - \mu \cdot \mathcal{E}_0 \cos \nu t] |\psi\rangle \quad (2.1)$$

where \hat{H}_0 is the unperturbed atomic Hamiltonian; μ is the dipole operator; \mathcal{E}_0 is the nonresonant field amplitude; and ν is the field frequency.

Using the essential states approximation with two unperturbed states represented by $|1\rangle$ and $|2\rangle$, the solution for a perturbed state can be written as

$$|\psi_1\rangle = [a|1\rangle + b|2\rangle] e^{-\frac{i}{\hbar} \int_0^t f(t') dt'} \quad (2.2)$$

where, assuming the perturbation is small, $a \approx 1$ and b is small. The term $f(t)$ is approximately the energy of the unperturbed state E_1 . For a second order Stark effect, the wave function is found by substituting equation (2.2) into equation (2.1):

$$|\psi_1\rangle = [a|1\rangle + b|2\rangle] \exp\left\{-\frac{i}{\hbar}(E_1 t + \frac{\Delta E_1 t}{2} + \frac{\Delta E_1}{4\nu} \sin 2\nu t)\right\} \quad (2.3)$$

where ΔE_1 is the static Stark shift, $\frac{(\mu_{12} \mathcal{E}_0)^2}{\hbar \omega_{12}}$.

In the absorption experiment, transitions will occur between $|\psi_1\rangle$ and another state represented by $|\psi_3\rangle$. If the interaction is $\hat{H}'(t) = \mu \cdot \mathcal{E} \cos \omega t$, perturbation theory indicates that the first order transition probability [8] is

$$|a_3^{(1)}(t)|^2 = \frac{1}{\hbar^2} \left| \int_{-\infty}^t \langle \psi_3 | \hat{H}' | \psi_1 \rangle dt' \right|^2 \quad (2.4)$$

The intensity is then dependent on the matrix element:

$$\langle \psi_3 | \hat{H}' | \psi_1 \rangle \approx \mu_{31} \mathcal{E} \exp \left\{ i \left(\omega_{13} t + \frac{\Delta \omega_{13} t}{2} + \frac{\Delta \omega_{13}}{4\nu} \sin 2\nu t - \omega t \right) \right\} \quad (2.5)$$

Significant transitions will occur only when the exponential term is "slowly varying," that is when its argument is approximately zero. The exponential can be simplified using the relation $e^{\pm iz \sin \theta} = \sum_{n=-\infty}^{\infty} J_n(z) e^{\pm i n \theta}$ [9] yielding

$$\langle \psi_3 | \hat{H}' | \psi_1 \rangle \approx \mu_{31} \mathcal{E} \exp \left\{ i \left(\omega_{13} + \frac{\Delta \omega_{13}}{2} - \omega \right) t \right\} \sum_{n=-\infty}^{\infty} J_n \left[\frac{\Delta \omega_{13}}{4\nu} \right] e^{i 2 n \nu t} \quad (2.6)$$

Equation (2.6) describes transitions which will occur for

$$\omega = \omega_{13} + \frac{\Delta \omega_{13}}{2} + 2n\nu, \quad n = 0, \pm 1, \pm 2, \dots \quad (2.7)$$

with relative intensity $J_n^2 \left[\frac{\Delta \omega_{13}}{4\nu} \right]$. This is the case for an atom which exhibits a quadratic Stark effect. The calculation describes absorption sidebands resulting from the presence of a nonresonant electric field. The position of these sidebands is primarily dependent on the field frequency. These predictions agree with experimental results [7] within experimental error. For the case of a linear Stark

effect, transitions occur for $\omega = \omega_{13} \pm n\nu$, with relative intensity $J_n^2 \left[\frac{\Delta\omega_{13}}{\nu} \right]$, where $\Delta\omega_{13} = \frac{\mathcal{E}_0 \mu_{11}}{\hbar}$ [2].

Discovery of this effect has led to promising applications. Arimondo and Glorieux [10] and Rackley and Butcher [11] performed absorption experiments using a nonresonant RF field to tune an atomic transition into coincidence with a laser. In effect they adjusted the RF frequency until the fixed laser frequency matched one of the sidebands. In a second type of application, Skatrud and DeLucia [12] reported on using an RF field to Stark tune a laser. Here the sidebands of an atomic transition were used for the lasing transition and, hence, the laser was tuned by changing the frequency of the RF field.

In each of these examples, application of the Townes–Merritt effect demonstrated some significant advantages over a static or DC Stark shift. Because of its frequency dependence, as per equation (2.7), the Townes–Merritt effect is not limited in the shift magnitude due to breakdown voltage, thus allowing a wider range. Since the DC Stark shift depends on the electric field amplitude, a uniform field is important to reduce broadening. The Townes–Merritt effect does not rely on field uniformity, as the intensity only determines relative intensities of the sidebands. Finally, the measurement or control of field frequency is substantially more accurate than that of field intensity. This allows greater experimental accuracy. These advantages lead to the proposed application of the Townes–Merritt effect, the use of level crossings to determine fine/hyperfine structure.

Level Crossings and Quantum Beats

Level crossings and quantum beats are related quantum phenomenon that arise from interference between two atomic transitions which have the same final energy state [13] as shown in Figure 4. Level crossings occur when the two initial

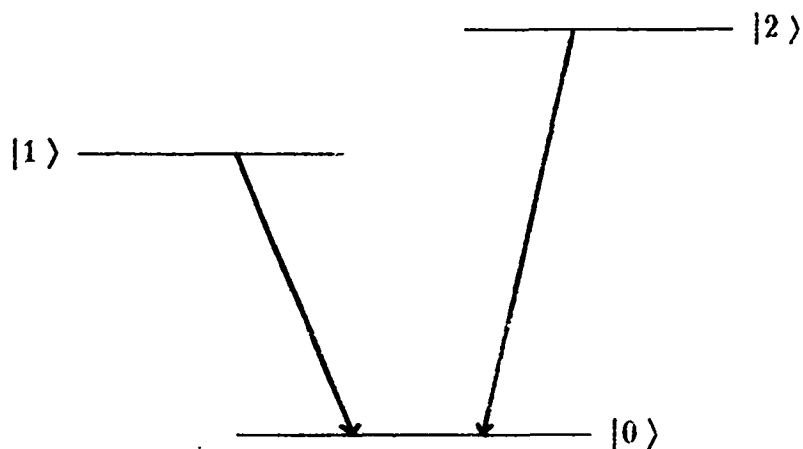


Figure 4. Three-Level Atomic System. Transitions can occur from either excited state to the ground state

states $|1\rangle$ and $|2\rangle$ coincide, resulting in a change in the polarization and angular dependence of the fluorescence pattern. Quantum beats can occur when the initial states are slightly different in energy; the result is a modulation of the total radiated power at a frequency equivalent to the energy difference. In both cases, the initial states must be excited coherently to achieve the interference effect.

In level crossing experiments, one observes the resonant fluorescence of the atom as a function of an external field. A change in the intensity or polarization at a specific observation angle signifies the occurrence of a level crossing, see Figure 5 [14]. The crossing, or degeneracy, is due to Stark or Zeeman shifts in the original atomic energy states resulting from an external static field. [6,15] The Hanle effect is a special case of a zero field level crossing. The primary application of the level crossing technique is the determination of original energy separation based on the field strength at which crossing occurs. The sensitivity of this method is comparable to the natural line width of the excited states. Several experiments have reported using this method [16,17,18] to measure various parameters, establishing it as a high resolution spectroscopic technique. One of the drawbacks is that the static field must be relatively strong and uniform.

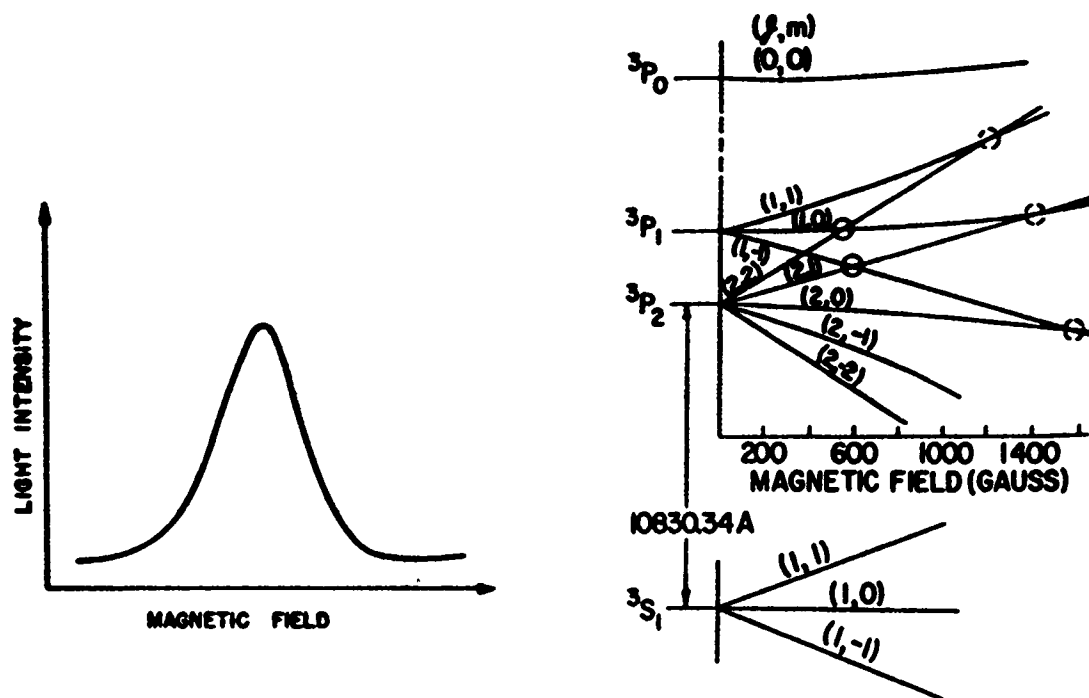


Figure 5. Level Crossing Experiment [6]. Fluorescence intensity as a function of magnetic field and the atomic energy level diagram.

The quantum beat phenomenon occurs when there is a slight difference in the energy of the initial excited states. When excited coherently, the transitions from these states interfere resulting in a modulation of the radiated power at the "beat" frequency. [19] Figure 6 shows a representative example of a beat signal in a fluorescence experiment. [20] A principal use of the quantum beat effect is to investigate very slight splittings in atomic levels [21,22] where other spectroscopic techniques do not have sufficient resolution.

To understand the theory describing level crossings and quantum beats, consider the simple three level model shown in Figure 4 in which two excited states can decay to a common ground state. The hypothetical experiment involves coherently exciting the two upper states and observing the resonant fluorescence.

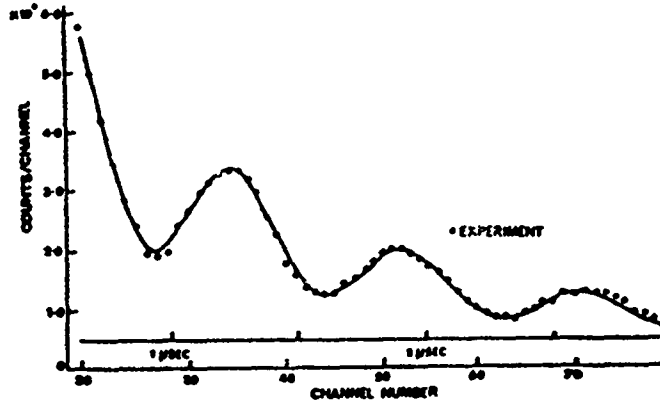


Figure 6. Quantum Beats in Zeeman states of Cd: 5 $3P_1$, [20]. Beats result in a modulation of the exponential decay curve.

fluorescence. The Poynting vector describes the radiation from the atom; in QED form this is

$$\hat{S} = \frac{c}{4\pi} (\hat{E}^{(-)} \times \hat{B}^{(+)} - \hat{B}^{(-)} \times \hat{E}^{(+)}) \quad (2.8)$$

where the superscript plus and minus refer to the positive and negative frequency parts of the \mathbf{E} and \mathbf{B} fields. [23] An ideal detector measures the expectation value of this expression which reduces to

$$S = \langle \hat{E}^{(-)} \cdot \hat{E}^{(+)} \rangle \quad (2.9)$$

This is consistent with the photo ionization process which takes place in the detector, described by Glauber. [24]

From dipole radiation theory [25], the E field can be expressed as

$$\hat{\mathbf{E}}(\pm) = \frac{\mathbf{r} \times \mathbf{r} \times \ddot{\boldsymbol{\mu}}^{(\pm)}}{c^2 r^3} \quad (2.10)$$

where $\ddot{\boldsymbol{\mu}}$ is the dipole acceleration operator. From Cook [3], an expression for radiation intensity, in terms of the dipole operator, results from substitution of equation (2.10) into equation (2.9):

$$S = \frac{r^2 \langle \ddot{\boldsymbol{\mu}}_i^{(-)} \cdot \ddot{\boldsymbol{\mu}}_i^{(+)} \rangle - x_i x_j \langle \ddot{\boldsymbol{\mu}}_i^{(-)} \cdot \ddot{\boldsymbol{\mu}}_j^{(+)} \rangle}{2\pi c^3 r^4} \quad (2.11)$$

using the summation notation for the vector components. equation (2.11) gives a means of predicting the fluorescence radiation at any point by the expectation value of the second time derivative of the dipole operators, $\langle \ddot{\boldsymbol{\mu}}_i^{(-)} \cdot \ddot{\boldsymbol{\mu}}_j^{(+)} \rangle$. This forms the basis for both the level crossings and quantum beat descriptions. In level crossings, the item of interest is the radiation intensity in a particular direction as a function of the energy difference in the excited states. For quantum beats, the total power radiated as a function of time is of concern.

First consider the case of quantum beats. The total power radiated is equal to the integral of equation (2.11) over a sphere of radius r :

$$P = \frac{4 \langle \ddot{\boldsymbol{\mu}}^{(-)} \cdot \ddot{\boldsymbol{\mu}}^{(+)} \rangle}{3c^3} \quad (2.12)$$

Now to find an expression for the dipole moment, let the energy eigenstates of the atom be defined by

$$\hat{H}|n\rangle = E_n|n\rangle \quad (2.13)$$

These states are orthogonal and complete. Then a convenient operator basis set is $\hat{\sigma}_{nm} = |n\rangle\langle m|$, such that in the Heisenberg picture,

$$\hat{\mu}(t) = \sum_{n,m} \mu_{nm} \hat{\sigma}_{nm} e^{i\omega_{nm}t} \quad (2.14)$$

where $\mu_{nm} = \langle n|\hat{\mu}|m\rangle$ are the dipole transition moments. This can be separated into the separate negative and positive frequency components as

$$\hat{\mu}^{(-)} = \sum_{n>m} \mu_{nm} \hat{\sigma}_{nm} e^{i\omega_{nm}t} \quad (2.15a)$$

$$\hat{\mu}^{(+)} = \sum_{m>n} \mu_{nm} \hat{\sigma}_{nm} e^{i\omega_{nm}t} = \sum_{p>q} \mu_{pq}^* \hat{\sigma}_{pq}^\dagger e^{i\omega_{pq}t} \quad (2.15b)$$

Taking the second derivative with respect to time and multiplying,

$$\ddot{\mu}^{(-)} \cdot \ddot{\mu}^{(+)} = \sum_{n>m} \sum_{p>q} \omega_{nm}^2 \omega_{pq}^2 \mu_{nm} \mu_{pq}^* \hat{\sigma}_{nm} \hat{\sigma}_{pq}^\dagger e^{i(\omega_{nm}-\omega_{pq})t} \quad (2.16)$$

The last term in this equation shows the presence of the beat frequency, $\omega_{nm}-\omega_{pq}$.

At this point it is worth noting that beats will not occur for all combinations of transitions, as semiclassical theory would predict. Only those pairs which have a common final state exhibit the beats. To see this, consider the $\hat{\sigma}$ terms,

$$\hat{\sigma}_{nm} \hat{\sigma}_{pq}^\dagger = |n\rangle\langle m| \left[|p\rangle\langle q| \right]^\dagger = |n\rangle\langle m|q\rangle\langle p| = \delta_{mq} \hat{\sigma}_{np} \quad (2.17)$$

which shows that the final states, $|m\rangle$ and $|q\rangle$ must be the same.

Equation (2.16) is then simplified by eliminating the sum over q :

$$\ddot{\vec{\mu}}^{(-)} \cdot \ddot{\vec{\mu}}^{(+)} = \sum_{n, p > m} \omega_{nm}^2 \omega_{pm}^2 \vec{\mu}_{nm} \cdot \vec{\mu}_{pm}^* \hat{\sigma}_{np} e^{i\omega_{np}t} \quad (2.18)$$

where $\omega_{np} \equiv \omega_{nm} - \omega_{pm}$ is the beat frequency. In taking the expectation value of this sum in the state $|\psi\rangle = \sum_n a_n |n\rangle$, we find

$$\langle \hat{\sigma}_{np} \rangle = \langle \psi | n \rangle \langle p | \psi \rangle = a_p a_n^* = \rho_{pn}^H \quad (2.19)$$

which is the density matrix in the Heisenberg picture. Hence, the expression for the total power becomes

$$P = \frac{4}{3c^3} \sum_{n, p > m} \omega_{nm}^2 \omega_{pm}^2 \vec{\mu}_{nm} \cdot \vec{\mu}_{pm}^* \rho_{pn}^H e^{i\omega_{np}t} \quad (2.20)$$

As an example, consider a three-level atomic system as shown in Figure 4. With the ground state defined by $m=0$, there are four combinations of n, p . The radiated power is then given by

$$P = \frac{4\omega_{10}^4 |\mu_{10}|^2}{3c^3} P_1 + \frac{4\omega_{20}^4 |\mu_{20}|^2}{3c^3} P_2 + \frac{4\omega_{20}^2 \omega_{10}^2}{3c^3} \left[\mu_{10} \cdot \mu_{20}^* \rho_{21}^H e^{i\omega_{12}t} + \mu_{20} \cdot \mu_{10}^* \rho_{12}^H e^{i\omega_{21}t} \right] \quad (2.21)$$

This clearly demonstrates the presence of a beat frequency ω_{21} , provided the upper states are coherently excited, $\rho_{21}^H \neq 0$.

For level crossings, specific characteristics of the radiation field as a function of the energy level separation are important. Generally, a change in the fluorescent intensity at a given observation point indicates the level crossing. To develop an expression for this, rewrite equation (2.11) as

$$S = \frac{(r^2 \delta_{ij} - x_i x_j)}{2\pi c^3 r^4} \langle \ddot{\mu}_i^{(-)} \cdot \ddot{\mu}_j^{(+)} \rangle \quad (2.22)$$

Using the expression for the dipole product in equation (2.18)

$$S = \frac{(r^2 \delta_{ij} - x_i x_j)}{2\pi c^3 r^4} \sum_{n, p > m} \omega_{nm}^2 \omega_{pm}^2 \mu_{nm}^i \cdot \mu_{pm}^{j*} \rho_{pn}(t) \quad (2.23)$$

Once again consider the three level atomic system shown in figure 4. As before the summation yields four terms. Assuming $\omega_{10} \approx \omega_{20} \approx \omega_0$,

$$S = \frac{(r^2 \delta_{ij} - x_i x_j)}{2\pi c^3 r^4} \omega_0^4 \left[\mu_{10}^i \mu_{10}^{j*} P_1 + \mu_{20}^i \mu_{20}^{j*} P_2 + \mu_{10}^i \mu_{20}^{j*} \rho_{21}(t) + \mu_{20}^i \mu_{10}^{j*} \rho_{12}(t) \right] \quad (2.24)$$

This describes the fluorescence as a function of position. It depends on the dipole moments and the density matrix.

To gain further insight, consider a relatively simple case of Zeeman splitting in the 2p states of hydrogen, specifically the $m = \pm 1$ states. The dipole moments for these states can be written [27]

$$\begin{aligned} \mu_{10} &= \mu_0(\mathbf{x} + i\mathbf{y}) \\ \mu_{20} &= \mu_0(\mathbf{x} - i\mathbf{y}) \end{aligned} \quad (2.25)$$

If the spontaneous emission rate is A for both states, the density matrix elements associated with the upper levels can be written as:

$$P_1 = P_2 = \frac{1}{2} \mu_0^2 Q^2 e^{-At} \quad (2.26a)$$

$$\rho_{12} = \rho_{21}^* = -\frac{1}{2} \mu_0^2 Q^2 e^{i\Lambda t - At} \quad (2.26b)$$

where Q is the time integral of the exciting pulse envelope divided by \hbar and Λ is the frequency corresponding to the energy difference between the excited states [28].

Using these equations in equation (2.24),

$$S = \frac{\omega_0^4 \mu_0^4 Q^2}{4 \pi c^3 r^2} e^{-At} [1 + \cos^2 \theta + \sin^2 \theta \cos(2\phi - \Lambda t)] \quad (2.27)$$

where θ and ϕ define the observation angle, in spherical coordinates.

A detector placed at a given angle will see an energy pulse whose total energy is defined by integrating equation (2.27) over time:

$$J = \frac{\omega_0^4 \mu_0^4 Q^2}{4 \pi c^3 r^2} \left[\frac{1 + \cos^2 \theta}{A} + \frac{\sin^2 \theta}{\Lambda^2 + A^2} (A \cos 2\phi + \Lambda \sin 2\phi) \right] \quad (2.28)$$

For the direction $\theta = \frac{\pi}{2}$, $\phi = 0$ this becomes

$$J = \frac{\omega_0^4 \mu_0^4 Q^2}{4 \pi c^3 r^2} \left[\frac{1}{A} + \frac{A}{\Lambda^2 + A^2} \right] \quad (2.29)$$

Figure 7 shows equation (2.29) as a function of the energy difference. There is a

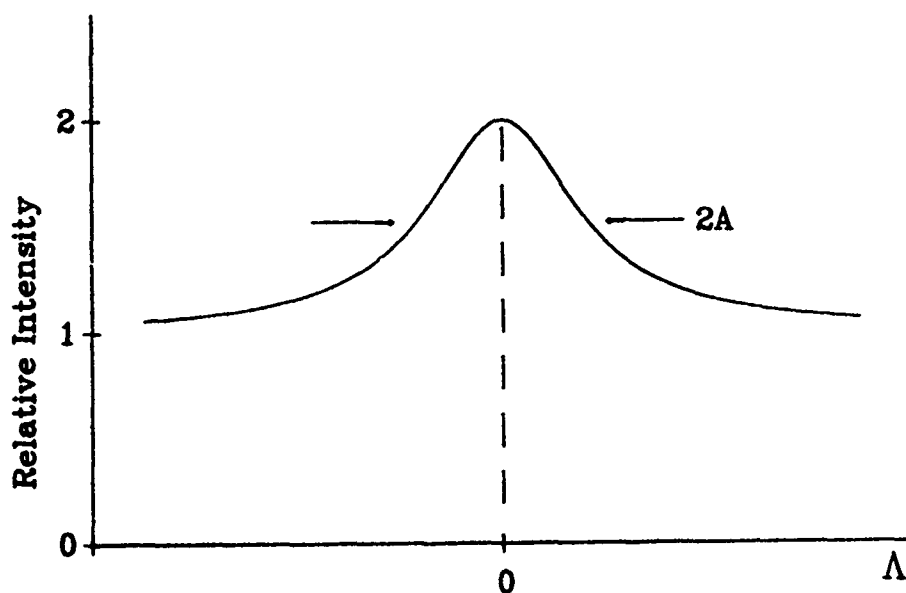


Figure 7. Fluorescent Intensity at Level Crossing. Crossing occurs at $\Lambda = 0$.

significant change in the observed fluorescence at $\Lambda = 0$. In addition, this has a narrow width, on the order of the natural linewidth ($\text{FWHM} = 2A$), making this technique potentially useful for high resolution spectroscopy.

The mathematical descriptions of quantum beats and level crossings in this section provide the necessary framework to address the effects of a nonresonant RF field on the atomic fluorescence. Equation (2.20) for quantum beats and equation (2.28) for level crossings describe signals as a function of the energy difference between the excited states. Similar expressions will be developed for the atom in an RF field, except that the energy difference will be a function of the field frequency due to the Townes–Merritt effect. The next section examines the Townes–Merritt effect using the Heisenberg operator formalism to describe the atomic dynamics.

III. QED Description of the Townes–Merritt Effect

To understand the impact of the Townes–Merritt effect on level crossings and quantum beats requires a reformulation of the Townes–Merritt description in terms of quantum electrodynamics (QED). It is convenient to use the Heisenberg operator formalism in developing a model to describe the effect. Initially, a two level atom in a resonant field is examined to gain insight in using the formalism. Then the case of the atom in a nonresonant field is discussed. Here the adiabatic approximation is introduced, which will be central in the description of level crossings and quantum beats. Combining the nonresonant field with a near resonant field, using the adiabatic approximation, results in a description of the Townes–Merritt effect. Two cases will be considered: a linear Stark shift of a single excited state and a quadratic Stark shift. A QED model is then developed, and the results compared to the adiabatic approach. This validates the adiabatic approach as a means to describe the atomic dynamics in a nonresonant field. As a final step, the dressed states model is used to describe the Townes–Merritt effect. The results further corroborate the adiabatic solution which will be used in level crossings and quantum beats.

Heisenberg Operator Formalism.

In the Heisenberg operator formalism the set of operators defined by

$$\hat{\sigma}_{ij} \equiv |i\rangle\langle j| \quad (3.1)$$

forms a complete operator basis, where $\hat{H}|i\rangle = E_i|i\rangle$. An arbitrary operator \hat{A} can then be described by

$$\hat{A} = \sum_{i,j} A_{ij} \hat{\sigma}_{ij} \quad (3.2)$$

where $A_{ij} \equiv \langle i | \hat{A}(0) | j \rangle$. In the Heisenberg picture, then, the $\hat{\sigma}$ operators obey the equation of motion

$$\dot{\hat{\sigma}}_{ij}^H = \frac{1}{i\hbar} [\hat{\sigma}_{ij}^H, \hat{H}] \quad (3.3)$$

with the initial condition $\hat{\sigma}_{ij}^H(0) = |i\rangle\langle j|$. Thus, the time evolution of any operator can be determined by solving for $\hat{\sigma}_{ij}^H(t)$, and the expectation value of the operator, which represents a physical observable, can be found by taking the expectation values of $\hat{\sigma}_{ij}^H$.

The $\hat{\sigma}$ operators exhibit useful mathematical properties. They are a closed set under multiplication

$$\hat{\sigma}_{ij} \hat{\sigma}_{nm} = \delta_{jn} \hat{\sigma}_{im} \quad (3.4)$$

which is useful in evaluating equations, such as commutation relations. The commutation rule for these operators is

$$[\hat{\sigma}_{ij}, \hat{\sigma}_{nm}] = \delta_{jn} \hat{\sigma}_{im} - \delta_{mi} \hat{\sigma}_{nj} \quad (3.5)$$

In addition, the Hamiltonian for an unperturbed atom can be represented by

$$\hat{H}_0 = \sum_n \hbar \omega_n \hat{\sigma}_{nn} \quad (3.6)$$

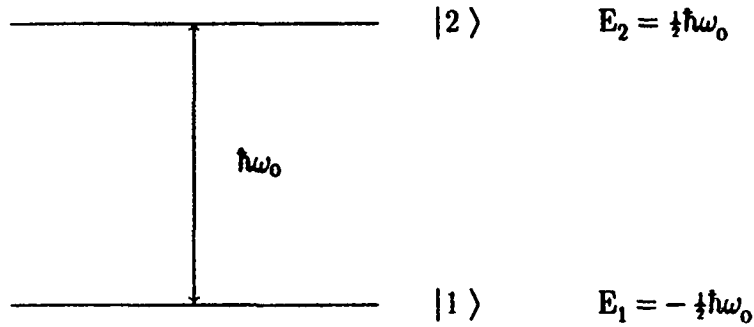


Figure 8. Two Level Atom

The time evolution of $\hat{\sigma}_{ij}^H$ is then given by

$$\dot{\hat{\sigma}}_{ij}^H(t) = i\omega_{ij}\hat{\sigma}_{ij}^H(0) \quad (3.7)$$

where $\omega_{ij} = \frac{E_i - E_j}{\hbar}$.

Consider now the two level atom with energy eigenstates shown in figure 8.

Define the $\hat{\sigma}$ operator basis in the following way:

$$\begin{aligned} \hat{\sigma} &\equiv |1\rangle\langle 2| \\ \hat{\sigma}_3 &\equiv |2\rangle\langle 2| - |1\rangle\langle 1| \end{aligned} \quad (3.8)$$

These two operators contain all the information for the two level atom. The unperturbed atomic Hamiltonian can be represented as $\hat{H}_0 = \frac{1}{2}\hbar\omega_0\hat{\sigma}_3$. In the electric dipole approximation, the interaction Hamiltonian for the atom in the electric field is given by

$$\hat{H}_1 = -\hat{\mu} \cdot \hat{E}(t) \quad (3.9)$$

The electric dipole approximation is valid when the E field spatial variation is negligible over the extent of the atom [8], which is the case here as the RF and optical wavelengths are large compared to the atomic diameter. The form of $\hat{\mu}$ and \hat{E} will define specific cases for the interaction. Initially consider the atomic levels to have definite parity and treat the E field classically. The dipole moment is then

$$\hat{\mu} = \begin{bmatrix} 0 & \mu \\ \mu & 0 \end{bmatrix} \epsilon = \mu(\hat{\sigma} + \hat{\sigma}^\dagger) \epsilon \quad (3.10)$$

where ϵ is the unit orientation vector. Let the electric field be classically prescribed in the form $\hat{E} = \mathcal{E} \cos \omega t$, which is oriented in the same direction as the atomic dipole. For a strong field this is reasonable as will be shown in the QED treatment. The total Hamiltonian is then

$$\hat{H} = \frac{1}{2} \hbar \omega_0 \hat{\sigma}_3 - \mu \mathcal{E} (\hat{\sigma} + \hat{\sigma}^\dagger) \cos \omega t \quad (3.11)$$

Using the Heisenberg equation of motion and the commutation relations for the $\hat{\sigma}$ operators,

$$\dot{\hat{\sigma}} = -i\omega_0 \hat{\sigma} - i\Omega \cos \omega t \hat{\sigma}_3 \quad (3.12a)$$

$$\dot{\hat{\sigma}}_3 = -i2\Omega \cos \omega t (\hat{\sigma} - \hat{\sigma}^\dagger) \quad (3.12b)$$

where $\Omega = \frac{\mu \mathcal{E}}{\hbar}$ is the Rabi frequency.

If the field frequency is close to the transition frequency, $\omega \approx \omega_0$, a near resonance condition exists. The first term on the right hand side of equation (3.12a) is the dominant term, so an approximate trial solution can be written

$$\hat{\sigma} = \hat{\mathcal{S}} e^{-i\omega_0 t} \quad (3.13)$$

where $\hat{\mathcal{S}}$ is slowly varying in time. Substitution into equations (3.12) yields

$$\dot{\hat{\mathcal{S}}} = -i\frac{\Omega}{2}(e^{i\omega t} + e^{-i\omega t})e^{i\omega_0 t} \hat{\sigma}_3 \quad (3.14a)$$

$$\dot{\hat{\sigma}}_3 = -i\Omega(e^{i\omega t} + e^{-i\omega t})(\hat{\mathcal{S}}e^{-i\omega_0 t} - \hat{\mathcal{S}}^\dagger e^{i\omega_0 t}) \quad (3.14b)$$

Since $\omega \approx \omega_0$, the terms with frequency of $\sim 2\omega_0$ can be ignored, as they are rapidly oscillating. These do not contribute significantly to the solution since they average to zero over a short time period, much less than the period of an observation. This is commonly referred to as the rotating wave approximation. Thus,

$$\dot{\hat{\mathcal{S}}} = -i\frac{\Omega}{2} e^{-i\Lambda t} \hat{\sigma}_3 \quad (3.15a)$$

$$\dot{\hat{\sigma}}_3 = -i\Omega(\hat{\mathcal{S}}e^{i\Lambda t} - \hat{\mathcal{S}}^\dagger e^{-i\Lambda t}) \quad (3.15b)$$

where $\Lambda \equiv \omega - \omega_0$ is the detuning.

Of particular interest is the on resonance case, when $\Lambda = 0$. Equations (3.15) can then be reduced to

$$\ddot{\hat{\sigma}}_3 = -\Omega^2 \hat{\sigma}_3 \quad (3.16)$$

A solution for the inversion operator, $\hat{\sigma}_3$, can easily be found, after taking the expectation value of equation (3.16):

$$\sigma_3(t) = \sigma_3(0) \sin(\Omega t + \phi) \quad (3.17)$$

This shows the Rabi oscillations at frequency Ω . The Rabi frequency depends directly on the field intensity, and a higher frequency indicates greater absorption.

In order to more precisely define the absorption rate, spontaneous emission needs to be considered. From a phenomenological argument [29], spontaneous emission can be included as additional terms in equations (3.12)

$$\dot{\hat{\sigma}} = -i\omega_0 \hat{\sigma} - i\Omega \cos \omega t \hat{\sigma}_3 - \frac{A}{2} \hat{\sigma} \quad (3.18a)$$

$$\dot{\hat{\sigma}}_3 = -i2\Omega \cos \omega t (\hat{\sigma} - \hat{\sigma}^\dagger) - A(\hat{\sigma}_3 + 1) \quad (3.18b)$$

Justification for these terms will be shown later in the QED section where the electric field is quantized.

Following an approach similar to the previous case, let $\hat{\sigma} = \hat{S}e^{-i\omega t}$. The equations of motion then become

$$\dot{\hat{S}} = i\Lambda \hat{S} - i\Omega \hat{\sigma}_3 - \frac{A}{2} \hat{S} \quad (3.19a)$$

$$\dot{\hat{\sigma}}_3 = -i\Omega(\hat{S} - \hat{S}^\dagger) - A(\hat{\sigma}_3 + 1) \quad (3.19b)$$

For steady state conditions, $\dot{\hat{S}} = \dot{\hat{\sigma}} = 0$, the solution for the expectation value of $\hat{\sigma}_3$ is

$$\sigma_3 = -\frac{\Lambda^2 + 4\Lambda^2}{\Lambda^2 + 4\Lambda^2 + 2\Omega^2} \quad (3.20)$$

The probability of being in the upper state is then

$$P_2 = \frac{1}{2}(1 + \sigma_3) = \frac{\Omega^2}{\Lambda^2 + 4\Lambda^2 + 2\Omega^2} \quad (3.21)$$

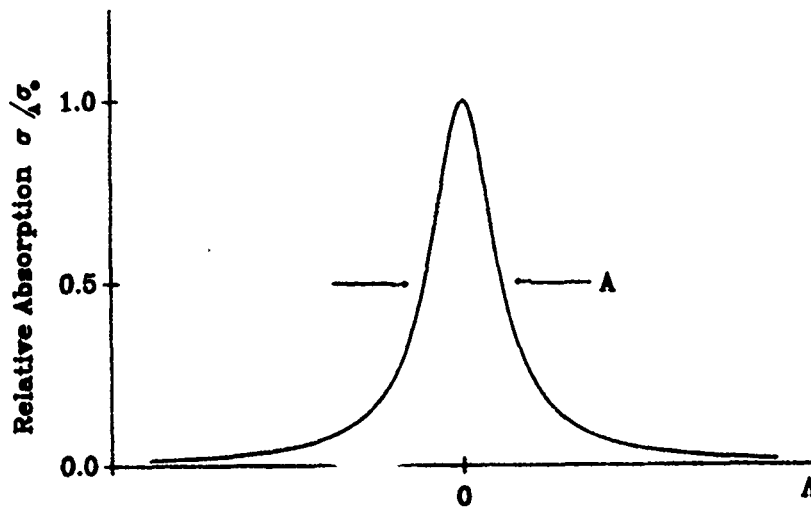


Figure 9. Absorption Cross-Section. The lineshape is Lorentzian, with a weak field width (FWHM) of A .

This is a Lorentzian function of width (FWHM) $\sqrt{A^2 + 2\Omega^2}$. The term $2\Omega^2$ represents power broadening. For weak field conditions, $A^2 \gg 2\Omega^2$, the probability of being in the upper state is directly proportional to Ω^2 . The absorption cross-section σ_A is equal to the rate of spontaneous emission, AP_2 , divided by the incident photon flux density $\frac{I}{\hbar\omega}$. I is the light intensity which can be expressed as $I = \frac{c\mathcal{E}^2}{8\pi}$. Thus,

$$\sigma_A = \frac{\hbar\omega AP_2}{I} = \frac{8\pi\omega A\mu^2}{\hbar c[A^2 + 4\Omega^2 + 2\Omega^2]} \quad (3.22)$$

where $\Omega^2 = \frac{\mu^2 \mathcal{E}^2}{\hbar^2}$. Figure 9 shows the absorption cross-section as a function of the detuning Δ . The A coefficient can be expressed as $A = \frac{4\mu^2\omega_0^3}{3\hbar c^3}$, so for a weak field the peak is $\sigma_0 = 6\pi\frac{c^2}{\omega_0^2}$.

Adiabatic Approximation

The Townes-Merritt effect occurs when there are two electric fields present, one nonresonant which will be referred to as the RF field and one resonant probe

field with a frequency near the transition frequency, $\omega \approx \omega_0$. The RF field frequency ν is much less than the transition frequency. The Hamiltonian is then

$$\hat{H} = \hat{H}_0 - \hat{\mu} \cdot \hat{E}_\nu - \hat{\mu} \cdot \hat{E}_0 \quad (3.23)$$

To find a solution describing the atomic dynamics, first consider only the effect of the RF field on the atom. Since it is far off resonance and is slowly varying as compared to the transition frequency, the adiabatic approximation is useful [8,30]. Here the instantaneous energy eigenstates form a convenient basis set:

$$\hat{H}_A(t) |n(t)\rangle = E_n(t) |n(t)\rangle \quad (3.24)$$

where $\hat{H}_A(t) = \hat{H}_0 - \hat{\mu} \cdot \hat{E}_\nu$. The physical interpretation of this approach is that as the RF field changes, the eigenstates evolve adiabatically with the field. The state $|n(0)\rangle$ at time zero, with field strength zero, will evolve to a state $|n(t)\rangle$ at time t that is Stark shifted by the field $E(t)$. Since the RF frequency is far off resonance, it is reasonable to assume no transitions occur. Additionally, these eigenstates remain orthonormal throughout. The total wave function is written as

$$|\psi(t)\rangle = \sum_n a_n |n(t)\rangle e^{-\frac{i}{\hbar} \int_0^t E_n(t') dt'} \quad (3.25)$$

This approach is valid so long as \dot{a}_n , which represents transitions, is small.

As stated, the adiabatic approximation is useful for cases in which the Hamiltonian changes slowly in time, in comparison to the atomic dynamics. This is just the case for the atom in an RF field when the frequency ν is much less than the

transition frequency ω_{ij} . In the adiabatic treatment, the energy eigenstates and eigenvalues are smooth functions of time which change in a continuous manner with the Hamiltonian satisfying the 'time independent' wave equation (3.24).

Of particular interest is the Heisenberg equation of motion for $\hat{\sigma}_{ij}^H \equiv |i(t)\rangle\langle j(t)|$. In the adiabatic approach, the equation of motion will be approximated as

$$\dot{\hat{\sigma}}_{ij}^H \approx i\omega_{ij}(t) \hat{\sigma}_{ij}^H \quad (3.26)$$

The additional terms will be small and rapidly oscillating, such that they do not contribute to the evolution of the states from which physical transitions occur.

Conversion to the Heisenberg picture is defined by a unitary transformation $\hat{U}(t)$ which satisfies

$$|\psi(t)\rangle = \hat{U}(t)|\psi(0)\rangle \quad (3.27)$$

where $|\psi\rangle$ is the solution to the Schrödinger wave equation. Substituting equation (3.27) into the wave equation

$$i\hbar \frac{\partial |\psi(t)\rangle}{\partial t} = i\hbar \frac{\partial \hat{U}(t)}{\partial t} |\psi(0)\rangle = \hat{H}(t) \hat{U}(t) |\psi(0)\rangle \quad (3.28)$$

From this, the time dependence of \hat{U} can be seen:

$$\dot{\hat{U}}(t) = \frac{1}{i\hbar} \hat{H}(t) \hat{U}(t) \quad (3.29)$$

An operator is defined in the Heisenberg picture by

$$\hat{A}^H = \hat{U}^\dagger \hat{A}^S \hat{U} \quad (3.30)$$

Now Take the derivative and use equation (3.29) to get

$$\begin{aligned} \dot{\hat{A}}^H &= \dot{\hat{U}}^\dagger \hat{A}^S \hat{U} + \hat{U}^\dagger \dot{\hat{A}}^S \hat{U} + \hat{U}^\dagger \hat{A}^S \dot{\hat{U}} \\ &= \frac{1}{i\hbar} [\hat{A}^H, \hat{H}] + \frac{\partial \hat{A}^H}{\partial t} \end{aligned} \quad (3.31)$$

where the last term is defined as $\frac{\partial \hat{A}^H}{\partial t} \equiv \dot{\hat{U}}^\dagger \hat{A}^S \hat{U}$, which arises if \hat{A}^S has an explicit time dependence. This then is the equation of motion for any operator in the Heisenberg picture.

For $\hat{\sigma}_{ij}^H$, using equation (3.24), the equation of motion becomes

$$\dot{\hat{\sigma}}_{ij}^H = i\omega_{ij}(t)\hat{\sigma}_{ij}^H + \frac{\partial \hat{\sigma}_{ij}^H}{\partial t} \quad (3.32)$$

where $\omega_{ij}(t) = \frac{E_i(t) - E_j(t)}{\hbar}$. An expression for the last term can be developed by first finding

$$\frac{\partial \hat{\sigma}_{ij}}{\partial t} = |\dot{i}\rangle \langle j| + |i\rangle \langle \dot{j}| \quad (3.33)$$

Using the identity operator

$$\begin{aligned} \frac{\partial \hat{\sigma}_{ij}}{\partial t} &= \sum_k |k\rangle \langle k|\dot{i}\rangle \langle j| + \sum_m |i\rangle \langle j|m\rangle \langle m|\dot{} \\ &= \sum_k \langle k|i\rangle \dot{\sigma}_{kj} + \sum_m \langle j|m\rangle \dot{\sigma}_{im} \end{aligned} \quad (3.34)$$

Now an expression for the inner products is found by differentiating equation (3.24)

$$\frac{\partial \hat{H}}{\partial t} |i\rangle + \hat{H} |i\rangle = \frac{\partial E_i}{\partial t} |i\rangle + E_i |i\rangle \quad (3.35)$$

Then multiply by $\langle k|$, where $k \neq i$

$$\langle k|i\rangle = \frac{\langle k|\frac{\partial \hat{H}}{\partial t}|i\rangle}{\hbar\omega_{ik}} \quad (3.36)$$

For $k = i$, $\langle i|i\rangle = 1$ since $\langle i|i\rangle = 1$. Thus,

$$\frac{\partial \hat{\sigma}_{ii}^H}{\partial t} = \sum_{k \neq i} \frac{\langle k|\frac{\partial \hat{H}}{\partial t}|i\rangle}{\hbar\omega_{ik}} \hat{\sigma}_{kj}^H + \sum_{m \neq j} \frac{\langle j|\frac{\partial \hat{H}}{\partial t}|m\rangle}{\hbar\omega_{jm}} \hat{\sigma}_{im}^H \quad (3.37)$$

If the RF field is written as $E(t) = \mathcal{E} \cos \nu t$, then

$$\frac{\partial \hat{H}}{\partial t} = -\hat{\mu} \cdot \frac{\partial E(t)}{\partial t} = \hat{\mu} \cdot \mathcal{E} \nu \sin \nu t \quad (3.38)$$

The equation of motion then becomes

$$\dot{\hat{\sigma}}_{ij}^H = i\omega_{ij}(t) \hat{\sigma}_{ij}^H + \sum_{k \neq i} \frac{\mu_{ki} \cdot \mathcal{E}}{\hbar\omega_{ik}} \nu \sin \nu t \hat{\sigma}_{kj}^H + \sum_{m \neq j} \frac{\mu_{jm} \cdot \mathcal{E}}{\hbar\omega_{jm}} \nu \sin \nu t \hat{\sigma}_{im}^H \quad (3.39)$$

The first term on the right hand side is the dominant term, which is seen by comparing magnitudes of the coefficients.

$$\left| \frac{\Omega_{ki} \nu}{\omega_{ik}} \right| \ll |\omega_{ij}| \quad (3.40)$$

where $\Omega_{ki} = \frac{\mu_{ki} \cdot \mathcal{E}}{\hbar}$ is the Rabi frequency, and is typically less than ν . This is the condition of validity for the adiabatic approximation [30]. As a result, an approximate solution for $\hat{\sigma}_{ij}^H(t)$ can be written

$$\hat{\sigma}_{ij}^H(t) = \hat{S}_{ij}(t) e^{i\omega_{ij}^0 t} \quad (3.41)$$

where \hat{S}_{ij} is a slowly varying function and ω_{ij}^0 is the unperturbed transition frequency. Substituting this into equation (3.39)

$$\begin{aligned} \dot{\hat{S}}_{ij} = & i[\omega_{ij}(t) - \omega_{ij}^0] \hat{S}_{ij} + \sum_{k \neq i} \frac{\Omega_{ki} \nu \sin \nu t}{\omega_{ik}} \hat{S}_{kj} e^{i\omega_{ki} t} \\ & + \sum_{m \neq j} \frac{\Omega_{jm} \nu \sin \nu t}{\omega_{jm}} \hat{S}_{im} e^{i\omega_{jm} t} \end{aligned} \quad (3.42)$$

Notice that all terms in the summations have frequencies of order $\omega_{ki} \pm \nu$. Since $\nu \ll \omega_{ki}$, these terms are all rapidly oscillating and can be neglected. The result is that the terms arising from $\frac{\partial \hat{\sigma}_{ij}^H}{\partial t}$ can be ignored in the equation of motion, which can then be approximated as $\dot{\hat{\sigma}}_{ij}^H \approx i\omega_{ij}(t) \hat{\sigma}_{ij}^H$ for the atom in an RF field. The solution takes the form

$$\hat{\sigma}_{ij}^H(t) = \hat{\sigma}_{ij}^H(0) e^{i \int_0^t \omega_{ij}(t') dt'} \quad (3.43)$$

This result will be most useful in describing the atomic dynamics in a nonresonant field. When a near resonant field is added, the Townes-Merritt effect results. For level crossings and quantum beats spontaneous emission is considered. But in all cases, evaluation of equation (3.43) for a specific set of energy states is central.

Townes-Merritt Effect

The adiabatic approximation defined a set of energy eigenstates for the atom in an RF field. Application of a near resonant field will now cause transitions to occur between the energy states. These transitions will occur not only at the fundamental frequency, but also at frequencies shifted by integer multiples of the RF frequency; this is the Townes-Merritt effect. The analysis here is very similar to that of an atom in a resonant field, except in this case the energy states are the instantaneous eigenstates from the adiabatic approach.

Consider the two level system depicted in figure 8. An exact solution exists for the energy states when an RF field is applied [27]:

$$|1\rangle = \begin{bmatrix} \cos \theta \\ -\sin \theta \end{bmatrix} \quad |2\rangle = \begin{bmatrix} \sin \theta \\ \cos \theta \end{bmatrix} \quad (3.44)$$

where $\tan 2\theta = -\frac{\Omega_v}{\omega_0} \cos \nu t$. This assumes a quadratic Stark shift, the linear case will be covered later. Note that since usually $\Omega_v \ll \omega_0$, values of θ will typically be small, the new states will be approximately the same as the original. The instantaneous energy levels are

$$E_{\pm} = \pm \frac{\hbar}{2} [\omega_0^2 + 4\Omega_v^2 \cos^2 \nu t]^{\frac{1}{2}} \quad (3.45)$$

where the plus and minus refer to the upper and lower states respectively. The instantaneous frequency difference is then given by

$$\omega'(t) = \frac{E_+ - E_-}{\hbar} = [\omega_0^2 + 4\Omega_v^2 \cos^2 \nu t]^{\frac{1}{2}} \quad (3.46)$$

In the Heisenberg operator formalism the σ operators will be defined by these

adiabatic states such that,

$$\hat{\sigma}_{ij}(t) \equiv |i(t)\rangle \langle j(t)| \quad (3.47)$$

and their time evolution will in turn define the atomic dynamics.

The Hamiltonian of equation (3.23) can be rewritten as $\hat{H} = \hat{H}_A + \hat{H}_\omega$, where the interaction with the resonant field is given by $\hat{H}_\omega = -\mu\mathcal{E} \cos \omega t$. The Heisenberg equation of motion for the σ operators is then

$$\dot{\hat{\sigma}}_{ij} = \frac{1}{i\hbar} [\hat{\sigma}_{ij}, \hat{H}_A + \hat{H}_\omega] = i\omega_{ij}(t)\hat{\sigma}_{ij} + \frac{1}{i\hbar} [\hat{\sigma}_{ij}, \hat{H}_\omega] \quad (3.48)$$

where the \hbar superscripts for the Heisenberg picture have been dropped. Now consider the case of the two level atom with σ operator defined by equations (3.8):

$$\dot{\hat{\sigma}} = -i\omega'(t) \hat{\sigma} - i\Omega_\omega \cos \omega t \hat{\sigma}_3 \quad (3.49a)$$

$$\dot{\hat{\sigma}}_3 = -i2\Omega_\omega \cos \omega t (\hat{\sigma} - \hat{\sigma}^\dagger) \quad (3.49b)$$

These equations are very similar to the case of only the resonant interaction except for the time dependence of ω' . The solution follows much the same approach.

Assume

$$\hat{\sigma}(t) = \hat{S}(t) e^{i \int_0^t \omega'(t') dt'} \quad (3.50)$$

This is reasonable since, in equation (3.49a), $-i\omega'(t)\hat{\sigma}$ is the major contributing term. Substituting the assumed solution into the equation of motion and discarding

the rapidly oscillating terms (rotating wave approximation), one obtains

$$\dot{\hat{S}} = -\frac{\Omega}{2} e^{-i \int_0^t \dot{\Lambda}(t') dt'} \hat{\sigma}_3 \quad (3.51a)$$

$$\dot{\hat{\sigma}}_3 = -i\Omega_{\omega} \left[\hat{S} e^{i \int_0^t \dot{\Lambda}(t') dt'} - \hat{S}^\dagger e^{-i \int_0^t \dot{\Lambda}(t') dt'} \right] \quad (3.51b)$$

where $\Lambda(t) \equiv \omega - [\omega_0^2 + 4\Omega_{\nu}^2 \cos^2 \nu t]^{1/2}$. First consider the exponential terms,

$$e^{i \int_0^t \dot{\Lambda}(t') dt'} = e^{i \int_0^t \omega - [\omega_0^2 + 4\Omega_{\nu}^2 \cos^2 \nu t']^{1/2} dt'} \quad (3.52)$$

Since $\Omega_{\nu} \ll \omega_0$,

$$[\omega_0^2 + 4\Omega_{\nu}^2 \cos^2 \nu t]^{1/2} \approx \omega_0 + \frac{2\Omega_{\nu}^2}{\omega_0} \cos^2 \nu t + \dots \quad (3.53)$$

Ignoring higher order terms leads to

$$\int_0^t (\omega_0 + \frac{2\Omega_{\nu}^2}{\omega_0} \cos^2 \nu t') dt' = \omega_0 t + \frac{\Omega_{\nu}^2}{\omega_0} t + \frac{\Omega_{\nu}^2}{2\omega_0 \nu} \sin 2\nu t \quad (3.54)$$

An exponential term with a sine argument can be expanded as a Bessel function series:

$$e^{-i \frac{\Omega_{\nu}^2}{2\omega_0 \nu} \sin 2\nu t} = \sum_{n=-\infty}^{\infty} J_n \left(\frac{\Omega_{\nu}^2}{2\omega_0 \nu} \right) e^{-i 2n \nu t} \quad (3.55)$$

The exponential then becomes

$$e^{i \int_0^t \Lambda(t') dt'} = \sum_n J_n\left(\frac{\Omega_v^2}{2\omega_0\nu}\right) e^{i(\omega - \omega_0 - \frac{\Omega_v^2}{\omega_0} - 2n\nu)t} \quad (3.56)$$

Now consider an on resonance case where

$$\omega \approx \omega_m \equiv \omega_0 + \frac{\Omega_v^2}{\omega_0} + 2m\nu \quad (3.57)$$

Then,

$$e^{i \int_0^t \Lambda(t') dt'} = \sum_n J_n\left(\frac{\Omega_v^2}{2\omega_0\nu}\right) e^{i2(m-n)\nu t} \quad (3.58)$$

Similarly,

$$e^{-i \int_0^t \Lambda(t') dt'} = \sum_n J_n\left(\frac{\Omega_v^2}{2\omega_0\nu}\right) e^{-i2(m-n)\nu t} \quad (3.59)$$

The equations of motion become

$$\dot{\hat{S}} = -i\frac{\Omega_\omega}{2} \hat{\sigma}_3 \sum_n J_n\left(\frac{\Omega_v^2}{2\omega_0\nu}\right) e^{i2(m-n)\nu t} \quad (3.60a)$$

$$\dot{\hat{\sigma}}_3 = -i\Omega_\omega \left[\hat{S} \sum_n J_n\left(\frac{\Omega_v^2}{2\omega_0\nu}\right) e^{-i2(m-n)\nu t} - \hat{S}^\dagger \sum_n J_n\left(\frac{\Omega_v^2}{2\omega_0\nu}\right) e^{-i2(m-n)\nu t} \right] \quad (3.60b)$$

For the case of interest the RF frequency is much greater than the Rabi frequency, $\nu \gg \Omega_\omega$, so that power broadening does not cause individual sidebands to overlap. For a similar reason, the RF field frequency must be greater than the natural linewidth, $\nu \gg \Lambda$. Since the operators evolve at the frequency Ω_ω , the only contributing factors in the expansion series is for $m = n$; the others rapidly average to zero. This is the equivalent of the rotating wave approximation. Thus, the equations of motion become

$$\dot{\hat{S}} = -\frac{\Omega_{\omega}}{2} J_m\left(\frac{\Omega_{\nu}^2}{2\omega_0\nu}\right) \hat{\sigma}_3 \quad (3.61a)$$

$$\dot{\hat{\sigma}}_3 = -i\Omega_{\omega} J_m\left(\frac{\Omega_{\nu}^2}{2\omega_0\nu}\right) [\hat{S} - \hat{S}^{\dagger}] \quad (3.61b)$$

These are similar to the previous case without the RF field, equations (3.16), except for the Bessel function coefficients. With a zero RF field strength, they revert to the earlier form. The solution for the inversion operator $\hat{\sigma}_3$ is

$$\hat{\sigma}_3 = \hat{\sigma}_3(0) \sin[J_m\left(\frac{\Omega_{\nu}^2}{2\omega_0\nu}\right) \Omega_{\omega}t + \phi] \quad (3.62)$$

Again, this shows Rabi oscillations at frequency $J_m\Omega_{\omega}$ reflecting the relative absorption strength of the sidebands. The result agrees with the original Townes-Merritt calculation for a quadratic Stark shift. The absorption occurs at frequencies $\omega_m \equiv \omega_0 + \frac{\Omega_{\nu}^2}{\omega_0} + 2m\nu$, with relative intensity $J_m^2\left(\frac{\Omega_{\nu}^2}{2\omega_0\nu}\right)$.

To include the effects of spontaneous emission, consider a more general case of the equations of motion where the incident radiation is slightly off resonance:

$$\dot{\hat{S}} = -i\frac{\Omega_{\omega}}{2} e^{-i\int_0^t \Lambda(t') dt'} \hat{\sigma}_3 - \frac{A}{2} \hat{S} \quad (3.63a)$$

$$\dot{\sigma}_3 = -i\Omega_{\omega} \left[\hat{S} e^{i\int_0^t \Lambda(t') dt'} - \hat{S}^{\dagger} e^{-i\int_0^t \Lambda(t') dt'} \right] - A(\hat{\sigma}_3 + 1) \quad (3.63b)$$

where again $\Lambda(t) \equiv \omega - [\omega_0^2 + 4\Omega_{\nu}^2 \cos^2 \nu t]^{\frac{1}{2}}$. Now let $\omega = \omega_0 + \frac{\Omega_{\nu}^2}{\omega_0} + 2m\nu + \Delta\omega$,

where $\Delta\omega$ is small, describing the condition where ω is slightly detuned from the m sideband. The exponential terms can be expanded similar to the Following the

development of equation (3.59), which results in

$$e^{\pm i \int_0^t \Lambda(t') dt'} = e^{\pm i \Delta \omega t} \sum_n J_n\left(\frac{\Omega_p^2}{2\omega_0\nu}\right) e^{\pm i 2(m-n)\nu t} \quad (3.64)$$

Elimination of all terms in the expansion except for $m = n$, results in

$$\dot{\hat{S}} = -i\frac{\Omega_p}{2} J_m\left(\frac{\Omega_p^2}{2\omega_0\nu}\right) \hat{\sigma}_3 e^{-i\Delta\omega t} - \frac{A}{2} \hat{S} \quad (3.65a)$$

$$\dot{\hat{\sigma}}_3 = -i\Omega_p J_m\left(\frac{\Omega_p^2}{2\omega_0\nu}\right) [\hat{S} e^{i\Delta\omega t} - \hat{S}^\dagger e^{-i\Delta\omega t}] - A(\hat{\sigma}_3 + 1) \quad (3.65b)$$

To remove the remaining exponential terms, let $\hat{S} = \hat{S}' e^{-i\Delta\omega t}$. The equations of motion for the expectation values are then

$$\dot{S}' = i\Delta\omega S' - i\frac{\Omega_p}{2} J_m\left(\frac{\Omega_p^2}{2\omega_0\nu}\right) \sigma_3 - \frac{A}{2} S' \quad (3.66a)$$

$$\dot{\sigma}_3 = -i\Omega_p J_m\left(\frac{\Omega_p^2}{2\omega_0\nu}\right) [S' - S'^*] - A(\sigma_3 + 1) \quad (3.66b)$$

The steady state solution for the inversion operator is

$$\sigma_3 = -\frac{A^2 + 4\Delta\omega^2}{A^2 + 4\Delta\omega^2 + 2\Omega_p^2 J_m^2} \quad (3.67)$$

This result is similar to that without the RF field, equation (3.20). The only difference is the Bessel function term $J_m^2\left(\frac{\Omega_p^2}{2\omega_0\nu}\right)$ which serves to determine the relative strengths of the sidebands. For $\Omega_p = 0$, $J_m(0) = \delta_{0m}$ and the equation reverts to the non-RF case.

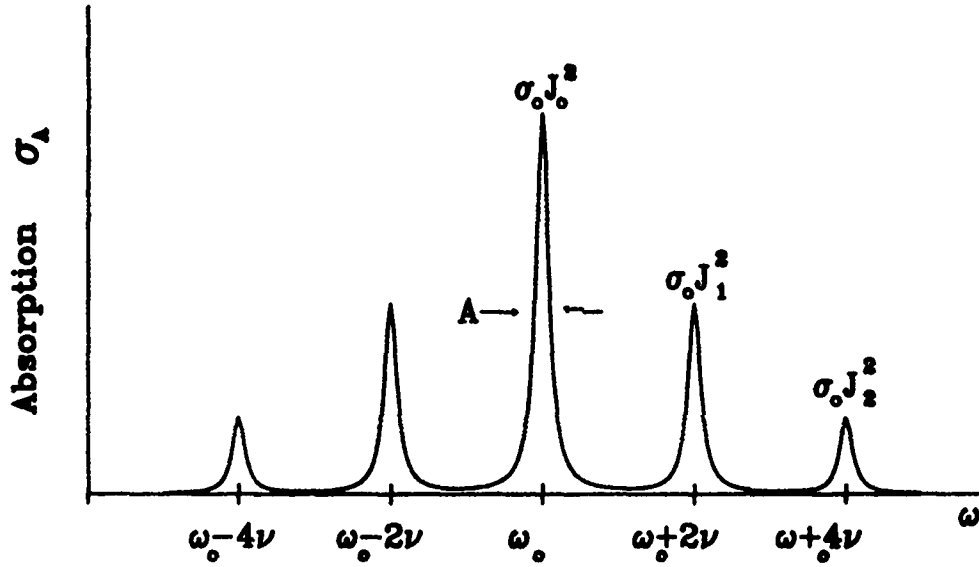


Figure 10. Absorption cross-section for an atom in a nonresonant field of frequency ν .

The absorption spectrum consists of a series of peaks separated by 2ν . Near each peak the probability of being in the upper state is given by

$$P_2 = \frac{1}{2}(1 + \sigma_3) = \frac{\Omega^2 J_m^2}{A^2 + 4\Delta\omega^2 + 2\Omega_\omega^2 J_m^2} \quad (3.68)$$

where $\Delta\omega$ is the local detuning. From equation (3.22), the absorption cross-section is

$$\sigma_A = \frac{8\pi\omega A \mu^2 J_m^2}{\hbar c [A^2 + 4\Delta\omega^2 + 2\Omega_\omega^2 J_m^2]} \quad (3.69)$$

Each peak is a Lorentzian function centered at $\omega = \omega_0 + \frac{\Omega_\nu^2}{\omega_0} + 2m\nu$, having a linewidth (FWHM) $\sqrt{A^2 + 2\Omega_\omega^2 J_m^2}$. For a weak field, $\Omega^2 \ll A^2$, the individual absorption peaks are $\sigma_0 J_m^2$, where σ_0 is the peak absorption in the non RF case. The spectrum is shown in figure 10, which shows the expected absorption sidebands. This agrees with the original Townes-Merritt analysis [2,7].

The case for the linear Stark shift is very similar to the quadratic case, except the calculation for the instantaneous energy states is much simpler, as will be shown. Recall, the Hamiltonian for the atom in an RF field is

$$\hat{H}_A = \frac{1}{2}\hbar\omega_0\hat{\sigma}_3 - \hat{\mu} \cdot \hat{E}_\nu \quad (3.70)$$

For a linear shift, the interaction term can be written

$$\hat{\mu} \cdot \hat{E}_\nu = \begin{bmatrix} \mu_{11} & 0 \\ 0 & \mu_{22} \end{bmatrix} \mathcal{E} \cos \nu t \quad (3.71)$$

To determine the energy levels, let $\hat{H}_A |n\rangle = E_n |n\rangle$, which results in

$$E_1 = -\frac{1}{2}\hbar\omega_0 - \mathcal{E}\mu_{11} \cos \nu t \quad (3.72a)$$

$$E_2 = \frac{1}{2}\hbar\omega_0 - \mathcal{E}\mu_{22} \cos \nu t \quad (3.72b)$$

The instantaneous transition frequency is then

$$\omega'(t) = \omega_0 - \Omega_\nu \cos \nu t \quad (3.73)$$

where $\Omega_\nu \equiv \frac{(\mu_{22} - \mu_{11})}{\hbar}$.

As in the previous case, when a probe beam is turned on, the equations of motion for the Heisenberg operators become

$$\dot{\hat{\sigma}} = -i\omega'(t) \hat{\sigma} - i\Omega_\nu \cos \omega t \hat{\sigma}_3 \quad (3.74a)$$

$$\dot{\hat{\sigma}}_3 = -i2\Omega_\nu \cos \omega t (\hat{\sigma} - \hat{\sigma}^\dagger) \quad (3.74b)$$

The solution is similar to the previous case. Define $\Lambda(t) = \omega - \omega_0 + \Omega_\nu \cos \nu t$, then

$$e^{i \int_0^t \Lambda(t') dt'} = \sum_{n=-\infty}^{\infty} J_n\left(\frac{\Omega_\nu}{\nu}\right) e^{i(\omega - \omega_0 + n\nu)t} \quad (3.75)$$

Let $\omega \approx \omega_0 - m\nu$, and consider only terms where $n = m$:

$$\dot{\hat{S}} = -\frac{\Omega_\omega}{2} J_m\left(\frac{\Omega_\nu}{\nu}\right) \hat{\sigma}_3 \quad (3.76a)$$

$$\dot{\hat{\sigma}}_3 = -\Omega_\omega J_m\left(\frac{\Omega_\nu}{\nu}\right) [\hat{S} - \hat{S}^\dagger] \quad (3.76b)$$

This reduces to $\ddot{\hat{\sigma}}_3 = -\Omega_\omega^2 J_m^2\left(\frac{\Omega_\nu}{\nu}\right) \hat{\sigma}_3$, and the solution can be expressed as

$$\hat{\sigma}_3 = \hat{\sigma}_3(0) \sin[J_m\left(\frac{\Omega_\nu}{\nu}\right) \Omega_\omega t + \phi] \quad (3.77)$$

This differs from the result in the quadratic case by the Bessel function argument and that the transitions occur for every integer multiple of the RF frequency ν with no static shift, instead of just the even harmonics. The expression for steady state absorption in the linear case is the same as equation (3.69) except again the Bessel function term has a different argument. The relative strength of the absorption sidebands is given by $J_m^2\left(\frac{\Omega_\nu}{\nu}\right)$.

The descriptions of the Townes–Merritt effect derived using the Heisenberg operator formalism and the adiabatic approximation agree exactly with previous published approaches and experimental results [2,26]. This gives a great deal of credibility to the approach, which will be used to describe level crossings and quantum beats. But before moving on to those subject, it is important to consider a quantum electrodynamic analysis of the Townes–Merritt effect.

Quantum Electrodynamic Treatment

In the previous section, spontaneous emission was included based on a phenomenological argument. A more rigorous approach involves quantization of the radiation field. This QED approach gives stronger justification for the spontaneous emission terms, and provides a more accurate representation of the atom-field system. Recall, that level crossings and quantum beats result from QED effects. It will be shown, however, that for a strong, classical-like field the QED description of the Townes-Merritt effect agrees with the Heisenberg operator approach presented.

The Hamiltonian for the atom-field system in QED is

$$\hat{H} = \frac{1}{2}\hbar\omega_0\hat{\sigma}_3 + \sum_{\mathbf{k},\lambda} \hbar\omega_{\mathbf{k}}\hat{a}_{\mathbf{k}\lambda}^{\dagger}\hat{a}_{\mathbf{k}\lambda} - \hat{\boldsymbol{\mu}} \cdot \hat{\mathbf{E}} \quad (3.78)$$

The first term is the Hamiltonian for the isolated atom. The second represents the electromagnetic field where $\hat{a}_{\mathbf{k}\lambda}^{\dagger}$ and $\hat{a}_{\mathbf{k}\lambda}$ are the creation and destruction operators. The third term is the interaction Hamiltonian in which the electric field is now quantized. In the Townes-Merritt effect, the electric field consists of the nonresonant RF field and a near resonant probe beam:

$$\hat{\mathbf{E}} = \hat{\mathbf{E}}_{\nu} + \hat{\mathbf{E}}_{\omega} \quad (3.79)$$

First consider the atom and the RF field. Following the adiabatic approach, define a set of basis states which satisfy the equation

$$\hat{H}_A |n(t)\rangle = E_n(t) |n(t)\rangle \quad (3.80)$$

where $\hat{H}_A = \frac{1}{2}\hbar\omega_0\hat{\sigma}_3 - \hat{\boldsymbol{\mu}} \cdot \hat{\mathbf{E}}_{\nu}$, as before. These states are the instantaneous energy

eigenstates of the atom in the RF field, which adiabatically follow the relatively slowly changing field. In the Townes–Merritt effect, the RF field is sufficiently strong that \hat{E}_ν can be treated. Thus, expressions for the energy states and values would agree with those previously developed. Also recall, in the adiabatic approximation, the equation of motion for $\hat{\sigma}_{ij}$ is

$$\dot{\hat{\sigma}}_{ij} = \frac{1}{\hbar} [\hat{\sigma}_{ij}, \hat{H}_A] = i\omega_{ij}(t) \hat{\sigma}_{ij} \quad (3.81)$$

Here the H superscript for the Heisenberg picture has been dropped for simplicity.

Adding the probe field, \hat{E}_ω , the equation of motion becomes

$$\dot{\hat{\sigma}}_{ij} = \frac{1}{\hbar} [\hat{\sigma}_{ij}, \hat{H}] = i\omega_{ij}(t) \hat{\sigma}_{ij} - \frac{1}{\hbar} [\hat{\sigma}_{ij}, \hat{\mu} \cdot \hat{E}_\omega] \quad (3.82)$$

The operator $\hat{\sigma}_{ij}$ commutes with the \hat{a} and \hat{a}^\dagger operators so the electromagnetic field term of the Hamiltonian has no impact on the equation of motion. To derive an expansion for the remaining commutator relation, recall $\hat{\mu} = \mu(\hat{\sigma} + \hat{\sigma}^\dagger)$. Also for the two level system, use

$$\hat{\sigma} = |1\rangle\langle 2| \quad (3.83a)$$

$$\hat{\sigma}_3 = |2\rangle\langle 2| - |1\rangle\langle 1| \quad (3.83b)$$

as the $\hat{\sigma}$ basis set. The equations of motion are then

$$\dot{\hat{\sigma}} = -i\omega'(t) \hat{\sigma} - \frac{i}{\hbar} \mu \cdot \hat{E}_\omega \hat{\sigma}_3 \quad (3.84a)$$

$$\dot{\hat{\sigma}}_3 = -\frac{2}{\hbar} (\hat{\sigma} - \hat{\sigma}^\dagger) \mu \cdot \hat{E}_\omega \quad (3.84b)$$

where $\omega(t) = \frac{E_2(t) - E_1(t)}{\hbar}$. The total field \hat{E}_ω commutes with the atomic operators since it is a function of \hat{a} and \hat{a}^\dagger .

The electric field \hat{E}_ω can be separated into free field and source field terms:

$$\hat{E}_\omega = \hat{E}_0 + \hat{E}_s \quad (3.85)$$

The free field term represents incident electromagnetic radiation. The source field results from the radiation reaction field of the atom. These terms can be further separated into positive and negative frequency components, after Glauber [24]:

$$\hat{E} = \hat{E}^{(+)} + \hat{E}^{(-)} \quad (3.86)$$

This is easily seen in the quantized expression for the free field:

$$\hat{E}_0 = \sum_{\mathbf{k}, \lambda} \left[\frac{2\pi\hbar\omega_{\mathbf{k}}}{V} \right]^{\frac{1}{2}} \left[\epsilon_{\mathbf{k}\lambda} \hat{a}_{\mathbf{k}\lambda} e^{i(\mathbf{k} \cdot \mathbf{x} - \omega_{\mathbf{k}} t)} + \epsilon_{\mathbf{k}\lambda} \hat{a}_{\mathbf{k}\lambda}^\dagger e^{-i(\mathbf{k} \cdot \mathbf{x} - \omega_{\mathbf{k}} t)} \right] \quad (3.87)$$

where the first term with \hat{a} is $\hat{E}_0^{(+)}$ and the second term $\hat{E}_0^{(-)}$. Before discussing the source field, there are some relations between the \hat{a} and \hat{a}^\dagger operators and field coherent states to cover, which are important in evaluating the equations of motion.

A coherent state provides the closest quantum mechanical representation of a classical electromagnetic wave. It is a good description of laser radiation, which is the case of interest here. The coherent state is a linear combination of number states given by

$$|\alpha\rangle \equiv e^{-\frac{1}{2}|\alpha|^2} \sum_{n=0}^{\infty} \frac{\alpha^n}{\sqrt{n!}} |n\rangle \quad (3.88)$$

where α is any complex number. Unlike for the number states $|n\rangle$, the expectation value of the $\hat{\mathbf{E}}$ and $\hat{\mathbf{B}}$ fields are non-zero for coherent states. Coherent states are also described as minimum uncertainty states, for the product of the position and momentum uncertainties is the minimum $\frac{\hbar}{2}$ allowed by the Heisenberg uncertainty principle. This type of state is then the closest description of a strong classical field.

The coherent state is an eigenvector of the destruction operator \hat{a} :

$$\hat{a}|\alpha\rangle = \alpha|\alpha\rangle \quad (3.89)$$

The field coherent state, $|\alpha\rangle_F$, is defined as the product of individual coherent states:

$$|\alpha\rangle_F \equiv |\alpha_1\rangle |\alpha_2\rangle \cdots \quad (3.90)$$

where the indices represent all possible \mathbf{k} and λ . Relations for field coherent states are

$$\hat{a}_{\mathbf{k}\lambda}|\alpha\rangle_F = \alpha_{\mathbf{k}\lambda}|\alpha\rangle_F \quad (3.91a)$$

$${}_F\langle\alpha|\hat{a}_{\mathbf{k}\lambda}^\dagger = \alpha_{\mathbf{k}\lambda}^* {}_F\langle\alpha| \quad (3.91b)$$

With these expressions, it can be shown that

$$\hat{\mathbf{E}}_0^{(+)}|\bar{\alpha}\rangle_F = \mathcal{E}_0^{(+)}|\bar{\alpha}\rangle_F \quad (3.92a)$$

$${}_F\langle\alpha|\hat{\mathbf{E}}_0^{(-)} = \mathcal{E}_0^{(-)}{}_F\langle\alpha| \quad (3.92b)$$

where

$$\mathcal{E}_0^{(+)} = \sum_{\mathbf{k}, \lambda} \left[\frac{2\pi\hbar\omega_{\mathbf{k}}}{V} \right]^{\frac{1}{2}} \epsilon_{\mathbf{k}\lambda} \alpha_{\mathbf{k}\lambda} e^{i(\mathbf{k}\cdot\mathbf{x} - \omega_{\mathbf{k}}t)} \quad (3.93a)$$

$$\mathcal{E}_0^{(-)} = \sum_{\mathbf{k}, \lambda} \left[\frac{2\pi\hbar\omega_{\mathbf{k}}}{V} \right]^{\frac{1}{2}} \epsilon_{\mathbf{k}\lambda} \alpha_{\mathbf{k}\lambda}^* e^{-i(\mathbf{k}\cdot\mathbf{x} - \omega_{\mathbf{k}}t)} \quad (3.93b)$$

Equation (3.92) will be useful in developing equations of motion for the σ operators.

The source field, $\hat{\mathbf{E}}_s$, occurs due to the presence of the atom. It is also referred to as the self field or radiation reaction field. It arises from the need to compensate for energy lost from the system due to radiation. Classically, as the atom radiates energy, the energy of the atomic dipole must decrease accordingly. Quantum mechanically, the expectation value of the electric field due to the atomic dipole decreases. From classical electrodynamics and the correspondence principle, a QED expression for the source field is [31]

$$\hat{\mathbf{E}}_s = \frac{2\ddot{\boldsymbol{\mu}}(t)}{3c^3} = \frac{2}{3c^3} \boldsymbol{\mu} (\ddot{\hat{\sigma}} - \ddot{\hat{\sigma}}^\dagger) \quad (3.94)$$

This agrees with the QED derivation [29]. In the equation of motion for $\hat{\sigma}$, equation (3.84a), the primary term on the right hand side is $-\omega'(t)\hat{\sigma}$ since $\omega' \gg \Omega_\omega$. Thus, the third derivative can be approximated as

$$\ddot{\hat{\sigma}} \approx i\omega'^3(t) \hat{\sigma} \quad (3.95)$$

The source field expression then becomes

$$\hat{\mathbf{E}}_s = \hat{\mathbf{E}}_s^{(+)} + \hat{\mathbf{E}}_s^{(-)} = i\frac{2\mu\omega'^3(t)}{3c^3}(\hat{\sigma} - \hat{\sigma}^\dagger) \quad (3.96)$$

which will be used in developing the equations of motion.

The equations of motion are put in the normal form, where the \hat{a}^\dagger operators are to the left and the \hat{a} operators are to the right, by separating the electric field into positive and negative frequency portions:

$$\dot{\hat{\sigma}} = -i\omega'(t) \hat{\sigma} - \frac{i}{\hbar} \left[\hat{\mu} \cdot \hat{\mathbf{E}}^{(+)} \hat{\sigma}_3 + \hat{\sigma}_3 \hat{\mu} \cdot \hat{\mathbf{E}}^{(+)} \right] \quad (3.97a)$$

$$\dot{\hat{\sigma}}_3 = -2\frac{i}{\hbar} \left[(\hat{\mu} \cdot \hat{\mathbf{E}}^{(-)} (\hat{\sigma} - \hat{\sigma}^\dagger) + (\hat{\sigma} - \hat{\sigma}^\dagger) \hat{\mu} \cdot \hat{\mathbf{E}}^{(+)} \right] \quad (3.97b)$$

This is possible since the positive and negative frequency portions individually commute with the atomic operators. Each field term can then be split into free field and source field terms. Using equation (3.96) and the $\hat{\sigma}$ operator product rule

$$\dot{\hat{\sigma}} = -i\omega'(t) \hat{\sigma} - \frac{i}{\hbar} \left[\hat{\mu} \cdot \hat{\mathbf{E}}^{(-)} \hat{\sigma}_3 + \hat{\sigma}_3 \hat{\mu} \cdot \hat{\mathbf{E}}^{(+)} \right] - \frac{A}{2} (\hat{\sigma} - \hat{\sigma}^\dagger) \quad (3.98a)$$

$$\dot{\hat{\sigma}}_3 = -2\frac{i}{\hbar} \left[\hat{\mu} \cdot \hat{\mathbf{E}}^{(-)} (\hat{\sigma} - \hat{\sigma}^\dagger) + (\hat{\sigma} - \hat{\sigma}^\dagger) \hat{\mu} \cdot \hat{\mathbf{E}}^{(+)} \right] - A(\hat{\sigma}_3 + \hat{I}) \quad (3.98b)$$

where $A \equiv \frac{4|\mu|^2\omega'^3}{3\hbar c^3}$ is the Einstein A coefficient, representing the rate of spontaneous emission. This leaves only the free field terms.

Since the atom-field system is fully quantized, the state of the system can be represented by the product of the atomic state and the field state:

$$|\Psi\rangle = |\psi_A\rangle |\alpha\rangle_F \quad (3.99)$$

where $|\alpha\rangle_F$ is a field coherent state. Taking the expectation values and using the eigenvalue relations of equations (3.92), the equations of motion are

$$\dot{\sigma} = -i\omega'(t) \sigma - \frac{i}{\hbar} \hat{\mu} \cdot \mathcal{E}_0(t) \sigma_3 - \frac{A}{2} (\sigma - \sigma^*) \quad (3.100a)$$

$$\dot{\sigma}_3 = -2\frac{i}{\hbar} \hat{\mu} \cdot \mathcal{E}_0(t) [\sigma - \sigma^*] - A(\sigma_3 + 1) \quad (3.100b)$$

where $\mathcal{E}_0(t) = \mathcal{E}_0^{(+)} + \mathcal{E}_0^{(-)}$, represents the incident probe beam and can be written as $\mathcal{E}_0(t) = \mathcal{E}_0 \cos \omega t$. In this case, the equations of motion are equivalent to those in

the previous section using the adiabatic approach. To demonstrate this, let $\sigma = S(t) \exp\left\{-i \int_0^t \omega'(t') dt'\right\}$, where $S(t)$ is a slowly varying function. Since $\omega \approx \omega'$, the rotating wave approximation is valid, and the equations become

$$\dot{S} = -\frac{\Omega_\omega}{2} e^{-i \int_0^t \Lambda(t') dt'} \sigma_3 - \frac{A}{2} S \quad (3.101a)$$

$$\dot{\sigma}_3 = -i\Omega_\omega \left[S e^{i \int_0^t \Lambda(t') dt'} - S^* e^{-i \int_0^t \Lambda(t') dt'} \right] - A(\sigma_3 + 1) \quad (3.101b)$$

where $\Omega_\omega = \frac{\mu \cdot \mathcal{E}_0}{\hbar}$ and $\Lambda(t) = \omega - \omega'(t)$. These are equivalent to equations (3.63) in the adiabatic approach; hence, the results are the same.

For a quadratic Stark shift, the instantaneous transition frequency is $\omega'(t) = [\omega_0^2 + \Omega_\nu^2 \cos^2 \nu t]^{\frac{1}{2}}$. Transitions then occur at frequencies $\omega_m = \omega_0 + \frac{\Omega_\nu^2}{\omega_0} + 2m\nu$, where m is an integer, with relative intensity $J_m^2\left(\frac{\Omega_\nu^2}{2\omega_0\nu}\right)$. The instantaneous transition frequency for a linear shift is $\omega'(t) = \omega_0 - \Omega_\nu \cos \nu t$, and transitions occur at $\omega_m = \omega_0 + m\nu$ with relative intensity $J_m^2\left(\frac{\Omega_\nu}{\nu}\right)$.

The results of this more rigorous description of the Townes–Merritt effect agree exactly with the previous method and with the original Townes–Merritt experiment. This adds greatly to the confidence of the model using the Heisenberg operator formalism and the adiabatic approximation to describe the effect of the nonresonant RF field. This adiabatic approach will be used to model a three level atom in level crossings. But first, a third method using dressed states to describe the Townes–Merritt effect will be examined to provide further insights to the physical processes.

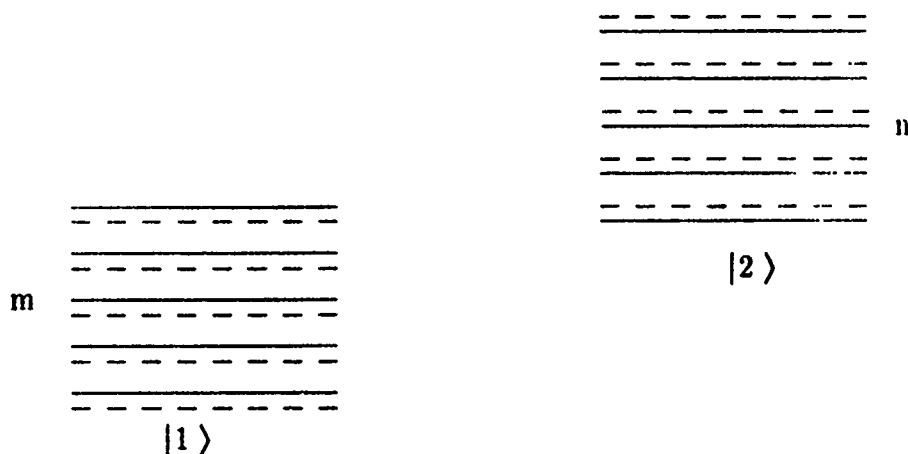


Figure 11 Dressed States for a Two Level Atom. Each atomic state is combined with a photon ladder representing the possible number of photons in the field. The combined energy states are represented by dashed lines.

Dressed States Model

Dressed states are useful in visualizing the transitions which can occur in the Townes–Merritt effect, although the mathematics is cumbersome. The purpose here is to describe, with the dressed states model, transitions which give rise to the absorption sidebands, and thus, further validate the adiabatic approach. Cases for both the linear and quadratic Stark shift will be examined.

A given dressed state is a combination of the atomic state and the photon number state. The energy level diagram consists of the atomic energy states superimposed with a ladder of the photon states. Figure 11 shows a two level atom in a nonresonant field. The state $|1, m\rangle$ represents the ground atomic state with m photons present, and is equal to the product of the two states, $|1\rangle_a |m\rangle_p$. When a probe beam is applied, transitions may occur between the ground state ladder and the excited state ladder, say between $|1, m\rangle$ and $|2, n\rangle$. Allowed transitions depend on the actual energy states. If only the original states are considered, the dipole matrix would be

$$\mu_{1m2n} = \langle 1,m | \hat{\mu} | 2,n \rangle = \mu_{12} \langle m | n \rangle = \mu_{12} \delta_{mn} \quad (3.102)$$

This would prescribe that only transitions where $n = m$ could occur. However, the actual energy states are linear combinations of the unperturbed states,

$$|\bar{1},n\rangle = \sum_{j,m} C_{ijnm} |j,m\rangle \quad (3.103)$$

so transitions where $n \neq m$ may occur. These states are indicated by dashed lines in figure 11, and are slightly shifted in energy. The transition strength is proportional to the square of the dipole moment and is then dependent on the coefficient C_{ijnm} . The transition frequency is a function of the new energy levels. The new states satisfy

$$\hat{H} |\bar{1},n\rangle = E_{1n} |\bar{1},n\rangle \quad (3.104)$$

and thus, are dependent on the Hamiltonian. Two cases will be considered here, the linear Stark shift of the excited state and a quadratic Stark shift.

For the linear case, the Hamiltonian can be written as

$$\hat{H} = \hbar\omega_0 \hat{\sigma}^\dagger \hat{\sigma} + \hbar\nu \hat{a}^\dagger \hat{a} - \mu_0 \cdot \mathbf{E} |2\rangle \langle 2| (\hat{a} + \hat{a}^\dagger) \quad (3.105)$$

where $|\mathbf{E}| \equiv \left[\frac{\hbar\nu}{2\epsilon_0 V} \right]^{\frac{1}{2}} = \mathcal{E}_\nu / 2\sqrt{m}$ and m is the average number of photons [29]. The ground state is unchanged, so $|\bar{1},m\rangle = |1,m\rangle$. The new excited state ladder is a linear combination of the $|2,m\rangle$ states only, given by

$$|\bar{2},n\rangle = \sum_m C_{nm} |2,m\rangle \quad (3.106)$$

Note that the coefficient C_{nm} should tend towards δ_{nm} as the field strength goes to zero. Substituting this into equation (3.104)

$$\sum_n C_{nm}(\hbar\omega_0 + \hbar\nu m) |2, m\rangle - \sum_n C_{nm} \mu_0 \cdot E [\sqrt{m} |2, m-1\rangle + \sqrt{m+1} |2, m+1\rangle] = E_{2n}' \sum_n C_{nm} |2, m\rangle \quad (3.107)$$

Multiplying by $\langle 2, m' |$ results in

$$C_{nm}(\hbar\omega_0 + \hbar\nu m) - C_{nm-1} \mu_0 \cdot E \sqrt{m+1} + C_{nm+1} \mu_0 \cdot E \sqrt{m} = E_{2n}' C_{nm} \quad (3.108)$$

Let $E_{2n}' = \hbar\omega_0 + n\hbar\nu$, and assume $\sqrt{m+1} \approx \sqrt{m} \approx \sqrt{m}$ which is valid for high photon occupation states. Equation (3.108) then becomes

$$C_{nm} \frac{2(m-n)\nu}{\Omega} = C_{nm-1} + C_{nm+1} \quad (3.109)$$

where $\Omega \equiv \frac{2\mu E \sqrt{m}}{\hbar} = \frac{\mu \mathcal{E}}{\hbar} = \Omega_\nu$ as before. This recursion relation is equivalent to one for Bessel functions [9], where $C_{nm} = J_{m-n}(\frac{\Omega_\nu}{\nu})$. Thus the energy eigenstates are

$$| \overline{2, n} \rangle = \sum_m J_{m-n}(\frac{\Omega_\nu}{\nu}) |2, m\rangle \quad (3.110)$$

with energy

$$E_{2n}' = \hbar\omega_0 + n\hbar\nu \quad (3.111)$$

Note as \mathcal{E} tends toward zero, $J_{m-n}(\frac{\Omega_\nu}{\nu})$ becomes δ_{nm} .

Transitions from the atomic ground state to the excited state are a function of the dipole matrix element. For an atom initially in the $| \overline{1, m} \rangle$ state, the

transition probability to the $|\overline{2,n}\rangle$ state is proportional to

$$\begin{aligned}
 |\mu_{1m2n}|^2 &= |\langle \overline{1,m} | \hat{\mu} | \overline{2,n} \rangle|^2 \\
 &= |\mu_0|^2 \left| \sum_k J_{k-n}(\frac{\Omega}{\nu}) \langle m | k \rangle \right|^2 \\
 &= \mu_0^2 J_{n-n}^2(\frac{\Omega}{\nu})
 \end{aligned} \tag{3.112}$$

The transition would occur at frequency $\omega = \omega_0 + (n-m)\hbar\nu$, with relative intensity $J_{m-n}^2(\frac{\Omega}{\nu})$. This agrees with the result in the adiabatic approach; here the difference term, $n-m$, represents the $n-m$ sideband. For the total transition strength, the individual moments are summed over the distribution in the ground state ladder, but the relative strengths of the sidebands would remain the same.

For the quadratic case, the situation is a little more complex since the energy eigenstates are functions of both original atomic states summed over the photon states:

$$|\overline{j,n}\rangle = \sum_{k,m} C_{jnk m} |k,m\rangle \tag{3.113}$$

The Hamiltonian for a many level atom in the RF field is

$$\hat{H} = \sum_n \hbar\omega_n \hat{\sigma}_{nn} + \hbar\nu \hat{a}^\dagger \hat{a} - \sum_{n,m} \hat{\sigma}_{nm} \mu_{nm} \cdot \mathbf{E} [\hat{a} + \hat{a}^\dagger] \tag{3.114}$$

Substituting equations (3.113) and (3.114) into (3.104)

$$\begin{aligned}
 \sum_{k,m} C_{jnk m} (\hbar\omega_k + m\hbar\nu) |k,m\rangle - \sum_{p,k,m} C_{jnk m} \mu_{pk} \cdot \mathbf{E} [\sqrt{m} |p,m-1\rangle + \sqrt{m+1} |p,m+1\rangle] \\
 = E_{jn} \sum_{k,m} C_{jnk m} |k,m\rangle
 \end{aligned} \tag{3.115}$$

Multiplying by $\langle k', m' |$ results in the following recursion relation:

$$[\hbar\omega_k + m\hbar\nu - E_{jn}'] C_{jnk m} = \sum_p \mu_{kp} \cdot E[\sqrt{m+1} C_{jn p m+1} + \sqrt{m} C_{jn p m-1}] \quad (3.116)$$

This is still a general relation; the linear Stark shift of the previous example occurs when μ_{kp} is non-zero only for $k = p = 2$. For the quadratic shift, $\mu_{kp} = 0$ for $k = p$.

Consider initially the upper state of the two level atom, $j = 2$. Let

$E_{2n} = \hbar\omega_0 + n\hbar\nu + \epsilon_n$. The index k can take on values of 1 or 2. For $k = 2$,

$$[(m-n)\hbar\nu - \epsilon_n] C_{2n2m} = \mu_{21} \cdot E[\sqrt{m+1} C_{2n1m+1} + \sqrt{m} C_{2n1m-1}] \quad (3.117)$$

For $k = 1$,

$$[-\hbar\omega_0 + (m-n)\hbar\nu - \epsilon_n] C_{2n1m} = \mu_{12} \cdot E[\sqrt{m+1} C_{2n2m+1} + \sqrt{m} C_{2n2m-1}] \quad (3.118)$$

Then substitute equation (3.118) into equation (3.117):

$$\begin{aligned} [(m-n)\hbar\nu - \epsilon_n] C_{2n2m} = -|\mu_{21} \cdot E|^2 & \left[\frac{(m+1) C_{2n2m} + \sqrt{(m+2)(m+1)} C_{2n2m+2}}{\hbar\omega_0 - (m-n+1)\hbar\nu + \epsilon_n} \right. \\ & \left. + \frac{m C_{2n2m} + \sqrt{m(m-1)} C_{2n2m-2}}{\hbar\omega_0 - (m-n-1)\hbar\nu - \epsilon_n} \right] \end{aligned} \quad (3.119)$$

Again assume a highly populated photon state, $m \approx m+1 \approx m$, and let $\epsilon_n = \frac{\hbar\Omega^2}{2\omega_0}$, where $\Omega \equiv \frac{2|\mu \cdot E|}{\hbar} \sqrt{m}$. Noting that $\hbar\omega_0 \gg \hbar\nu, \epsilon_n$, the recursion relation simplifies to

$$\frac{4(n-m)\nu\omega_0}{\Omega^2} C_{2n2m} = C_{2n2m+2} + C_{2n2m-2} \quad (3.120)$$

This relates alternate coefficients in the photon ladder of the excited state. Since

the perturbation is relatively small, the largest coefficient is for $m = n$. In fact, when the RF field goes to zero this is the only coefficient in the series. In the presence of an RF field, the other non-zero coefficients could only be the even series, or where $m = n \pm 2k$; k is an integer. This result agrees with the experiment; absorption sidebands exist only for the even harmonics of ν .

Equation (3.120) is a Bessel function recursion relation where $C_{2n2m} \equiv J_{\frac{n-n}{2}}(\frac{\Omega^2}{2\omega_0\nu})$, imposing the condition $m = n \pm 2k$, for the even series. The energy states can then be written

$$|\overline{2,n}\rangle = \sum_k J_k(\frac{\Omega^2}{4\omega_0\nu}) |2,n+2k\rangle \quad (3.121)$$

with energy

$$E'_{2n} = \hbar\omega_0 + n\hbar\nu + \frac{\hbar\Omega^2}{2\omega_0} \quad (3.122)$$

This ignores terms involving the ground atomic state since the coefficients C_{2n1m} are smaller by a factor of $\frac{\Omega}{\omega_0}$, as can be seen in equation (3.118). The last term in the expression for the energy is the static Stark shift, which agrees with previous theory. Similar expressions for the ground state ladder can be developed:

$$|\overline{1,m}\rangle = \sum_j J_j(\frac{\Omega^2}{4\omega_0\nu}) |1,m-2j\rangle \quad (3.123)$$

$$E'_{1m} = m\hbar\nu - \frac{\hbar\Omega^2}{2\omega_0} \quad (3.124)$$

Now consider a transition from the $|\overline{1,m}\rangle$ state to the $|\overline{2,n}\rangle$ state as a result of the probe beam. The strength of this transition is directly proportional to

$$\begin{aligned}
|\mu_{1m2n}|^2 &= |\langle 1, m | \hat{\mu} | 2, n \rangle|^2 \\
&= \mu_{12}^2 \left| \sum_{k, j} J_j\left(\frac{\Omega^2}{4\omega_o\nu}\right) J_k\left(\frac{\Omega^2}{4\omega_o\nu}\right) \langle m-2j | n+2k \rangle \right|^2 \\
&= \mu_{12}^2 \left| \sum_k J_k\left(\frac{\Omega^2}{4\omega_o\nu}\right) J_{\frac{m-n}{2}-k}\left(\frac{\Omega^2}{4\omega_o\nu}\right) \right|^2 \quad (3.125)
\end{aligned}$$

The last line results from the relation $m - 2j = n + 2k$. Notice also that for this to be satisfied, the indices m and n must differ by a multiple of 2, $m - n = 2p$. This becomes a selection rule for the transition. The sum of the Bessel function products can be further reduced by the relation $\sum_k J_k(z) J_{v-k}(z) = J_v(2z)$ [9]; thus,

$$|\mu_{1m2n}|^2 = \mu_{12}^2 J_{\frac{m-n}{2}}^2\left(\frac{\Omega^2}{2\omega_o\nu}\right) \quad (3.126)$$

Transitions can then occur at frequencies $\omega_k = \omega_o + \frac{\Omega^2}{\omega_o} + 2p\nu$, where $p \equiv \frac{m-n}{2}$ is an integer. The relative strengths are given by $J_k^2\left(\frac{\Omega^2}{2\omega_o\nu}\right)$.

The result here agrees with previous approaches in describing the Townes–Merritt effect, which provides an added degree of confidence in the adiabatic approximation for defining the energy states of an atom in a nonresonant field. The dressed states model provides a convenient picture for understanding the physical transitions; however, its complexity warrants use of the adiabatic approach in describing the three level atom for level crossings and quantum beats. The dressed states picture raises one other issue, the question of quantum beats in a two level atom due to interference between transitions from adjacent atom–field states, which will now be discussed.

Quantum Beats in a Two Level Atom

Quantum beats have not been observed in a two level atom, nor are they predicted in the adiabatic model. In the dressed states picture, the possibility arises if adjacent photon states in the excited atomic state ladder transition to a common state in the ground state ladder. These type of transitions, n, p photons to m photons, are allowed due to the mixing of states, as shown in the previous section. This is, however, a simplistic view of the transitions from excited state to ground state since it ignores the total contribution from all states in the ladder. It will be shown that when all possible transitions are considered, there is no beating effect, although the sidebands are still present.

The quantum beat phenomenon occurs when two excited states can transition to a common ground state. Interference between the two possible transitions can produce a beat signal. In the dressed states picture, it is possible in a two level atom for two different excited states to transition to the same ground state, if one considers the various atom-field states. To demonstrate this, consider the simplest example, where only the upper state exhibits a linear Stark shift. Recall $|\overline{1, n}\rangle = |1, n\rangle$, and from equation (3.110),

$$|\overline{2, n}\rangle = \sum_k J_{k-n}\left(\frac{\Omega}{\nu}\right) |2, k\rangle \quad (3.127)$$

The mixing of states allows this situation to exist. Figure 12 depicts relaxation from various levels in the excited state ladder to a single level in the ground state ladder, which could conceivably produce the beat signal at multiples of the RF frequency. To fully evaluate the potential for interference, these type of transitions must be summed over the entire excited ladder.

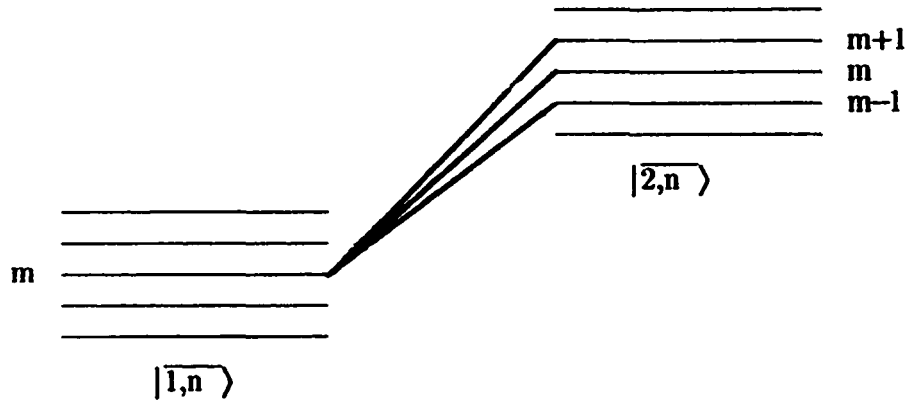


Figure 12 Quantum Beats in a Two Level Atom. Transitions occur between combined atom-RF field states.

The quantum beat signal is given by equation (2.20), which is repeated here, assuming $\omega_{10} \approx \omega_{20} \approx \omega_0$:

$$P = \frac{4\omega_0^4}{3c^3} \sum_{n, P > n} \mu_{nm} \mu_{pm}^* e^{i\omega_{np}t} \rho_{pn}^H \quad (3.128)$$

The dipole matrix elements are between the excited state $\langle \overline{2,n} |$ and the lower state $| \overline{1,m} \rangle$. If the field is considered to be a coherent state, then it can be assumed that the excited states of interest have equal initial populations. This is reasonable since in a strong field, the coefficients of the coherent state change little between adjacent states, and the coefficients of the energy states $| \overline{2,n} \rangle$ drop off rapidly as k differs from n .

The dipole matrix can be written as

$$\begin{aligned} \mu_{nm} &= \langle \overline{2,n} | \mu | \overline{1,m} \rangle = \sum_k J_{k-n} \left(\frac{\Omega_\nu}{\nu} \right) \langle 2,k | \mu | 1,m \rangle \\ &= \mu_0 J_{m-n} \left(\frac{\Omega_\nu}{\nu} \right) \end{aligned} \quad (3.129)$$

Upon substitution of this into equation (3.128), the power radiated is

$$P = \frac{4\omega_0^4\mu_0^2}{3c^3} \sum_{n,p} J_{n-n}(\frac{\Omega}{\nu}) J_{p-n}(\frac{-\Omega}{\nu}) e^{i\nu(n-p)t} \rho_{pn}^H \quad (3.130)$$

The Bessel function series reduces to $\sum_n J_{n-n} J_{p-n} = \delta_{np}$; thus ,

$$P = \frac{4\omega_0^4\mu_0^2}{3c^3} \sum_n \rho_{nn}^H = \frac{4\omega_0^4\mu_0^2}{3c^3} \quad (3.131)$$

Since P is constant, there are no quantum beats present despite the existence of transitions on the various harmonic sidebands. An interpretation of this is the individual beat signals, which would be present if the atom were initially excited to only two states in the ladder, become washed out when combined with all other possible transition pairs. Quantum beats can still occur in a three level atom as will be shown later.

IV. Quantum Beats and Level Crossings

Three Level Atom

Level crossings and quantum beats result from interference between the spontaneous decay of two coherently excited states which have the same final or ground state. To treat this phenomenon, the simplest atomic model is that of a three level atom with the two excited states close in energy; refer to figure 4. A level crossing occurs when the upper states coincide, resulting in a shift of the fluorescence pattern depending on the original transition characteristics. When the energy states are slightly separated, quantum beats may result which modulate the radiated power during spontaneous emission.

When the atom is placed in a nonresonant RF field, additional transitions can occur, as discussed in the section on the Townes–Merritt effect. These transitions give rise to other possible level crossings or quantum beats, which is precisely the subject of this study. The adiabatic and the dressed states models, used to describe the Townes–Merritt effect, provide the mathematical basis and an intuitive understanding of the physical processes occurring. The dressed states model gives a clear picture in terms of identifying transitions which fit the three level model for quantum beats or level crossings. Figure 13 shows the photon ladders associated with each atomic state. Here a level crossing condition exists when the $|1,n\rangle$ and $|2,p\rangle$ states coincide and can each decay to the $|0,m\rangle$ state. This of course represents but one of the possible combinations in the dressed states model. To arrive at the total solution, all possible combinations need be included. This added complexity is the prime motivation for using the adiabatic approach to mathematically describe the level crossing and quantum beat effects. In the description of the Townes–Merritt effect, the adiabatic solution agreed with the

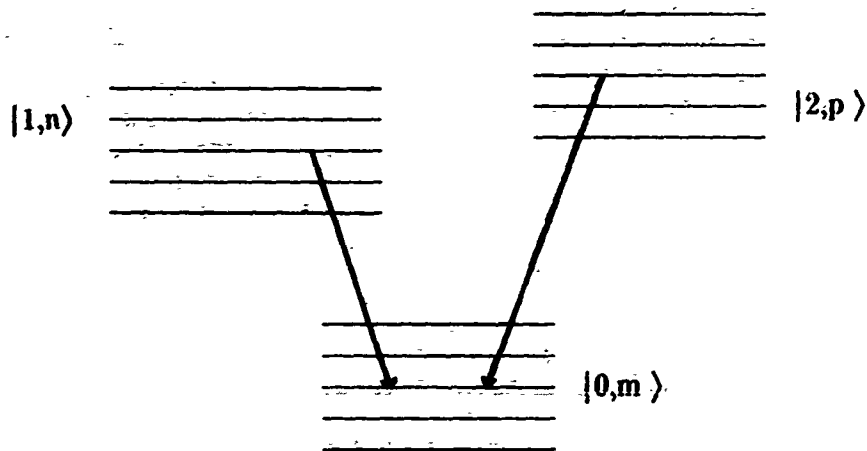


Figure 13 Dressed states picture of a three level atom in an RF field. Energy levels represent an atomic states combined with a photon state with n photons present.

dressed states solution as well as the original experimental results, which gives the approach significant credibility.

The primary difference between the Townes-Merritt experiment and either level crossings or quantum beats is that in the latter there is no second applied field to trigger a transition. Both level crossings and quantum beats result from spontaneous emission of the atom after it has been excited by a short pulse; however, the energy eigenstates which result from the RF field are the same. Thus, the calculations will consider spontaneous emission transitions from the excited energy eigenstates to the ground state of the three level atom.

The first requirement is to determine the instantaneous energy eigenstates for the atom in the RF field. Two cases will be considered: a linear Stark shift of a single excited state and a quadratic Stark shift of all three states. The first case is relatively simple and the atomic operators, $\hat{\sigma}_{ij}$, can be determined exactly. The second requires an approximate solution, using perturbation theory. These solutions will then be used to calculate the quantum beat and level crossing effects.

Linear Stark Shift. For the linear Stark shift case, two methods will be used to calculate the atomic operators, $\hat{\sigma}_{ij}$. The first solves the time independent Schrödinger equation for the instantaneous energy eigenstates, then uses them to construct the $\hat{\sigma}$ operators. The second uses the unperturbed atomic states as a basis and solves the Heisenberg equation of motion for the $\hat{\sigma}$ operators in the Heisenberg picture. Both methods result in the same expression, but the latter can be easily adjusted to include spontaneous emission.

The Hamiltonian for the atom in the RF field is given by

$$\hat{H} = \hat{H}_A = \sum_n \hbar \omega_n \hat{\sigma}_{nn} - \hat{\mu} \cdot \hat{E} \quad (4.1)$$

where

$$\hat{\mu} = \sum_{i,j} \hat{\sigma}_{ij} \hat{\mu}_{ij} \quad (4.2)$$

For the case of a single level linear Stark shift, the only non-zero term of μ_{ij} is $\mu_{11} \equiv \mu \epsilon$. Let the RF field be given by $\hat{E} = \epsilon \mathcal{E} \cos \nu t$. Then the Hamiltonian becomes

$$\hat{H} = \sum_n \hbar \omega_n \hat{\sigma}_{nn} - \hbar \Omega_\nu \hat{\sigma}_{11} \cos \nu t \quad (4.3)$$

The instantaneous energy eigenstates are solutions of

$$\hat{H}(t) |n(t)\rangle = E_n(t) |n(t)\rangle \quad (4.4)$$

which yields $|n(t)\rangle = |n\rangle$ and

$$E_0 = 0 \quad (4.5a)$$

$$E_1 = \hbar\omega_1 - \hbar\Omega_\nu \cos \nu t \quad (4.5b)$$

$$E_2 = \hbar\omega_2 \quad (4.5c)$$

The $\hat{\sigma}$ operators are then defined by $\hat{\sigma}_{ij} \equiv |i(t)\rangle\langle j(t)|$. In the Heisenberg picture,

$$\dot{\hat{\sigma}}_{ij}^H = \frac{1}{i\hbar}[\hat{\sigma}_{ij}^H, \hat{H}^H] = i\omega_{ij}(t)\hat{\sigma}_{ij}^H \quad (4.6)$$

The solution of this equation results in

$$\hat{\sigma}_{ij}^H(t) = \hat{\sigma}_{ij}^H(0) e^{i \int_0^t \omega_{ij}(t') dt'} \quad (4.7)$$

which defines the time evolution of the $\hat{\sigma}$ operators.

The second method starts by defining $\hat{\sigma}_{ij} \equiv |i\rangle\langle j|$, where $|i\rangle$ represents an unperturbed atomic state. The Heisenberg equation of motion gives

$$\begin{aligned} \dot{\hat{\sigma}}_{ij}^H &= \frac{1}{i\hbar}[\hat{\sigma}_{ij}^H, \hat{H}^H] \\ &= -i \sum_n [\hat{\sigma}_{ij}^H, \hat{\sigma}_{nn}^H] \omega_n + i[\hat{\sigma}_{ij}^H, \hat{\sigma}_{11}^H] \Omega_\nu \cos \nu t \\ &= i\omega_{ij} \hat{\sigma}_{ij}^H + i[\delta_{j1} \hat{\sigma}_{i1}^H - \delta_{i1} \hat{\sigma}_{1j}^H] \Omega_\nu \cos \nu t \end{aligned} \quad (4.8)$$

The solution of equation (4.8) is the same as the previous method. For example, consider

$$\dot{\hat{\sigma}}_{12}^H = i\omega_{12} \hat{\sigma}_{12}^H - i\Omega_\nu \cos \nu t \hat{\sigma}_{12}^H \quad (4.9)$$

The solution is

$$\hat{\sigma}_{12}^H(t) = \hat{\sigma}_{12}^H(0) e^{i \int_0^t \omega_{12}(t') dt'} \quad (4.10)$$

where $\omega_{12}(t) = \omega_{12} - \Omega_\nu \cos \nu t$.

These solutions, however, have not considered spontaneous emission. This can be included by adding a decay term to equation (4.9)

$$\dot{\hat{\sigma}}_{12}^H = i\omega_{12}\hat{\sigma}_{12}^H - i\Omega_\nu \cos \nu t \hat{\sigma}_{12}^H - A\hat{\sigma}_{12}^H \quad (4.11)$$

Here it is assumed for simplicity that the decay coefficients for the two transitions are equal to A . The result agrees with the previous treatment of spontaneous emission in the section on the Townes–Merritt effect, which lead to equation (3.98a). The factor of 2 difference arises from the fact that both the $|1\rangle$ and $|2\rangle$ states are excited states. The solution then reads

$$\hat{\sigma}_{12}^H(t) = \hat{\sigma}_{12}^H(0) e^{-At} e^{i \int_0^t \omega_{12}(t') dt'} \quad (4.12)$$

This will be useful in calculating the effects of quantum beats and level crossings.

Quadratic Stark Shift. For a quadratic Stark shift, the methods used in the previous section to find the energy states do not yield simple solutions. In fact, the second method involving the Heisenberg equation of motion would require solving six coupled differential equations. The primary reason for this is the form of the dipole matrix, which can be written

$$\mu \equiv \begin{bmatrix} 0 & \mu_{01} & \mu_{02} \\ \mu_{10} & 0 & 0 \\ \mu_{20} & 0 & 0 \end{bmatrix} \quad (4.13)$$

This assumes that transitions between the ground state and each of the excited states are allowed, but not between excited states. Additionally, each state is of definite parity so $\mu_{ii} = 0$.

The time independent Schrödinger equation can be rewritten in matrix form, using equation (4.13), to read

$$\hbar \begin{bmatrix} 0 & \Omega_1 \cos \nu t & \Omega_2 \cos \nu t \\ \Omega_1^* \cos \nu t & \omega_1 & 0 \\ \Omega_2^* \cos \nu t & 0 & \omega_2 \end{bmatrix} |\bar{n}\rangle = E_n' |\bar{n}\rangle \quad (4.14)$$

where $\Omega_1 \equiv \frac{\mu_{01} \cdot \mathcal{E}}{\hbar}$. An exact solution requires the characteristic equation, in this case a cubic equation of E_n' .

A more tractable approach is to use time independent perturbation theory to find the instantaneous energy states. This is valid for small perturbations, when $\Omega \ll \nu$. To second order, the perturbed states are given by [8]

$$|\bar{n}\rangle = |n\rangle + \sum_{k \neq n} \left\{ \frac{\langle k | \hat{H}' | n \rangle}{E_n - E_k} \left[1 - \frac{\langle n | \hat{H}' | n \rangle}{E_n - E_k} \right] + \sum_{m \neq n} \frac{\langle k | \hat{H}' | m \rangle \langle m | \hat{H}' | n \rangle}{(E_n - E_k)(E_n - E_m)} \right\} |k\rangle \quad (4.15)$$

$$E_n' = E_n + \langle n | \hat{H}' | n \rangle + \sum_{k \neq n} \left| \frac{\langle n | \hat{H}' | k \rangle}{E_n - E_k} \right|^2 \quad (4.16)$$

where $\hat{H}' = -\boldsymbol{\mu} \cdot \hat{\mathbf{E}}$. For the three level atom, equations (4.15) and (4.16) yield

$$|\overline{0}\rangle = |0\rangle - \frac{\hbar\Omega_1^*}{\omega_1} \cos \nu t |1\rangle - \frac{\hbar\Omega_2^*}{\omega_2} \cos \nu t |2\rangle \quad (4.17a)$$

$$|\overline{1}\rangle = |1\rangle + \frac{\hbar\Omega_1}{\omega_1} \cos \nu t |0\rangle + \frac{\Omega_1\Omega_2^*}{\omega_1\omega_{12}} \cos \nu t |2\rangle \quad (4.17b)$$

$$|\overline{2}\rangle = |2\rangle + \frac{\hbar\Omega_2^*}{\omega_2} \cos \nu t |0\rangle + \frac{\Omega_1^*\Omega_2}{\omega_{21}\omega_2} \cos \nu t |1\rangle \quad (4.17c)$$

and

$$E_0 = - \left[\frac{\hbar\Omega_1^2}{\omega_1} + \frac{\hbar\Omega_2^2}{\omega_2} \right] \cos^2 \nu t \quad (4.18a)$$

$$E_1 = \hbar\omega_1 + \frac{\hbar\Omega_1^2 \cos^2 \nu t}{\omega_1} \quad (4.18b)$$

$$E_2 = \hbar\omega_2 + \frac{\hbar\Omega_2^2 \cos^2 \nu t}{\omega_2} \quad (4.18c)$$

From these expressions, the $\hat{\sigma}$ operators may be written. Note that in forming $\hat{\sigma}_{ij}$, $\Omega \ll \omega$, so,

$$\dot{\hat{\sigma}}_{ij} \equiv \overline{|i\rangle\langle j|} \approx |i\rangle\langle j| \quad (4.19)$$

Thus, the $\frac{\partial \hat{\sigma}_{ij}^H}{\partial t}$ term can be ignored, and the Heisenberg equation of motion is, as before

$$\dot{\hat{\sigma}}_{ij} = i\omega_{ij}(t) \hat{\sigma}_{ij} \quad (4.20)$$

Spontaneous emission is again included by adding an exponential decay term in the solution. In the case of $\hat{\sigma}_{12}$, the result is

$$\hat{\sigma}_{12}(t) = \hat{\sigma}_{12}(0) e^{-At} e^{i \int_0^t \omega_{12}(t') dt'} \quad (4.21)$$

where

$$\omega_{12}(t) = \omega_{12} + \frac{\omega_2\Omega_1^2 - \omega_1\Omega_2^2}{\omega_1\omega_2} \cos^2 \nu t \quad (4.22)$$

Equation (4.21) is the same result as for the linear case, equation (4.12), except for the definition of the instantaneous transition frequency. These equations will be central to calculating level crossing and quantum beat effects in the next section. It is worth noting that the effects for the quadratic shift are expected to be much less due to the smaller instantaneous shifts; of order $\frac{\Omega}{\omega}$ less. Also if $\Omega_1 = \Omega_2$, the effects will be negligible.

Quantum Beats Calculation

Before addressing level crossings, the effect of the Townes–Merritt sidebands on quantum beats will be discussed. Specifically, this section will cover the presence of quantum beats in which the magnitude and frequency are dependent on the RF field. This is a simpler calculation, primarily since it considers the total radiation from the atom as a function of time instead of radiation in a specific direction. Both the single linear Stark shifted level and the quadratic Stark shift, covered in the last section, will be considered. The calculation follows the adiabatic approach, but for the simpler linear case, the dressed states model is also used as a comparison.

Quantum beats can occur when the atom is initially excited by a pulse such that there is a finite probability of being in either upper state. In this way, the off diagonal elements of the initial density matrix are non-zero. The off diagonal terms are defined as the product of the amplitude coefficients of the wave function for each of the excited states, for example $\rho_{12} \equiv a_1 a_2^*$. As the atom decays back to the ground state from the 'mixed' upper state via spontaneous emission, there is potential interference between the two distinct transitions. The interference results in a beating effect, or an amplitude modulation of the radiated power, which has a frequency directly related to the energy separation of the two excited states. The

Townes-Merritt effect causes a splitting of these excited states raising the possibility of other beat signals dependent on the RF field frequency. The following calculations will show this dependence.

Equation (2.12) described the power emitted from the atom as a function of the expectation value of the inner product of the positive and negative frequency portions of the dipole acceleration operator:

$$P = \frac{4 \langle \ddot{\mu}^{(-)} \cdot \ddot{\mu}^{(+)} \rangle}{3c^3} \quad (4.23)$$

In the adiabatic approach, the dipole operator can be represented as

$$\hat{\mu}^{\pm}(t) = \sum_{n,m} \mu_{nm} \hat{\sigma}_{nm}^{\pm}(t) \quad (4.24)$$

where $\hat{\sigma}_{nm}(t)$ is defined by the adiabatic energy states. Following the development in chapter II, an expression for the inner product, similar to equation (2.18), results:

$$\ddot{\mu}^{(-)} \cdot \ddot{\mu}^{(+)} = \sum_{n,p>m} \omega_{nm}^2 \omega_{pm}^2 \mu_{nm} \cdot \mu_{pm}^* \hat{\sigma}_{np}(t) \quad (4.25)$$

The expression for the power radiated then becomes

$$P = \frac{4}{3c^3} \sum_{n,p>m} \omega_{nm}^2 \omega_{pm}^2 \mu_{nm} \cdot \mu_{pm}^* \langle \hat{\sigma}_{np}(t) \rangle \quad (4.26)$$

Considering the possible values for the indices in the case of the three level atom, the index m must be zero, and (n,p) can be (1,1), (1,2), (2,1), or (2,2). The first and last possibilities are trivial since

$$\langle \hat{\sigma}_{11}(t) \rangle = P_1(t) = P_1(0) e^{-At} \quad (4.27a)$$

$$\langle \hat{\sigma}_{22}(t) \rangle = P_2(t) = P_2(0) e^{-At} \quad (4.27b)$$

where P_n is the probability of being in state n , and it is assumed that both excited states have a spontaneous emission rate A . The middle two cases are equivalent, representing complex conjugates of each other. Taking the expectation value of equation (4.21),

$$\langle \hat{\sigma}_{12}(t) \rangle = \rho_{21}^H e^{-At} e^{i \int_0^t \omega_{12}(t') dt'} \quad (4.28)$$

Note, this is the same for both the linear and quadratic cases; only the expressions for $\omega_{12}(t)$ is different.

Finally, using equations (4.27) and (4.28), the equation for power radiated becomes

$$P = \left\{ \frac{4\omega_{20}^4 |\mu_{20}|^2}{3c^3} P_2 + \frac{4\omega_{10}^4 |\mu_{10}|^2}{3c^3} P_1 + \frac{4\omega_{20}^2 \omega_{10}^2}{3c^3} \left[\mu_{10} \cdot \mu_{20}^* \rho_{21}^H e^{i \int_0^t \omega_{12}(t') dt'} + \mu_{20} \cdot \mu_{10}^* \rho_{12}^H e^{-i \int_0^t \omega_{12}(t') dt'} \right] \right\} e^{-At} \quad (4.29)$$

Notice this is very similar to equation (2.21) in the original description of quantum beats, except for the exponential terms which are now dependent on the instantaneous transition frequency, $\omega_{12}(t)$. This reflects the Townes-Merriitt effect in the atomic energy states, and will give rise to beat signals that depend on the RF field. Again, the distinction between the linear and quadratic cases is the expression for $\omega_{12}(t)$.

Linear Stark Shift. For a linear Stark shift of a single excited level, the instantaneous energy difference is represented by the frequency

$$\omega_{12}(t) = \omega_{12} - \Omega_{\nu} \cos \nu t \quad (4.30)$$

The exponential term in equation (4.29) then becomes

$$e^{i \int_0^t \omega_{12}(t') dt'} = e^{i \omega_{12} t} e^{-i \frac{\Omega_{\nu}}{\nu} \sin \nu t} \quad (4.31)$$

The last exponential term in equation (4.31) can be expanded into a Bessel function series:

$$e^{i \int_0^t \omega_{12}(t') dt'} = \sum_{n=-\infty}^{\infty} J_n\left(\frac{\Omega_{\nu}}{\nu}\right) e^{i(\omega_{12} - n\nu)t} \quad (4.32)$$

The expression for radiated power, equation (4.29), is then

$$P = \left\{ \frac{4\omega_{10}^4 |\mu_{20}|^2}{3c^3} P_2 + \frac{4\omega_{10}^4 |\mu_{10}|^2}{3c^3} P_1 + \frac{4\omega_{10}^2 \omega_{20}^2}{3c^3} \left[\mu_{10} \cdot \mu_{20}^* \rho_{21}^H \sum_{n=-\infty}^{\infty} J_n\left(\frac{\Omega_{\nu}}{\nu}\right) e^{i(\omega_{12} - n\nu)t} \right. \right. \\ \left. \left. + \mu_{20} \cdot \mu_{10}^* \rho_{12}^H \sum_{n=-\infty}^{\infty} J_n\left(\frac{\Omega_{\nu}}{\nu}\right) e^{i(\omega_{12} - n\nu)t} \right] \right\} e^{-\Lambda t} \quad (4.33)$$

The series of exponential terms indicate the possibility of quantum beats at frequencies $\omega_{12} - n\nu$ depending on the magnitude of the coefficients. To illustrate this, assume $\omega_{10} \approx \omega_{20} \approx \omega_0$ and $\mu_{10} = \mu_{20} = \mu_0$. In addition, let the initial excitation result in $P_1 = P_2 = \rho_{12}^H = \rho_{21}^H$. Then,

$$P = 2P_0 e^{-At} \left[1 + \sum_n J_n\left(\frac{\Omega}{\nu}\right) \cos(\omega_{12} - n\nu)t \right] \quad (4.34)$$

where $P_0 = \frac{4\omega_0^4 |\mu_0|^2}{3c^3} P_1$. Expanding the series to a few terms around $n = 0$,

$$P \approx 2P_0 e^{-At} \left[1 + J_0\left(\frac{\Omega}{\nu}\right) \cos \omega_{12} t + J_1\left(\frac{\Omega}{\nu}\right) \cos(\omega_{12} - \nu)t + J_{-1}\left(\frac{\Omega}{\nu}\right) \cos(\omega_{12} + \nu)t \dots \right] \quad (4.35)$$

This shows the presence of beats with frequencies ω_{12} , $\omega_{12} \pm \nu$, \dots , with relative magnitude $J_n(\frac{\Omega}{\nu})$. Since one expects $\nu \gg \Omega$, only a few terms around $n = 0$ will be significant, and the greatest contribution is likely to come from the J_0 term, which corresponds to the beat frequency of the unperturbed atom. To detect the other beat frequencies, consider experimental apparatus. In measuring the decay curve, the equipment will be limited by an effective bandwidth, BW. Only those signals which vary at a frequency less than this bandwidth can be measured. Any beat frequency which satisfies $\omega_{12} + n\nu \gg BW$, will average to, resulting in no impact on the decay measurement. If, however, for some value m , $\omega_{12} - m\nu < BW$, the beat signal would be detectable and would have magnitude $J_m(\frac{\Omega}{\nu})$. The radiative decay would then follow

$$P = 2P_0 e^{-At} \left[1 + J_m\left(\frac{\Omega}{\nu}\right) \cos(\omega_{12} - m\nu)t \right] \quad (4.36)$$

Another possible means exists for a very large field such that the term $J_0(\frac{\Omega}{\nu}) \approx 0$. In this case, the higher order Bessel functions would be significant, representing various beat signals. These experimental considerations will be covered in more detail later.

Dressed States Calculation. The linear Stark shift provides a relatively simple case which can be examined with the dressed states model, without great mathematical complexity. This allows another comparison to the adiabatic approach, and further validates that model. For the dressed states calculation, consider the energy level diagram of figure 13. Beat signals can occur when there is the possibility of transitions from a level in each of the two excited state ladders to a common level in the ground state ladder. In figure 13, the $|1,n\rangle$ to $|0,m\rangle$ transition could interfere with the $|2,p\rangle$ to $|0,m\rangle$ transition producing a beat signal. Of course, in the dressed state picture, this combination is summed over the entire photon ladder, so the expression for the radiated power from equation (2.20),

$$P = \frac{4}{3c^3} \sum_{n,p} \omega_{nm}^2 \omega_{pm}^2 \mu_{nm} \cdot \mu_{pm}^* \rho_{pn}^H e^{i\omega_{np}t} e^{-At} \quad (4.37)$$

is summed over the combined atom-field states. The n and p indices each refer to the excited state ladders and m represents the ground state ladder.

When performing the summation, there are two cases of interest for the dipole operator, transitions from the first excited atomic state, which is Stark shifted, to the ground state, and those from the second excited state to the ground state. The dipole matrices can be simplified, using equation (3.110) to define the energy states, resulting in

$$\langle \overline{2,n} | \hat{\mu} | \overline{0,m} \rangle = \mu_{20} \delta_{nm} \quad (4.38a)$$

$$\langle \overline{1,n} | \hat{\mu} | \overline{0,m} \rangle = \mu_{10} J_{m-n} \left(\frac{\Omega}{\nu} \right) \quad (4.38b)$$

With the approximation $\omega_{nm} = \omega_{pm} = \omega_0$, equation (4.37) becomes

$$P = \frac{4\omega_0^4}{3c^3} \sum_{n, p > n} \left\{ |\mu_{20}|^2 \delta_{nm} \delta_{pm} \rho_{2p2n}^H e^{i(n-p)\nu t} + |\mu_{10}|^2 J_{m-n} J_{m-p} \rho_{1p1n}^H e^{i(n-p)\nu t} \right. \\ \left. + \mu_{10} \cdot \mu_{20}^* J_{m-n} \delta_{pm} \rho_{2p1n}^H e^{i[\omega_{12} + (n-p)\nu]t} \right. \\ \left. + \mu_{20} \cdot \mu_{10}^* J_{m-n} \delta_{pm} \rho_{1p2n}^H e^{-i[\omega_{12} + (n-p)\nu]t} \right\} e^{-At} \quad (4.39)$$

where the term ρ_{2p1n}^H represent the density matrix element between states $|2, p\rangle$ and $|1, n\rangle$. The first term in the summation reduces to

$$\sum_n |\mu_{20}|^2 \rho_{2m2m}^H = \sum_n |\mu_{20}|^2 P_{2m} = |\mu_{20}|^2 P_2 \quad (4.40)$$

where P_{2m} is the probability of being in state $|2, m\rangle$. Using the relation

$\sum_m J_{m-n} J_{m-p} = \delta_{np}$ [9] produces a similar result in the second term of the summation:

$$\sum_n |\mu_{10}|^2 \rho_{1n1n}^H = |\mu_{10}|^2 P_1 \quad (4.41)$$

This leaves the last two terms, which are similar to the last two terms of equation (4.33). The primary difference is in the density matrix ρ_{2p1n}^H which depends on the probability distribution in the two excited state ladders. To show equivalence between equations (4.33) and (4.39), first change the summation indices such that the combinations are summed over all decay pairs q with a constant difference in photon state $r = p - n$:

$$\sum_{n, p} \mu_{10} \cdot \mu_{20}^* J_{p-n} \rho_{2p1n}^H e^{i[\omega_{12} + (n-p)\nu]t} \\ \sum_{r=-\infty}^{\infty} \sum_q \mu_{10} \cdot \mu_{20}^* J_r \rho_{2q+r1q}^H e^{i(\omega_{12} - r\nu)t} \quad (4.42)$$

Consider now the density matrix summation, specifically the term $J_r \sum_q \rho_{2q+r1q}^H$. Since the Bessel function argument is small, the higher order Bessel functions, $|r| \gg 1$, are negligible. Thus, the summation over q need only consider a limited range of r . For a typical photon distribution in a real field, the coefficients of nearby number states will be approximately equal, so

$$J_r \sum_q \rho_{2q+r1q}^H \approx J_r \sum_q \rho_{2q1q}^H \quad (4.43)$$

This last sum is the equivalent of ρ_{21}^H . Equation (4.39) then becomes

$$P = \frac{4\omega_0^4}{3C^3} \left[|\mu_{20}|^2 P_2 + |\mu_{10}|^2 F_1 + \mu_{10}^* \mu_{20} \rho_{21}^H \sum_{n=-\infty}^{\infty} J_r\left(\frac{\Omega_n}{\nu}\right) e^{i(\omega_{12}-r\nu)t} + \mu_{20}^* \mu_{10} \rho_{12}^H \sum_{r=-\infty}^{\infty} J_r\left(\frac{\Omega_r}{\nu}\right) e^{-i(\omega_{12}-r\nu)t} \right] e^{-At} \quad (4.44)$$

which is of the same form as the adiabatic result, equation (4.33).

The dressed states calculation agrees with the adiabatic approach when an assumption is made concerning the photon state distribution. The assumption of equal populations in nearby states is quite reasonable for real fields. This agreement gives greater confidence in the adiabatic approach, which is far simpler, particularly for a quadratic shift or for level crossing calculations.

Quadratic Stark Shift. When a quadratic Stark shift is present, the instantaneous energy difference between upper levels is represented by the frequency given in equation (4.22)

$$\omega_{12}(t) = \omega_{12} + \Omega' \cos^2 \nu t \quad (4.45)$$

where $\Omega' \equiv \frac{\omega_2 \Omega_1^2 - \omega_1 \Omega_2^2}{\omega_1 \omega_2}$. Notice that if $\Omega_1 \approx \Omega_2$, then $\Omega' \approx 0$ and there would be no beating effect. Similar to the development in the linear case, the exponential term in equation (4.30) becomes

$$\begin{aligned} e^{i \int_0^t \omega_{12}(t') dt'} &= e^{i \omega_{12} t} e^{i \Omega' \int_0^t \cos^2 \nu t' dt'} \\ &= e^{i \omega_{12} t + i \frac{\Omega'}{2} t + i \frac{\Omega'}{4 \nu} \sin 2 \nu t} \\ &= \sum_n J_n\left(\frac{\Omega'}{2 \nu}\right) e^{i(\omega_{12} + \frac{\Omega'}{2} + 2n\nu)t} \end{aligned} \quad (4.46)$$

This is similar to equation (4.32) in the linear case, except the beat frequencies are at even harmonics of ν , given by $\omega_{12} + \frac{\Omega'}{2} + 2n\nu$. Also, there is a slight shift in the fundamental frequency by the amount $\frac{\Omega'}{2}$.

Using equation (4.46), the power radiated is

$$\begin{aligned} P = & \left\{ \frac{4\omega_{20}^4 |\mu_{20}|^2}{3c^3} P_2 + \frac{4\omega_{10}^4 |\mu_{10}|^2}{3c^3} P_1 \right. \\ & + \frac{4\omega_{20}^2 \omega_{10}^2}{3c^3} \left[\mu_{10}^* \mu_{20} \rho_{21}^H \sum_n J_n\left(\frac{\Omega'}{2 \nu}\right) e^{i(\omega_{12} + \frac{\Omega'}{2} + 2n\nu)t} \right. \\ & \left. \left. + \mu_{20}^* \mu_{10} \rho_{12}^H \sum_n J_n\left(\frac{\Omega'}{2 \nu}\right) e^{i(\omega_{12} + \frac{\Omega'}{2} + 2n\nu)t} \right] \right\} e^{-At} \end{aligned} \quad (4.47)$$

Beats at frequencies other than ω_{12} are expected to be much smaller than the linear case since Ω' is small compared to Ω_ν . The dominant term in the expansion is then $J_0(\frac{\Omega'}{2 \nu})$. To evaluate the possibility of beats at other frequencies, first consider Ω' . For Ω' to be non-zero, the individual Rabi frequencies Ω_1 and Ω_2 can not be equal, so $\mu_{10} \neq \mu_{20}$. In this case, assume the dipole moments differ by a constant, or

$\mu_{20} = K\mu_{10}$. Also, as before, let $\omega_{10} \approx \omega_{20}$ and $P_1 = P_2 = \rho_{12}^H = \rho_{21}^H$. Then, equation (4.47) becomes

$$P = P_0 e^{-At} \left[1 + K^2 + 2K \sum_n J_n\left(\frac{\Omega'}{2\nu}\right) \cos\left(\omega_{12} + \frac{\Omega'}{2} + 2n\nu\right)t \right] \quad (4.48)$$

To observe beats resulting from the Townes-Merritt interaction, consider again the effective bandwidth BW. If there is a value m for which

$$\omega_{12} + \frac{\Omega'}{2} + 2m\nu < BW \quad (4.49)$$

then an amplitude modulation in the decay curve at that frequency could be observed. The power radiated would then be

$$P = P_0 e^{-At} \left[1 + K^2 + 2K J_m\left(\frac{\Omega'}{2\nu}\right) \cos\left(\omega_{12} + \frac{\Omega'}{2} + 2m\nu\right)t \right] \quad (4.50)$$

It is anticipated that this modulation would be much less than in linear case due to a small Ω' and the factor K. Here the modulation amplitude would be

$$M_Q = \frac{2K J_m\left(\frac{\Omega'}{2\nu}\right)}{1 + K^2} \quad (4.51)$$

as opposed to the linear case where

$$M_L = J_m\left(\frac{\Omega}{\nu}\right) \quad (4.52)$$

Nonetheless, equations (4.36) and (4.50) demonstrate the possibility of quantum beats which result from interaction with the RF field.

The additional beat signals result from an effective splitting of the excited states due to the nonresonant RF field. When any one of the levels in an excited state ladder comes close to a level in the other excited state ladder, a beat signal in the radiative decay could be observed. The magnitude of this modulation depends primarily on the RF field strength and the experimental setup, as will be discussed in the next chapter.

Level Crossings

If the two excited states have the same energy, a level crossing condition exists, whether the crossing is the normal occurrence or a result of an energy shift of one or both levels. When a crossing occurs, the two possible transitions can interfere causing a shift in the atomic fluorescence pattern, as compared to the uncrossed situation. The interference is heavily dependent on the specific transitions involved and the observation angle. From equation (2.23), with the atom at the origin, the radiated energy as a function of the point of observation is given by

$$S = \frac{(r^2 \delta_{ij} - x_i x_j)}{2\pi c^3 r^4} \sum_{n, p \gg m} \omega_{nm}^2 \omega_{pm}^2 \mu_{nm}^i \mu_{pm}^{j*} \rho_{pn}(t) \quad (4.53)$$

Note the Einstein summation notation is used for the i and j indices. This section will explore level crossings resulting from an interaction with the RF field. As previously discussed, the RF field causes an effective splitting of the atomic levels, which is easily seen with the dressed states model. However, for mathematical simplicity, the calculations here will follow the adiabatic approach in defining the atomic dynamics, which has compared favorably with the dressed states result in simpler cases. Both the linear and the quadratic Stark shift will be covered, with equations (4.12) and (4.21) used to describe the atom in the RF field for their

respective cases. The approach is similar to that used in the case of quantum beats.

For the three level atom, the sum in equation (4.53) reduces to four terms:

$$S = \frac{(r^2 \delta_{ij} - x_i x_j)}{2\pi c^3 r^4} \omega_0^4 \left[\mu_{20}^i \mu_{20}^{j*} P_2 e^{-At} + \mu_{10}^i \mu_{10}^{j*} P_1 e^{-At} + \mu_{10}^i \mu_{20}^{j*} \rho_{21}(t) + \mu_{20}^i \mu_{10}^{j*} \rho_{12}(t) \right] \quad (4.54)$$

assuming $\omega_{10} \approx \omega_{20}$. In evaluating this equation, the geometry of the experiment and the dipole moments of the specific transitions involved become very important. With regard to the experimental geometry, the orientation of the excitation pulse polarization and the viewing angle are critical parameters. Geometries which yield the greatest effects will be considered here. The transition dipole moments impact the degree of interference, in much the same way as the orientation of radiating elements in an array determine the overall antenna pattern. Three possible combinations for the two transitions will be covered.

For a dipole transition, the moment can be written as

$$\mu_{nm} = \langle n | \hat{\mu} | m \rangle = \mu_{nm} \epsilon \quad (4.55)$$

where ϵ is a unit vector in the direction of μ . The orientation of ϵ influences the initial excitation and determines the polarization of the emitted radiation. This orientation depends on the initial and final orbital quantum numbers, l , and magnetic quantum numbers, m [8]. Table 1 summarizes the possibilities. For the transition in which the magnetic quantum numbers remain the same, the dipole moment is oriented in the z direction and radiation would then be linearly polarized in the same direction if view in the xy plane. The other cases result in circular polarization if viewed along the z axis. Note that even though these transitions are

Quantum Numbers		Dipole Moment
Orbital	Magnetic	
$l' = l \pm 1$	$m' = m$	$\mu_{nm}z$
$l' = l \pm 1$	$m' = m - 1$	$\mu_{nm}(x + iy)/\sqrt{2} \equiv \mu_{nm}\epsilon_+$
$l' = l \pm 1$	$m' = m + 1$	$\mu_{nm}(x - iy)/\sqrt{2} \equiv \mu_{nm}\epsilon_-$

Table 1. Transition Dipole Moments. Initial state is defined by l and m .

considered orthogonal, at other viewing angles, the radiation from these transitions do not have a simple polarization, and thus may interfere with each other. With regard to the initial excitation, the orientation of the excitation pulse, relative to the dipole moments, determines the initial values of the density matrix elements. For example, to excite a transition with the dipole moment in the z direction, the pulse should optimally be polarized in the z direction.

When the atom decays, the degree of interference depends on the relative orientation of the dipole moments. The three cases to be considered are

- 1) ϵ_+, ϵ_-
- 2) ϵ_+, z
- 3) z, z

These are representative of all possible combinations, and each case will be considered for both the linear and the quadratic shifts. In each of these case, an optimal orientation for the excitation pulse and the viewing angle will be specified.

Linear Stark Shift. As in the case of quantum beats, the diagonal elements of the density matrix represent the probability of the atom being in the given energy state. From equations (4.27), these are

$$\rho_{22}(t) = P_2 e^{-At} \quad (4.56a)$$

$$\rho_{11}(t) = P_1 e^{-At} \quad (4.56b)$$

The off diagonal elements ρ_{21} and ρ_{12} represent the interference, and are critical to the level crossing effect. These are complex conjugates, so only one will be treated explicitly. Recall from equation (4.28),

$$\rho_{21}(t) = \rho_{21}^H e^{-At} e^{i \int_0^t \omega_{12}(t') dt'} \quad (4.57)$$

For a linear Stark shift, the instantaneous frequency difference is

$\omega_{12}(t) = \omega_{12} - \Omega \cos \nu t$. Using equation (4.32), the second exponential term then reduces to a Bessel function series:

$$\rho_{21}(t) = \rho_{21}^H e^{-At} \sum_n J_n\left(\frac{\Omega}{\nu}\right) e^{i(\omega_{12} - n\nu)t} \quad (4.58)$$

Equation (4.54) then becomes

$$S = \frac{(r^2 \delta_{ij} - x_i x_j)}{2\pi c^3 r^4} \omega_0^4 \left[\mu_{20}^i \mu_{20}^{j*} P_2 + \mu_{10}^i \mu_{10}^{j*} P_1 + \mu_{10}^i \mu_{20}^{j*} \rho_{21}^H \sum_n J_n\left(\frac{\Omega}{\nu}\right) e^{i(\omega_{12} - n\nu)t} + \mu_{20}^i \mu_{10}^{j*} \rho_{12}^H \sum_n J_n\left(\frac{\Omega}{\nu}\right) e^{-i(\omega_{12} - n\nu)t} \right] e^{-At} \quad (4.59)$$

Further evaluation requires expressions for the the dipole moments and the initial density matrix, which depend on the specific combination of dipole moments. The three cases previously discussed will be covered here.

Case 1: First let the two dipole moments be given by

$$\mu_{10} = \mu_0 \epsilon_+ = \mu_0(x + iy)/\sqrt{2} \quad (4.60a)$$

$$\mu_{20} = \mu_0 \epsilon_- = \mu_0(x - iy)/\sqrt{2} \quad (4.60b)$$

Also, define the position coordinates using the standard spherical coordinate system:

$$\begin{aligned} x_1 &= r \sin \theta \cos \phi \\ x_2 &= r \sin \theta \sin \phi \\ x_3 &= r \cos \theta \end{aligned} \quad (4.61)$$

With these expressions, the summations over i and j in equation (4.59) can be reduced. Table 2 lists the individual terms involved in the summations.

$$\begin{aligned} \delta_{ij} \mu_{10}^i \mu_{10}^{j*} &= \delta_{ij} \mu_{20}^i \mu_{20}^{j*} = \mu_0^2 \\ \delta_{ij} \mu_{10}^i \mu_{20}^{j*} &= \delta_{ij} \mu_{20}^i \mu_{10}^{j*} = 0 \\ x_i x_j \mu_{10}^i \mu_{10}^{j*} &= \frac{r^2 \mu_0^2}{2} \sin^2 \theta \\ x_i x_j \mu_{20}^i \mu_{20}^{j*} &= \frac{r^2 \mu_0^2}{2} \sin^2 \theta \\ x_i x_j \mu_{10}^i \mu_{20}^{j*} &= \frac{r^2 \mu_0^2}{2} \sin^2 \theta e^{i2\phi} \\ x_i x_j \mu_{20}^i \mu_{10}^{j*} &= \frac{r^2 \mu_0^2}{2} \sin^2 \theta e^{-i2\phi} \end{aligned}$$

Table 2. Dipole Moment Products for Case 1.

The radiated power as a function of observation angle is then

$$S = \frac{\mu_0^2 \omega_0^4}{4\pi c^3 \Gamma^4} \left[(1 + \cos^2 \theta)(P_2 + P_1) - \sin^2 \theta \left[e^{i2\phi} \rho_{21}^H \sum_n J_n\left(\frac{\Omega}{\nu}\right) e^{i(\omega_{12} - n\nu)t} + e^{-i2\phi} \rho_{12}^H \sum_n J_n\left(\frac{\Omega}{\nu}\right) e^{-i(\omega_{12} - n\nu)t} \right] \right] e^{-\Lambda t} \quad (4.62)$$

Next, expressions for the initial density matrix elements are required. These depend on the orientation of the excitation pulse. An element of the density matrix can be written as

$$\rho_{np}^H = a_n a_p^* \quad (4.63)$$

where a_n is the wave function coefficient corresponding to the atomic state $|n\rangle$ after initial excitation. For the excited states, a_n is given by

$$a_n = i\epsilon \cdot \mu_{n0} Q \quad (4.64)$$

where ϵ is the polarization of the excitation pulse, and Q is the area of the pulse, specifically given by $Q = \frac{1}{\hbar} \int \mathcal{E}(t) dt$. This assumes a short pulse of frequency ω and duration T , such that $(\omega_{n0} - \omega)T \ll 1$.

Let the excitation pulse be linearly polarized in the y direction, so $\epsilon = y$, which will equally excite both transitions. Figure 14 shows the orientation for this case. The initial values for the density matrix are then

$$P_1 = P_2 = \frac{\mu_0^2 Q^2}{2} \quad (4.65a)$$

$$\rho_{21}^H = \rho_{12}^H = -\frac{\mu_0^2 Q^2}{2} \quad (4.65b)$$

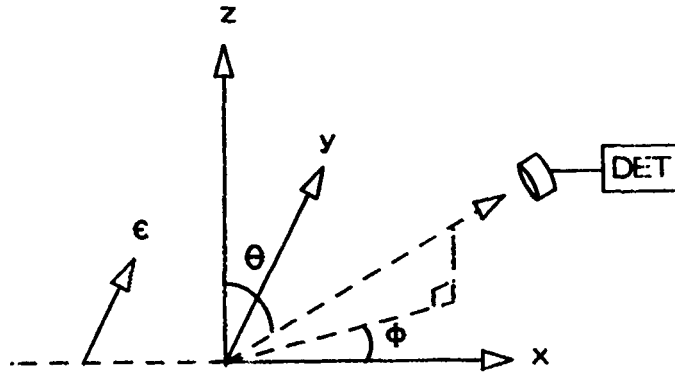


Figure 14. Level Crossing Geometry

Substituting the density matrix terms into equation (4.62) yields

$$S = \frac{\omega_0^4 \mu_0^4 Q^2}{4\pi c^3 \Gamma^2} e^{-\Lambda t} \left[(1 + \cos^2 \theta) + \sin^2 \theta \sum_n J_n\left(\frac{\Omega_\nu}{\nu}\right) \cos(\omega_{12}t - n\nu t - 2\phi) \right] \quad (4.66)$$

Integrating S over time gives the total energy radiated by the atom in the direction specified by θ and ϕ :

$$\begin{aligned} \mathcal{I} &= \int_0^\infty S(t) dt \\ &= \left\{ \frac{\omega_0^4 \mu_0^4 Q^2}{4\pi c^3 \Gamma^2} \right\} \left[\frac{1 + \cos^2 \theta}{\Lambda} + \sin^2 \theta \sum_n J_n\left(\frac{\Omega_\nu}{\nu}\right) \frac{A \cos 2\phi + (\omega_{12} - n\nu) \sin 2\phi}{(\omega_{12} - n\nu)^2 + \Lambda^2} \right] \quad (4.67) \end{aligned}$$

This result is useful in predicting the radiated energy as a function of the RF frequency, ν . Level crossings occur when $\omega_{12} - n\nu = 0$, which agrees with the dressed states picture. When a level crossing condition exists, there is a maximum in the interference term, depending on the observation angle, with relative magnitude $J_n(\frac{\Omega_\nu}{\nu})$.

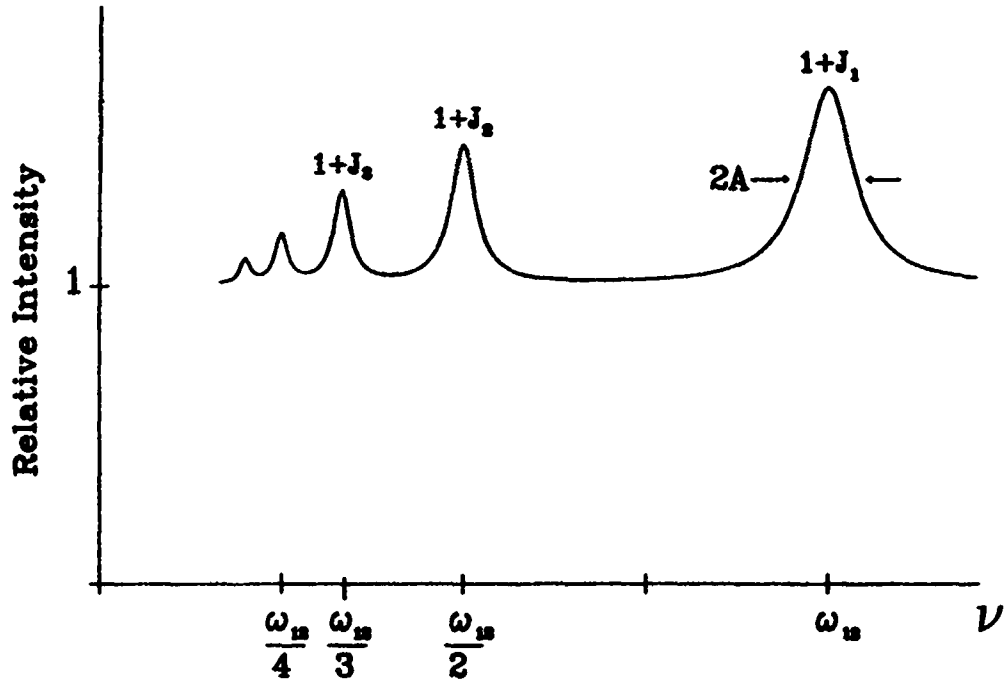


Figure 15. Level Crossing Signal for a Linear Stark Shift

For an example of a possible experimental geometry, let the observation angle be defined by $\theta = \frac{\pi}{2}$, $\phi = 0$. Then

$$J = J_0 \left[1 + \sum_n J_n \left(\frac{\Omega_n}{\nu} \right) \frac{A^2}{\Lambda_n^2 + A^2} \right] \quad (4.68)$$

where $J_0 \equiv \frac{\mu_0^4 \omega_0^4 Q^2}{4 \pi c^3 \Gamma^2 A}$ and $\Lambda_n^2 \equiv (\omega_{12} - n\nu)^2$. This indicates a series of peaks in the radiated energy as ν changes. Figure 15 shows a representative level crossing signal for this case. When $m\nu \approx \omega_{12}$, then for $n \neq m$, the interference term is negligible since $\frac{A^2}{\Lambda_n^2 + A^2} \ll 1$:

$$J = J_0 \left[1 + J_m \left(\frac{\Omega_m}{\nu} \right) \frac{A^2}{\Lambda_m^2 + A^2} \right] \quad (4.69)$$

This represents the signal strength near one of the peaks, and is similar to the

original level crossing calculation, equation (2.29). The magnitude of the peak is $J_{\max} = J_o[1 + J_m(\frac{\Omega}{\nu})]$ and the width is approximately $\frac{2A}{m}$. This becomes the basis for using a nonresonant RF field as a spectroscopic tool. If the peaks can be detected, then the values of ν at which the crossings occur determine the original energy level spacing. Note that other viewing angles will produce different types of level crossing curves than figure 15.

Case 2: When the relevant transitions have dipole moments given by

$$\mu_{10} = \mu_o \epsilon_+ \quad (4.70a)$$

$$\mu_{20} = \mu_o \epsilon_- \quad (4.70b)$$

the potential interference effect is expected to be diminished. This compares to antennae placed along orthogonal axes; there is limited overlap between the beam patterns. Table 3 lists the dipole products for this case.

$$\begin{aligned} \delta_{ij} \mu_{10}^i \mu_{10}^{j*} &= \delta_{ij} \mu_{20}^i \mu_{20}^{j*} = \mu_o^2 \\ \delta_{ij} \mu_{10}^i \mu_{20}^{j*} &= \delta_{ij} \mu_{20}^i \mu_{10}^{j*} = 0 \\ x_i x_j \mu_{10}^i \mu_{10}^{j*} &= \frac{r^2 \mu_o^2}{2} \sin^2 \theta \\ x_i x_j \mu_{20}^i \mu_{20}^{j*} &= r^2 \mu_o^2 \cos^2 \theta \\ x_i x_j \mu_{10}^i \mu_{20}^{j*} &= \frac{r^2 \mu_o^2}{2\sqrt{2}} \sin 2\theta e^{i\phi} \\ x_i x_j \mu_{20}^i \mu_{10}^{j*} &= \frac{r^2 \mu_o^2}{2\sqrt{2}} \sin 2\theta e^{-i\phi} \end{aligned}$$

Table 3. Dipole Moment Products for Case 2.

Substitution of the dipole products into equation (4.59) results in

$$S = \frac{\mu_0^2 \omega_0^4}{2\pi c^3 r^4} \left[(1 - \cos^2 \theta) P_2 + (1 - \frac{\sin^2 \theta}{2}) P_1 - \frac{\sin 2\theta}{2\sqrt{2}} \left[e^{i\phi} \rho_{21}^H \sum_n J_n(\frac{\Omega_\nu}{\nu}) e^{i(\omega_{12} - n\nu)t} + e^{-i\phi} \rho_{12}^H \sum_n J_n(\frac{\Omega_\nu}{\nu}) e^{-i(\omega_{12} - n\nu)t} \right] \right] e^{-At} \quad (4.71)$$

This shows that there is no interference for $\theta = 0, \frac{\pi}{2}$, which is consistent with the antenna analogy. Further, to obtain excitation of both levels, the initial pulse would have to be linearly polarized at an angle between the z axis and the xy plane.

For the excitation pulse, let $\epsilon = (y + z)/\sqrt{2}$, a 45 degree angle to the z axis. The initial values for the density matrix are then

$$P_1 = \frac{\mu_0^2 Q^2}{4} \quad (4.72a)$$

$$P_2 = \frac{\mu_0^2 Q^2}{2} \quad (4.72b)$$

$$\rho_{21}^H = -\frac{\mu_0^2 Q^2}{2\sqrt{2}} \quad (4.72c)$$

$$\rho_{12}^H = \frac{\mu_0^2 Q^2}{2\sqrt{2}} \quad (4.72d)$$

The expression for radiated power then becomes

$$S = \frac{\mu_0^4 \omega_0^4 Q^2}{4\pi c^3 r^4} \left[\frac{1}{2} + \frac{3\sin^2 \theta}{4} - \frac{\sin 2\theta}{4} \sum_n J_n(\frac{\Omega_\nu}{\nu}) \sin(\omega_{12}t - n\nu t + \phi) \right] e^{-At} \quad (4.73)$$

Integration results in

$$\mathcal{J} = \left\{ \frac{\omega_0^4 \mu_0^4 Q^2}{4\pi c^3 r^4} \right\} \left[\frac{2+3\sin^2 \theta}{4A} - \frac{\sin 2\theta}{4} \sum_n J_n(\frac{\Omega_\nu}{\nu}) \frac{A \sin \phi + (\omega_{12} - n\nu) \cos \phi}{(\omega_{12} - n\nu)^2 + A^2} \right] \quad (4.74)$$

which is similar to equation (4.67) in case 1. Again, maxima will occur whenever

$\omega_{12} - n\nu = 0$, coinciding with the level crossings.

If the detector is placed at $\theta = \frac{\pi}{4}$, $\phi = -\frac{\pi}{2}$, the total energy received is given by

$$J = J_0 \left[\frac{7}{8} + \frac{1}{4} \sum_n J_n \left(\frac{\Omega_n}{\nu} \right) \frac{A^2}{A^2 + \Lambda_n^2} \right] \quad (4.75)$$

The result compares to the previous case, except that the interference effect is reduced by approximately $\frac{1}{4}$. The energy received as a function of ν would look like figure 15, but the magnitude of the peaks is given by

$$J_{\max} = J_0 \left[\frac{7}{8} + \frac{1}{4} J_m \left(\frac{\Omega_m}{\nu} \right) \right] \quad (4.76)$$

The unfavorable geometry is the reason for the lesser effect.

Case 3: The most favorable geometry exists when the transition dipoles have the same orientation:

$$\mu_{10} = \mu_{20} = \mu_0 \hat{z} \quad (4.77)$$

This results in a maximum overlap in the radiation patterns. Using the dipole products given in table 4, the expression for radiated energy becomes

$$S = \frac{\mu_0^2 \omega_0^4}{2\pi c^3 \Gamma^4} e^{-\Lambda t} \left[P_2 + P_1 + \rho_{21}^H \sum_n J_n \left(\frac{\Omega_n}{\nu} \right) e^{i(\omega_{12} - n\nu)t} + \rho_{12}^H \sum_n J_n \left(\frac{\Omega_n}{\nu} \right) e^{-i(\omega_{12} - n\nu)t} \right] \sin^2 \theta \quad (4.71)$$

Notice there is no ϕ dependence.

$$\begin{aligned}
\delta_{ij}\mu_{10}^i\mu_{10}^{j*} &= \delta_{ij}\mu_{20}^i\mu_{20}^{j*} = \mu_0^2 \\
\delta_{ij}\mu_{10}^i\mu_{20}^{j*} &= \delta_{ij}\mu_{20}^i\mu_{10}^{j*} = \mu_0^2 \\
x_i x_j \mu_{10}^i \mu_{10}^{j*} &= x_i x_j \mu_{20}^i \mu_{20}^{j*} = r^2 \mu_0^2 \cos^2 \theta \\
x_i x_j \mu_{10}^i \mu_{20}^{j*} &= x_i x_j \mu_{20}^i \mu_{10}^{j*} = r^2 \mu_0^2 \cos^2 \theta
\end{aligned}$$

Table 4. Dipole Moment Products for Case 3.

The optimum excitation polarization is $\epsilon = z$, in which case

$$P_1 = P_2 = \rho_{21}^H = \rho_{12}^H = \mu_0^2 Q^2 \quad (4.79)$$

Equation (4.78) then becomes

$$S = \frac{\mu_0^4 \omega_0^4 Q^2}{\pi c^3 r^4} e^{-At} \left[1 + \sum_n J_n \left(\frac{\Omega_n}{\nu} \right) \cos(\omega_{12} - n\nu)t \right] \sin^2 \theta \quad (4.80)$$

Once again, integration results in

$$\mathcal{J} = \left\{ \frac{\omega_0^4 \mu_0^4 Q^2}{\pi c^3 r^2} \right\} \left[\frac{1}{A} + \sum_n J_n \left(\frac{\Omega_n}{\nu} \right) \frac{A}{A^2 + \Lambda_n^2} \right] \sin^2 \theta \quad (4.81)$$

It is obvious that the maximum radiation occurs for $\theta = \frac{\pi}{2}$. As in the previous two cases, peaks occur when $\Lambda_n = \omega_{12} - n\nu = 0$, and in this case have magnitude

$$\mathcal{J}_{\max} = 4\mathcal{J}_0 [1 + J_m \left(\frac{\Omega_m}{\nu} \right)] \quad (4.82)$$

This compares favorably with the first case, having the same relative magnitudes between the peaks and the background, but this case has a larger absolute value.

<u>I</u>	$\mu_{10} = \mu_0 \epsilon_+$ $\mu_{20} = \mu_0 \epsilon_-$	$\epsilon = y$	$\theta = \pi/2$ $\phi = 0$
$\mathcal{J} = \mathcal{J}_0 \left[1 + \sum_n J_n \left(\frac{\Omega}{\nu} \right) \frac{A}{A^2 + \Lambda_n^2} \right]$			
<u>II</u>	$\mu_{10} = \mu_0 \epsilon_+$ $\mu_{20} = \mu_0 z$	$\epsilon = (y+z)/\sqrt{2}$	$\theta = \pi/4$ $\phi = -\pi/2$
$\mathcal{J} = \mathcal{J}_0 \left[\frac{7}{8} + \frac{1}{4} \sum_n J_n \left(\frac{\Omega}{\nu} \right) \frac{A}{A^2 + \Lambda_n^2} \right]$			
<u>III</u>	$\mu_{10} = \mu_0 z$ $\mu_{20} = \mu_0 z$	$\epsilon = z$	$\theta = \pi/2$
$\mathcal{J} = 4\mathcal{J}_0 \left[1 + \sum_n J_n \left(\frac{\Omega}{\nu} \right) \frac{A}{A^2 + \Lambda_n^2} \right]$			

Table 5. Level Crossing Signals for a Linear Stark Shift

All three cases for an atom with a linear Stark shift of an excited state exhibit changes in the fluorescence resulting from the RF field. Table 5 summarizes the results for each case with a specific geometry. Recall, $\mathcal{J}_0 \equiv \frac{\mu_0^4 \omega_0^4 Q^2}{4\pi C^3 \Gamma^2}$ and $\Lambda_n \equiv \omega_{12} - n\nu$. In these results, the presence of a maximum indicates a level crossing condition. Other observation angles can result in different level crossing signals, for example a decrease in the energy received as the levels cross. In any case, if these can be measured, then the original energy separation can be determined by the RF frequencies at which crossings occurred. The magnitude of the Bessel function terms, $J_n(\frac{\Omega}{\nu})$, will be key in determining whether the peaks can be detected. Overall though, the linear case presents the best opportunity for observing the level

crossings, when compared to quadratic shifts, as will be shown.

Quadratic Stark Shift. For an atom with a quadratic Stark shift, the off diagonal density matrix elements are given by

$$\rho_{21}(t) = \rho_{21}^H e^{-\Lambda t} e^{i \int_0^t \omega_{12}(t') dt'} \quad (4.83)$$

where $\omega_{12}(t) = \omega_{12} + \Omega' \cos^2 \nu t$ and $\Omega' \equiv \frac{\omega_2 \Omega_1^2 - \omega_1 \Omega_2^2}{\omega_1 \omega_2}$. Using the Bessel function expansion, this becomes

$$\rho_{21}(t) = \rho_{21}^H e^{-\Lambda t} \sum_n J_n\left(\frac{\Omega'}{2\nu}\right) e^{i(\omega_{12} + \frac{\Omega'}{2} + 2n\nu)t} \quad (4.84)$$

Notice that this is of the same form as the linear Stark case, equation (4.58), except for the Bessel function argument and that only even harmonics of the RF frequency are included. As in the section on quantum beats, if $\Omega_1 \approx \Omega_2$, then $\Omega' \approx 0$ and there would be a negligible effect at level crossing, since the only significant term would be $J_0(\frac{\Omega'}{2\nu}) \approx 1$. Thus, once again, it is assumed the magnitudes of the dipole moments differ by a constant, such that $|\mu_{20}| = K |\mu_{10}|$.

Substitution of equation (4.84) into equation (4.54) yields an expression for the radiated power:

$$S = \frac{(r^2 \delta_{ij} - x_i x_j)}{2\pi c^3 r^4} \omega_0^4 \left[\mu_{20}^i \mu_{20}^{j*} P_2 + \mu_{10}^i \mu_{10}^{j*} P_1 + \mu_{10}^i \mu_{20}^{j*} \rho_{21}^H \sum_n J_n\left(\frac{\Omega'}{2\nu}\right) e^{i\Lambda_n' t} + \mu_{20}^i \mu_{10}^{j*} \rho_{12}^H \sum_n J_n\left(\frac{\Omega'}{2\nu}\right) e^{-i\Lambda_n' t} \right] e^{-\Lambda t} \quad (4.85)$$

<u>I</u> $\mu_{10} = \mu_0 \epsilon_+$ $\mu_{20} = \mu_0 \epsilon_-$	$\epsilon = y$
$J = J_0 \left[(1 + \cos^2 \theta)(1 + K^4) + K^2 \sin^2 \theta \sum_n J_n \left(\frac{\Omega'}{2\nu} \right) \frac{A^2 \cos 2\phi + A \Lambda_n' \sin 2\phi}{A^2 + \Lambda_n'^2} \right]$	
$\theta = \pi/2, \phi = 0$	
$J = J_0 \left[1 + K^4 + K^2 \sum_n J_n \left(\frac{\Omega'}{2\nu} \right) \frac{A^2}{A^2 + \Lambda_n'^2} \right]$	
<u>II</u> $\mu_{10} = \mu_0 \epsilon_+$ $\mu_{20} = \mu_0 z$	$\epsilon = (y+z)/\sqrt{2}$
$J = J_0 \left[\frac{2 + (4K^4 - 1)\sin^2 \theta}{4} - \frac{K^2 \sin 2\theta}{4} \sum_n J_n \left(\frac{\Omega'}{2\nu} \right) \frac{A^2 \sin \phi + A \Lambda_n' \cos \phi}{A^2 + \Lambda_n'^2} \right]$	
$\theta = \pi/4, \phi = -\pi/2$	
$J = J_0 \left[\frac{2 + (4K^4 - 1)}{8} + \frac{K^2}{4} \sum_n J_n \left(\frac{\Omega'}{2\nu} \right) \frac{A^2}{A^2 + \Lambda_n'^2} \right]$	
<u>III</u> $\mu_{10} = \mu_0 z$ $\mu_{20} = \mu_0 z$	$\epsilon = z$
$J = 2J_0 \left[1 + K^4 + 2K^2 \sum_n J_n \left(\frac{\Omega'}{2\nu} \right) \frac{A}{A^2 + \Lambda_n'^2} \right] \sin^2 \theta$	
$\theta = \pi/2$	
$J = 2J_0 \left[1 + K^4 + 2K^2 \sum_n J_n \left(\frac{\Omega'}{2\nu} \right) \frac{A^2}{A^2 + \Lambda_n'^2} \right]$	

Table 6. Level Crossing Signals for a Quadratic Stark Shift

where $\Lambda_n' \equiv \omega_{12} + \frac{\Omega'}{2} + 2n\nu$. This is comparable to equation (4.59) of the linear case; hence, the results for the three combinations previously considered would be similar here. These are summarized in table 6.

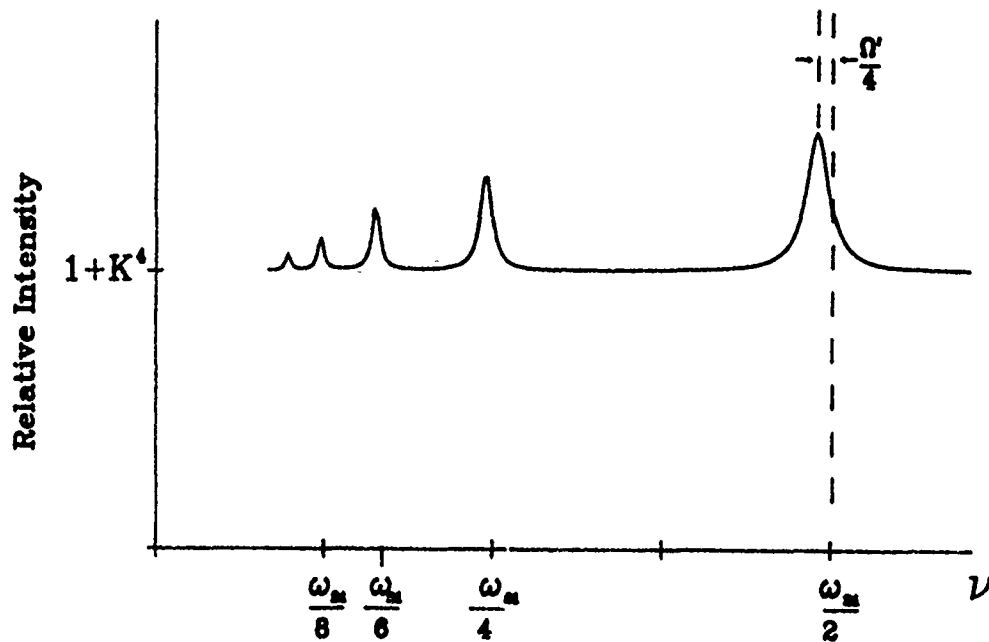


Figure 16. Level Crossing Signal for a Quadratic Stark Shift

In each case, the energy received varies as a function of ν , as a result of level crossings. Peaks occur when $\Lambda'_n = \omega_{12} + \frac{\Omega'}{2} + 2n\nu = 0$, with relative maxima determined by $J_n(\frac{\Omega'}{2\nu})$. Figure 16 shows the received energy versus RF frequency for case 1. This is very similar to the linear case, except the peaks occur at half the frequency, reflecting the even harmonics of the RF frequency. In addition, each peak is shifted slightly from even fractions of ω_{21} by the amount $\frac{\Omega'}{4n}$ due to the static Stark shift. The width of each peak is $\frac{\Lambda}{n}$, again making this potentially useful for high resolution spectroscopy. A noteworthy point is that this technique would be relatively doppler free. Normally, the doppler effect results in a significant line broadening; however, in this case, the level shifts result from interaction with the RF field. Doppler shifts at RF frequencies are very small compared to the transition frequency.

Limiting factors are the relative magnitudes of the dipole moments, indicated by the constant K , and the magnitude of the Bessel function coefficients $J_n(\frac{\Omega'}{2\nu})$. These will determine whether the peaks can be detected, and the technique usable.

V. Experimental Feasibility

The previous two chapters presented theoretical descriptions of the Townes—Merritt effect, quantum beats, and level crossings, which was the goal of this dissertation. As a final step, a brief look at some experimental aspects will provide further insight to these phenomena. An example is the field strengths required to observe these effects for a given atomic sample. The intent here is not to describe an experiment, but to give an idea of the feasibility of such an experiment by considering order of magnitude estimates of critical parameters. In the Townes—Merritt effect, the primary concern is the relative magnitude of the sidebands. Experimental requirements for observing the sidebands, in linear and quadratic cases, will be examined, and these conditions will also apply to level crossings and quantum beats. An additional concern in quantum beats is the beat frequency, and for level crossings, the viewing angle is important.

The calculations on the Townes—Merritt effect describe absorption sidebands at integer multiples of the RF frequency for a linear Stark shift and even integer multiples for a quadratic shift, with relative amplitudes of $J_n^2(\frac{\Omega}{\nu})$ and $J_n^2(\frac{\Omega^2}{2\omega_0\nu})$, respectively. In order to observe these sidebands there must be sufficient separation between adjacent signals so that the natural linewidth does not obscure individual sidebands, and the magnitudes governed by the Bessel function terms must be large enough for detection. A condition that $\nu \gg A$ ensures separation of individual sidebands. Typical values for A are on the order of $10^6 \rightarrow 10^9 \text{ sec}^{-1}$, so a nominal value for ν is 10 times A or $10^7 \rightarrow 10^{10} \text{ Hz}$.

The amount of energy in the sidebands is determined by the Bessel function coefficients. For a given sideband to be observable, the magnitude of the associated coefficient should be on the order of $J_n \approx .01 \rightarrow .1$ as a minimum. This then

places a bound on the Bessel function arguments and subsequently defines experimental constraints.

The key term, from an experimental perspective, in the Bessel function arguments is the Rabi frequency, $\Omega_\nu \equiv \frac{\mu \mathcal{E}_\nu}{\hbar}$. The dipole moment for an allowed transition can be approximated as $\mu \approx e a_0$, where a_0 is the Bohr radius, approximately 5×10^{-9} cm. The Rabi frequency can then be written

$$\Omega_\nu = 10^7 \mathcal{E}_\nu \quad (5.1)$$

where \mathcal{E}_ν is the magnitude of the RF field in V/cm. For $\mathcal{E}_\nu = 100 \rightarrow 1000$ V/cm, $\Omega_\nu = 10^9 \rightarrow 10^{10}$ Hz.

Now consider a specific example where $\nu = 10^9$ Hz and $\omega_0 = 5 \times 10^{15}$ Hz. The relative intensities of the sidebands are given by

$$\text{Linear:} \quad J_n^2\left(\frac{\Omega_\nu}{\nu}\right) = J_n^2(10^{-2} \mathcal{E}_\nu) \quad (5.2a)$$

$$\text{Quadratic:} \quad J_n^2\left(\frac{\Omega_\nu^2}{2\omega_0\nu}\right) = J_n^2(10^{-11} \mathcal{E}_\nu^2) \quad (5.2b)$$

This illustrates the significant decrease in effect for the quadratic case, as compared to a linear Stark shift. For an RF field with an amplitude of 100 to 1000 V/cm the argument for the Bessel function in the linear case is between 1 and 10, resulting in a significant amount of energy in the sidebands. Table 7 lists relative intensities for the lower order sidebands in this case.

For the quadratic case, with $\mathcal{E}_\nu = 1000$ V/cm, the sidebands are negligible. The first sideband has a relative intensity of $J_1^2(10^{-5}) \approx 2.5 \times 10^{-11}$. To observe sidebands for a quadratic shift would require very large field strengths in this case, or alternately consider transitions with lower frequencies such that the Bessel

z	$J_0^2(z)$	$J_1^2(z)$	$J_2^2(z)$	$J_3^2(z)$	$J_4^2(z)$	$J_5^2(z)$	$J_6^2(z)$	$J_7^2(z)$
1	.5855	.1936	.0132	.0003				
2	.0501	.3326	.1244	.0166	.0011			
3	.0676	.1149	.2362	.0955	.0174	.0018		
4	.1577	.0043	.1325	.1850	.0790	.0174	.0024	
5	.0315	.1073	.0021	.1331	.1530	.0681	.0171	.0028
6	.0226	.0765	.0589	.0131	.1279	.1311	.0604	.0167
7	.0900	.0000	.0908	.0280	.0249	.1210	.1150	.0545
8	.0294	.0550	.0127	.0847	.0111	.0345	.1139	.1027
9	.0081	.0601	.0209	.0327	.0704	.0030	.0417	.1072
10	.0604	.0018	.0648	.0034	.0482	.0547	.0002	.0469

Table 7. Sideband Intensities for a Linear Stark Shift

function arguments are near unity.

In determining a feasible range for the Townes–Merritt effect consider the relationships between ω_0 , A , and ν . As previously discussed, the RF frequency should be greater than the atomic decay rate, on the order of $\nu \approx 10A$, to break out individual sidebands. Further, the A coefficient is dependent on the transition frequency [23]:

$$A = \frac{\omega_0^3 \mu^2}{3\pi\epsilon_0 \hbar c^3} \quad (5.3)$$

in SI units. Again assuming $\mu \approx ea_0$, this can be simplified to $A \approx 3 \times 10^{-40} \omega_0^3$.

Thus, for a given transition frequency, the optimum RF frequency can be determined and subsequently, as in equations (5.2), the required field strength.

As an example, consider the hydrogen atom 1S to 2P transition. The 2P level exhibits a linear Stark shift due to mixing between the 2S and 2P states [32], resulting in energy shifts for the two states of $\pm 3ea_0\mathcal{E}$. The transition frequency is approximately $\omega_0 \approx 10^{16}\text{Hz}$ and the decay rate is about $6 \times 10^8\text{Hz}$. A reasonable choice for the RF frequency is then $\nu = 3 \times 10^9\text{Hz}$. The relative intensities of the sidebands in this case are given by equation (5.2a), $J_n^2(10^{-2}\mathcal{E}_\nu)$. Table 7 lists the intensities for typical values of \mathcal{E}_ν .

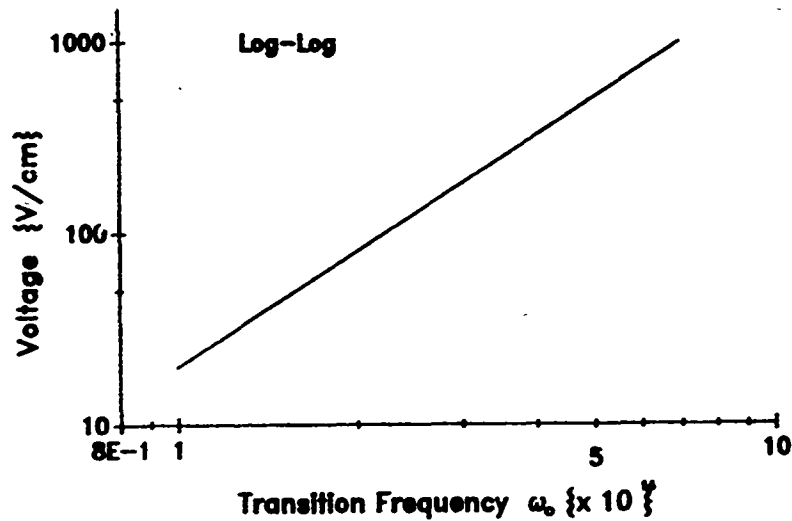


Figure 17. RF Field Strength Required for a Quadratic Shift

For the quadratic case the problem is to determine the approximate range where the effect could be observed for a given maximum field strength, representing an experimental constraint. Assuming $\nu = 10\text{A}$, the Bessel function argument can be rewritten using equation (5.3)

$$\frac{\Omega_{\nu}^2}{2\omega_0\nu} = \frac{3\pi\epsilon_0 c^3}{20\hbar\omega_0^4} \mathcal{E}_{\nu}^2 \approx 10^{52} \frac{\mathcal{E}_{\nu}^2}{\omega_0^4} \quad (5.4)$$

Considering only the first sideband, let $J_1^2(\frac{\Omega_{\nu}^2}{2\omega_0\nu}) > .01$ be the criteria for detection. For small arguments, much less than one, the Bessel function can be approximated as [9]

$$J_n(z) \approx \frac{(z/2)^n}{n!} \quad (5.5)$$

Then if $\mathcal{E} = 1000 \text{ V/cm}$, using equations (5.4) and (5.5), the transition frequency must be $\omega_0 < 5 \times 10^{14} \text{ Hz}$. Following the same approach, figure 17 shows the minimum required field strength for a range of typical transition frequencies.

Higher field strengths would allow higher order sidebands to be observed. Thus, based on these order of magnitude estimates, the effect can be observed in a wide range of potential samples, shown here to have transitions from about the middle of the visible into the infrared.

Another case of interest involves an atom which exhibits a Zeeman shift in the energy levels. This is a linear effect proportional to the magnetic field strength B. The interaction Hamiltonian for the Zeeman effect is

$$\hat{H}' \equiv -\hat{\mu}_m \cdot \hat{B} \quad (5.6)$$

where $\hat{\mu}_m$ is the magnetic moment and \hat{B} is an oscillating magnetic field. Development of the equations of motion is analogous to the linear Stark shift. For a two level atom in which only the excited state is shifted, the interaction Hamiltonian can be written

$$\hat{\mu}_m \cdot \hat{B} = \begin{bmatrix} 0 & 0 \\ 0 & \mu_m \end{bmatrix} B \quad (5.7)$$

The instantaneous transition frequency is then

$$\omega'(t) = \omega_0 - \Omega_b \cos \nu t \quad (5.8)$$

where $\Omega_b \equiv \frac{\mu_m B}{\hbar}$. As in the case of the linear Stark effect, there are absorption sidebands at $\omega_0 + n\nu$ with relative intensity $J_n^2(\frac{\Omega_b}{\nu})$.

To estimate the strength of the sidebands in this case, the magnetic dipole can be approximated by the Bohr magneton, $\mu_m \approx \frac{e\hbar}{2m_e}$. The intensities then depend directly on the B field strength:

$$J_n^2\left(\frac{\Omega_b}{\nu}\right) = J_n^2\left(\frac{eB}{2m_e\nu}\right) \approx J_n^2\left(10^{11} \frac{B}{\nu}\right) \quad (5.9)$$

where B is in webers/m². The primary experimental constraint arises in producing a strong B field at the relatively high frequency ν . The coil inductance limits the maximum field strength at a given frequency.

To analyze this constraint, consider a typical setup in which an AC power supply with a maximum voltage V drives a wire coil to produce a B field at frequency ν . The field strength is given by

$$B = \mu_0 I \frac{N}{l} \sin \theta_m \quad (5.10)$$

where μ_0 is the permeability of free space, I the instantaneous current, N the number of turns, l the length of the coil, and θ_m the angle from the center to the edge of the coil [33]. The current flow is limited by the maximum available voltage V and the coil impedance X_L according to Ohm's Law: $I = V/X_L$. The impedance is equal to the product of the field frequency and the coil inductance, which is

$$L = \mu_0 \frac{N^2}{l} A \quad (5.11)$$

where A is the cross-sectional area of the coil. Thus the maximum B field strength can be expressed as

$$B = \frac{V}{\nu N A} \sin \theta_m \quad (5.12)$$

For a power supply with a maximum voltage of $10^4 V$, and a coil which has $N = 100$, $A = 100 \text{ cm}^2$, and $\theta_m = 30^\circ$, the sideband intensities are given by

$$J_n^2\left(\frac{\Omega_b}{\nu}\right) = J_n^2\left(\frac{10^{15}}{2\nu^2}\right) \quad (5.13)$$

In order for the sidebands to be observable, the Bessel function argument should again be of order unity, so the maximum B field frequency is $\nu \approx 10^7 \rightarrow 10^8$ Hz . The atomic decay coefficient is then an order of magnitude lower, $A \approx 10^6 \rightarrow 10^7$ Hz , and using equation (5.3), the maximum transition frequency is on the order of 10^{15} Hz , which is comparable to the quadratic Stark shift case.

These order of magnitude calculations demonstrate the experimental constraints on observing the Townes–Merritt effect for a Stark or Zeeman shifted atom. As expected, the greatest effect occurs with the linear Stark shift; however, few atoms or molecules exhibit such a shift. The quadratic Stark effect and the Zeeman effect have comparable ranges in which the Townes–Merritt could be observed. These are generally limited by the maximum field strength available. Experimental constraints for level crossings and quantum beats are similar to the Townes–Merritt effect calculations.

Conditions for observing quantum beats in linear and quadratic Stark shifted atoms are similar to those for the Townes–Merritt effect previously discussed. To show this, consider the power radiated by a three level atom in an RF field. For the linear Stark case, this is given by equation (4.34)

$$P = 2P_o e^{-\Lambda t} \left[1 + \sum_n J_n^2\left(\frac{\Omega}{\nu}\right) \cos(\omega_{12} - n\nu)t \right] \quad (5.14)$$

The signal decays exponentially, at rate A , with a superimposed harmonic modulation defined by the terms in the Bessel function series. Oscillations occur with frequency $\omega_{12} - n\nu$ and relative amplitude $J_n(\frac{\Omega}{\nu})$. The modulation factor M_n for a given component is in fact equal to the Bessel function coefficient.

For the beats to be observable, two conditions must be met: the modulation factor has to be large enough to be detected and the beat frequency must be within the measuring capability of the experiment. Much as was discussed in the Townes-Merritt effect, to detect beats resulting from interactions with the sidebands, the Bessel function argument should be at least of order unity, so higher order terms are significant. The conditions on Ω_p and ν are the same here as for the linear shift in the Townes-Merritt effect, resulting in a wide range of possible transitions.

The second consideration is the beat frequency, and the primary concern is the signal bandwidth in the experiment. For example, in a decay rate measurement, the sample is repeatedly excited, then the radiated power is measured during a finite time period Δt which is delayed from the initial excitation. As the delay time is increased, the power received decreases according to the decay curve. The time period Δt establishes a maximum bandwidth, and hence, sets a limit on the measurable beat frequency.

Given a limiting bandwidth, BW, for a particular experimental setup; only those frequencies which are less than that bandwidth are detectable; the others average to zero. For example, assume $BW \approx 50A$ and $\omega_{12} = 100A$. If the RF frequency is on the order of $30A$, then the only measurable beats are those which satisfy

$$|100A - n30A| < 50A \quad (5.15)$$

In this case, $n = 2, 3, 4$, corresponding to beat frequencies of $10A$, $20A$, and $40A$.

It would be possible to adjust the RF frequency and the bandwidth such that only one beat signal is present, and the power radiated would be

$$P = 2P_0 e^{-At} \left[1 + J_n\left(\frac{\Omega_p}{\nu}\right) \cos(\omega_{12} - n\nu)t \right] \quad (5.16)$$

This raises the possibility of using the beat signal to measure the separation between widely separated upper states, with a large ω_{12} .

There is one further observation concerning the beat signals. It is possible that the beat signals resulting from interaction with the RF field could be obscured by the zero field beat signal, ω_{12} . This zero field signal can be eliminated by adjusting the field strength, such that the Bessel function coefficient $J_0(\frac{\Omega}{\nu}) = 0$. The first zero occurs for $\frac{\Omega}{\nu} = 2.4$.

In the case of the quadratic Stark shift, the experimental considerations are very similar to the linear case. From equation (4.48), the power radiated is

$$P = P_0 e^{-\Lambda t} \left[1 + K^2 + 2K \sum_n J_n\left(\frac{\Omega'}{2\nu}\right) \cos(\omega_{21} + \frac{\Omega'}{2} + 2n\nu)t \right] \quad (5.17)$$

The primary differences are the constant of proportionality K (defined by $|\mu_{10}| = K|\mu_{10}|$) and the beat frequencies occur on the even harmonics of ν . In addition, the Rabi frequency is now replaced by Ω' , which is equal to

$$\Omega' = \frac{\omega_2 \Omega_1^2 - \omega_1 \Omega_2^2}{\omega_1 \omega_2} \quad (5.18)$$

Assuming $\omega_1 \approx \omega_2$, this can be rewritten as $\Omega' = \frac{\Omega^2}{\omega_0} (1 - K^2)$.

The modulation factor for the n th beat signal is then

$$M_n = \frac{2K}{1+K^2} J_n \left[\frac{\Omega^2}{2\omega_0 \nu} (1 - K^2) \right] \quad (5.19)$$

which gives the relative intensity of the beat signal with frequency $\omega_{21} + \frac{\Omega'}{2} + 2n\nu$.

If $K \approx .5$, then

$$M_n = \frac{4}{5} J_n \left(\frac{3\Omega^2}{8\omega_0 \nu} \right) \quad (5.20)$$

This is very similar to the Bessel function coefficient in the quadratic case of the Townes-Merritt effect; thus, the same overall conditions for the experimental parameters apply. As in the linear case, the beat frequencies must be less than the bandwidth to enable detection.

In a level crossing experiment, instead of determining the radiated power as a function of time, the total energy radiated in a specific direction is measured. As shown in the last chapter, variations in the total energy as a function of the RF frequency are indications of level crossings. As in quantum beats and the Townes-Merritt effect, these variations are detectable if the Bessel function coefficients for higher order terms are significant. Again, this requires that the argument be at least of order unity. One other consideration in a level crossing experiment is the observation angle. The initial calculations were performed with peaks indicating the level crossings; another geometry may be more favorable for precise measurement of the RF frequency at which the crossings occur. For the purpose of brevity, only the first case, where $\mu_{10} = \mu_0 \epsilon_+$ and $\mu_{20} = \mu_0 \epsilon_-$, will be used; and assume the observation is in the xy plane, so $\theta = \frac{\pi}{2}$ and ϕ may vary.

From equation (4.67), the total energy in the linear Stark shifted case is

$$J = J_0 \left[1 + \sum_n J_n \left(\frac{\Omega}{\nu} \right) \frac{\Lambda^2 \cos 2\phi + \Lambda \Lambda_n \sin 2\phi}{\Lambda^2 + \Lambda_n^2} \right] \quad (5.22)$$

where $\Lambda_n = \omega_{12} - n\nu$. For $\phi = 0$, this results in a series of peaks occurring when $\Lambda_n = 0$, corresponding to a level crossing condition. The relative magnitude of each peak is $J_n \left(\frac{\Omega}{\nu} \right)$, so the detectability then depends on the RF field strength and frequency, as before. In fact, the same requirements exist here as for the linear Stark shifted case of quantum beats.

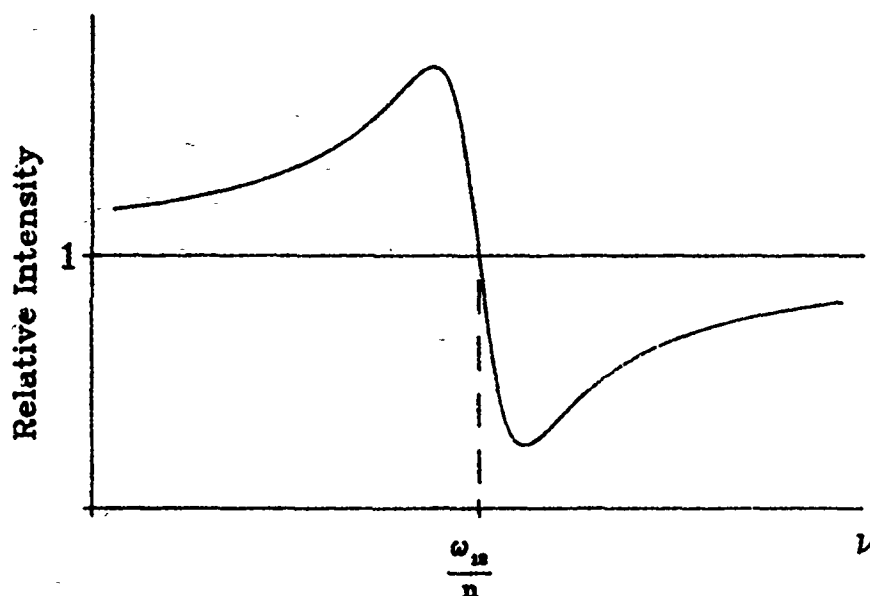


Figure 18. Level Crossing Signal for $\phi = \pi/4$

For experimental purposes, it may be more convenient to shift the detector to $\phi = \frac{\pi}{4}$. In this case, the detector is no longer in line with the initial excitation pulse, reducing potential degradation, and the level crossing signal has a different shape. For a single level crossing event, where $n\nu \approx \omega_{12}$, equation (5.22) becomes

$$\mathcal{I} = \mathcal{I}_0 \left[1 + J_n\left(\frac{\Omega\nu}{\nu}\right) \frac{A\Lambda_n}{A^2 + \Lambda_n^2} \right] \quad (5.23)$$

Figure 18 depicts the energy detected near a level crossing; the crossing occurs when $\Lambda_n = 0$ or when $\frac{\mathcal{I}}{\mathcal{I}_0}$ passes through one. The precise RF frequency at which the crossing occurs can more easily be determined in this case.

In the case of a Zeeman shift, the level crossing equation takes the same form as equation (5.22) except the Bessel function coefficient is replaced with $J_n\left(\frac{\Omega\nu}{\nu}\right)$. The conditions for observing level crossings here are the same as were discussed in the Townes–Merritt effect.

For a quadratic Stark shift, the total energy radiated is listed in table 6. For case I,

$$J = J_0 \left[1 + K^4 + K^2 \sum_n J_n \left(\frac{\Omega'}{2\nu} \right) \frac{A^2 \cos 2\phi + \frac{A \Lambda_n'}{\Lambda_n'^2} \sin 2\phi}{A^2 + \frac{A \Lambda_n'}{\Lambda_n'^2}} \right] \quad (5.24)$$

A level crossing occurs when $\Lambda_n' \equiv \omega_{12} + \frac{\Omega'}{2} + 2n\nu = 0$. The relative intensity of the individual peaks, when $\phi = 0$, is

$$\left[\frac{J}{J_0} \right]_{\max} = \frac{K^2}{1+K^4} J_n \left(\frac{\Omega'}{2\nu} \right) \quad (5.25)$$

If $K \approx 1/\sqrt{2}$, then using equation (5.18), this becomes

$$\left[\frac{J}{J_0} \right]_{\max} = \frac{2}{5} J_n \left(\frac{\Omega^2}{4\omega_0\nu} \right) \quad (5.26)$$

which is similar to equation (5.20) in the quadratic case of quantum beats. Thus, in order to detect at least the first order peak ($n=1$), the minimum RF field strength is about 1000 V/cm for an atomic transition frequency less than 5×10^{14} Hz and $\nu \approx 10^7$ Hz.

These order of magnitude calculations demonstrate the possibility of detecting quantum beats and level crossings resulting from interaction between the atom and a nonresonant RF field. Thus, it is feasible to use the level crossing technique to measure the spacing between nearby excited states, making this a useful spectroscopic tool.

VI. Conclusion

The primary purpose of this research was to investigate the possibility of using a nonresonant electromagnetic field as a means to measure closely spaced atomic energy levels by causing a level crossing. Level crossing experiments have been used to make spectroscopic measurements; however, in these experiments, static electric or magnetic fields were used to give rise to the energy shifts. Using static fields has the disadvantages of requiring relatively strong fields to create a significant shift, field nonuniformities result in broadening and lower resolution, and the lack of precision in measuring the actual field strength leads to significant uncertainty. If an oscillating field is used to create the energy shifts and subsequent crossings, these problems are alleviated.

A nonresonant field causes an effective splitting in the atomic energy states in what is referred to as the Townes-Merritt effect. The splitting can be viewed as individual states resulting from the combination of atom and field states into a single quantum system. In this 'dressed states' picture, photon ladders are superimposed on the atomic energy states. Transitions between the new states result in sidebands on the original atomic line separated by multiples of the nonresonant field frequency. The Townes-Merritt effect for a two level atom was analyzed here with a quantum electrodynamics (QED) approach, using the Heisenberg operator formalism to describe the atomic dynamics. The adiabatic approximation was used to include the effects of the nonresonant field on the atomic energy states for both linear and quadratic Stark shifts. The description of the Zeeman effect is mathematically equivalent to the linear case. The results agree with the dressed states model and the original experiment.

In a multi-level atom, the Townes-Merritt splitting can result in other

effects: specifically quantum beats and level crossings. These effects result from interference between separate transitions which originate in nearby excited states and end in a common ground state. Level crossings and quantum beats were analyzed for linear and quadratic Stark shifted atoms, again using the Heisenberg operator formalism. Quantum beats which depend on the field frequency were predicted in both cases, with the stronger effect in the linear case. If the quantum beat signals can be detected, this may provide a means to determine accurately the difference between widely spaced energy states.

In the case of level crossings, expressions were developed defining the total radiated energy, along a specific viewing axis, as a function of the field frequency. A level crossing results in a change in the fluorescence pattern indicated by a variation in the received energy. The peaks in the energy signal are relatively narrow, on the order of $2A$, allowing precise measurement of the crossing point. This can then be used to accurately determine the original energy spacing. Since the energy shifts here are a function of the field frequency, using an oscillating field alleviates the requirement for a strong field in the case of a static shift. In addition, a nonuniform field does not result in broadening as in the static case, and the critical parameter, frequency, can be measured with extreme accuracy. Thus, using a nonresonant field in a level crossing experiment can result in a very accurate spectroscopic technique.

Experimental confirmation of this technique will be the final proof of its usefulness. The last chapter provided a look at some of the critical parameter in such an experiment. It was shown that for an idealized atom, there is a wide range of possible transition frequencies that are applicable, infrared to the mid-visible. Typical RF field frequencies are on the order of 10^7 to 10^{10} Hz and field strengths of 100 to 1000 V/cm. The obvious follow-on work is to find an appropriate atomic or molecular sample and conduct an experiment to confirm this technique.

BIBLIOGRAPHY

1. Townes, C.H. and F.R. Merrit, "Stark Effect in High Frequency Fields," Physical Review **72**, 1266-7 (1947).
2. Townes, C.H. and A.L. Schawlow, Microwave Spectroscopy, p.273-9. McGraw-Hill, New York, 1955.
3. Cook, Richard J., Unpublished notes. November 1987.
4. Schenzle, A. and R.G. Brewer, "Quantum Electrodynamic Calculation of Quantum Beats in a Spontaneously Radiating Three Level System," Proceedings of the Second International Laser Spectroscopy Conference, edited by S. Haroche, et al. Springer-Verlag, Berlin, 1975.
5. Series, G.W., "Optical Pumping and Related Topics," in Quantum Optics, edited by S.M. Kay and A. Maitland. Academic Press, London, 1970.
6. Colegrove, F.D., P.A. Franken, R.R. Lewis, and R.H. Sands, "Novel Method of Spectroscopy with Applications to Precision Fine Structure Measurements," Physical Review Letters **3**, 420-422 (1959).
7. Autler, S.H., and C.H. Townes, "Stark Effect in Rapidly Varying Fields," Physical Review **100**, 703-722 (1955).
8. Schiff, Leonard I., Quantum Mechanics, (Third Edition). McGraw-Hill, New York, 1968.
9. Olver, F.W.S., "Bessel Functions of Integer Orders," Handbook of Mathematical Functions, edited by M. Abramowitz and I.A. Stegun. Government Printing Office, Washington, 1972.
10. Arimondo, E. and P. Glorieux, "Saturated Absorption on a Dressed Molecule: Application to the Spectroscopy of the ν_6 Band of CH_3I ," Physical Review A **19**, 1067-1083 (1979).
11. Rackley, S.A., and R.J. Butcher, "RF Modulation in IR Stark Spectroscopy," Molecular Physics **39**, 1265-1272 (1980).
12. Skatrud, D. and F. DeLucia, "RF Stark Tuning of Optically Pumped Far IR Lasers," Optics Letters **10**, 215-7 (1985).
13. Bonch-Bruevich, A.M. and V.A. Khodovoi, "Current Methods for the Study of the Stark Effect in Atoms," Soviet Physics Uspekhi **10**, 637-657, (1968).
14. Franken, P.A., "Interference Effects in the Resonance Fluorescence of 'Crossed' Excited Atomic States," Physical Review **121**, 508-512 (1961).
15. Khadjavi, A., W. Happer and A. Luno, "Electric Field Level Crossing Spectroscopy," Physical Review Letters **17**, 463-5, (1966).
16. Caldow, G.L., G. Duxbury, and L. Evans, "Laser Stark Saturation Spectroscopy of the ν_2 Band of CD_3I ," Journal of Molecular Spectroscopy **69**, 239-253 (1978).

17. Sakai, J. and M. Katayama, "Hyperfine Level Crossings in CD_3I ," Chemical Physics Letters **35**, 395 (1975)
18. Bheskar, N.D. and A. Lurio, "Tensor Polarizability of the 2^1P_1 state of He^+ by Electric Field Level Crossing," Physical Review A **10**, 1685-1699 (1974)
19. Series, G.W., "Double Resonance and Optical Pumping: The Early Days," Proceedings of the Ninth International Conference on Atomic Physics, edited by R.S. Van Dyck and E.N. Fortson.
20. Dodd, J.N., W.J. Sandle and D. Zisserman, "Study of Resonance Fluorescence in Cadmium: Modulation Effects and Lifetime Measurements," Journal of Physics **92**, 497 (1967).
21. Andra, H.J., "Stark-Induced Quantum Beats in $\text{H LY}\alpha$ Emission," Physical Review A **2**, 2200-7 (1970)
22. Haroche, S. J.A. Paisner and A.L. Schawlow, "Hyperfine Quantum Beats Observed in Cs Vapor under Pulsed Dye Laser Excitation," Physical Review Letters **30**, 948-954 (1973).
23. Loudon, R. The Quantum Theory of Light (Second Edition). Oxford University Press, New York, 1983.
24. Glauber, R.J., "Optical Coherence and Photon Statistics," in Quantum Optics and Electronics, edited by C. DeWitt, A. Blandin, and C. Cohen-Tannoudji. Gordon and Breach, New York, 1965.
25. Marion J.B. and M.A. Heald, Classical Electrodynamical Radiation (Second Edition), Academic Press, New York, 1980.
26. Macke, B. and J. LeGrand, "RF Sidebands in Microwave and IR Spectroscopy," Journal of Physics B **7**, 865-880, (1974).
27. Cohen-Tannoudji, C., B. Diu, and F. Laloe. Quantum Mechanics. Wiley, New York, 1977.
28. Coek, Richard J. Unpublished notes. December 1987.
29. Milonni, P.W., "Semiclassical and Quantum-Electrodynamical Approaches in Nonrelativistic Radiation Theory," Physics Reports **25**, 1-81 (1976).
30. Messiah, A., Quantum Mechanics. Wiley, New York, 1976.
31. Jackson, J.D., Classical Electrodynamics. Wiley, New York, 1962.
32. Merzbacher, E., Quantum Mechanics (Second Edition). Wiley, New York, 1970.
33. Lorrain, P. and D. Corson, Electromagnetic Fields and Waves (Second Edition). Freeman, San Francisco, 1970.

VITA

William Roc White [REDACTED]

[REDACTED] in Chelmsford, Massachusetts in 1972, and received a Bachelor of Science degree in physics and mathematics from the United States Air Force Academy in 1976, graduating in the top ten percent of his class. He was a distinguished graduate of both Undergraduate Navigator Training, in April 1977, and Electronic Warfare Training, in August 1977, at Mather Air Force Base, California. Following flight training, he was assigned to the 17 Defense Systems Evaluation Squadron, Malmstrom Air Force Base, Montana, as an EB-57 electronic warfare officer. He returned to Mather Air Force Base in August 1979 to instruct radar fundamentals and electronic countermeasures (ECM) with the 453 Flight Training Squadron. While at Mather, he successfully completed course requirements for a Masters of Science in Mechanical Engineering at California State University, Sacramento. In May 1983, he entered the School of Engineering, Air Force Institute of Technology, and earned a Masters of Science degree in physics, in December 1984. He also received the Mervin E. Gross award as the top graduate in his class. From January 1985 to February 1988, he was assigned to the 4950 Test Wing, Wright-Patterson Air Force Base, Ohio as a Flight Test Director. During this time he initiated and directed the Electronic Counter Countermeasures/Advanced Radar Test Bed (ECCM/ARTB) program, an effort to build the Air Force's first airborne integrated radar and sensor test platform on a modified C-141 aircraft. Also while at the Test Wing, he completed on his own time the course requirements and comprehensive exams for a Doctor of Philosophy degree through the Air Force Institute of Technology. Major White is currently assigned to the Frank J. Seiler Research Laboratory, United States Air Force Academy, Colorado as the Chief of the Laser Physics Division.

[REDACTED] [REDACTED]